

The Development of Capillary and Microchip Electrophoresis Methods for the Analysis of  
Pharmaceuticals in Developing Countries

By

Jessica S. Creamer

B.S., Chemistry, Northern Arizona University, 2008

M.S., Pharmaceutical Chemistry, University of Kansas, 2010

Submitted to the graduate degree program in Pharmaceutical Chemistry and the Graduate  
Faculty of the University of Kansas in partial fulfillment of the requirements for the degree of  
Doctor of Philosophy.

---

Chairperson – Dr. Susan M. Lunte

---

Dr. Karen J. Nordheden

---

Dr. Teruna J. Siahaan

---

Dr. John F. Stobaugh

---

Dr. Michael Zhuo Wang

Date Defended: May 30<sup>th</sup>, 2014



The Dissertation Committee for Jessica S. Creamer  
certifies that this is the approved version of the following dissertation:

Capillary and Microchip Electrophoresis Methods for the Analysis of  
Pharmaceuticals used in Developing Countries

---

Chairperson Dr. Susan M. Lunte

Date approved: \_\_\_\_\_



This dissertation is dedicated to my parents, Will and Cathy Creamer,  
for their unwavering love and support.



## Abstract

Maintaining a consistent supply of pharmaceuticals to developing countries could save millions of lives per year. One of the major roadblocks in this effort is an abundance of substandard and counterfeit drugs in the supply chain. To prevent these products from being distributed, improved methodology and instrumentation for drug screening is needed. In these low-resource areas the availability of proper funding and laboratory space is limited. To replace the expensive liquid chromatography and mass spectrometry instrumentation traditionally used for quality control, capillary electrophoresis (CE) can be used. CE has a low startup cost and, because of the small sample and reagent volume requirements, the cost per test is kept to a minimum. Additionally, any methodology developed for CE can be transferred to the miniaturized platform of microchip electrophoresis (ME). ME further reduces the cost-per-test and provides the potential for a fully portable analytical device that can be used for on-site analysis. This method is particularly useful for screening pharmaceuticals throughout the many distribution lines, store houses, and clinics across a large country.

In this dissertation, CE was used to develop methodology for the analysis of the peptide drug oxytocin (OT). OT is needed in developing countries to prevent death from post-partum hemorrhage. A major concern regarding the supply chain of peptide-based drugs is the degradation of these products when they are shipped and stored incorrectly. Several degradation products are produced when OT is subjected to heat-stress conditions. Deamidation, in particular, produces small molecular changes that have significant effects on the biological activity of the peptide. Initially, methodology for the separation and detection of desamino degradation products of OT was developed for CE-UV. OT contains three potential sites of deamidation, which leads to seven distinct desamino products. The separation was achieved following an optimization of the background electrolyte to include a pseudostationary phase and an organic modifier to increase selectivity and resolve the eight structurally similar peptides.

To improve the functionality of the CE assay for OT integrity screening, the next step of was to further optimize the method for a separation of all of the known degradation products formed under heat-stressed OT formulations. However, current literature on the degradation of OT does not yet addressed the degradation of Pitocin pharmaceutical formulations that are prepared in water containing a small amount of acetic acid, to adjust the pH between 3-5, and 0.5% chlorobutanol as a preservative. To investigate the effect that CB and CB-like products have on the degradation of OT, LC-UV-MS was used to monitor the formation of degradation products as a function of time. The preliminary data shows that CB, and the structurally similar trichloroethanol (TCE), significantly stabilize OT from the heat-stress degradation. The addition of either of these trichloro species substantially reduces the rate of degradation observed over a 48 h period at 70 °C. Further work is needed on this project to determine the cause of this protective effect by performing structural studies of OT in the presence of CB or TCE.

Finally, initial steps were taken towards the development of a low-cost portable ME device. A significant percentage of small molecule counterfeit drugs are formulated with the wrong amount of active ingredient. Current portable analytical methods available to monitor the pharmaceutical supply chain are limited in their quantitative abilities. By coupling ME to conductivity detection, it is possible to perform quantitative analysis of multiple species simultaneously. Initial experiments to evaluate system performance were performed using two first-line anti-tuberculosis drugs, ethambutol and isoniazid.



## Acknowledgements

Much effort has gone into the work published here and I could not have done it alone.

First and foremost I'd like to acknowledge my advisor, Dr. Susan Lunte, for the six years' worth of mentoring and guidance. From the very start she has worked with me to create unique projects which have led to exciting and unexpected research. Despite her busy schedule she never failed to make time to talk about research or make a much needed cup of Jet Fuel. Through her tireless efforts I have come into my own as scientist and writer. I cannot thank her enough for always pushing me to be my best, especially towards the end, when I needed it most.

The KU Pharmaceutical Chemistry Department is an excellent place to learn and this is due entirely to the efforts of the stellar faculty. In particular I'd like to thank the many teachers I have had over the years for helping fill my head with a tremendous amount of knowledge and for the solid foundation on which to build my future.

Nothing would run smoothly without the efforts of the staff. Thank you to Nancy Helm for all of your help and kindness throughout my time here. Thanks to Gary Weber for all of the work that you do for our group and for putting up with all of us constantly asking you where Sue was any given week; I hope that you enjoy your well-earned retirement!

Many thanks to my committee members, Dr. Siahaan, Dr. Stobaugh, Dr. Volkin, and Dr. Nordheden, who have taken time out of their busy schedules to give spot-on guidance during our many meetings, and to Dr. Wang for agreeing to be a part of my defense process in Dr. Volkin's stead. I am particularly grateful to my readers Dr. Siahaan and Dr. Stobaugh for their thoughtful feedback during the writing process.

I owe so much to all of the Lunte Lab members, past and present, for their constant support and camaraderie. You helped me work through so many research problems.

To the people that were in the lab when I joined, Dr. Pradyot Nandi, Dr. Dave Fisher, Dr. Matt Hulvey, Dr. Courtney Sloan, Dr. Phil Livanec, Dr. Anne Regel and Dr. Tom Linz, thank you for teaching me what it meant to be a part of the lab. Your hard work and worldly knowledge of BBQ, bacon, and beer helped me go from vegetarian to meat-lover in just one short year. In particular, I want to say thanks to Anne and Courtney for being excellent friends, in lab and out. Sharing a cube in grad school is like being roommates. Thanks for always telling me it was going to be okay, and for suggesting that we go out to eat when it was clear we needed a break from MRB.

A huge thank you to the rest of my Lunte Lab family, my fellow graduate students Dr. Dulan Gunasekara, Dr. David Scott, Joe Siegel, Shamal Durayalage, Manjula Wijesinghe, Abdullah Al-Hossaini, Rachel Saylor, and Nathan Oborny; the numerous, wonderful undergrads Erin Reid, Erin Evans, Emilie Mainz, Pann Pichetsurnthorn, Derek Jensen, and wine expert Jeff Bauman; and the host of talented visiting scientists Bruno Lucca, Diogenes Meneses, Richard Piffer, Giuseppe Caruso, and Dr. Fracassi da Silva that have lent their brains, humor, and insight into the research that we do. Having you all around has made the countless group meeting and odd hours in lab much more bearable.

I am especially thankful for the individuals with whom I have worked closely on projects. Thanks to Nathan Oborny for always stepping up to help me out even when your plate was already full. Thanks to Fracassi for leaping over the language barrier to teach me how to think outside the fabrication box. Thanks to Shannon Krauss, the goofball of an REU that I was fortunate enough to mentor, who helped to initiate the oxytocin project. And of course, thanks to Ryan Grigsby; none of

us would be able to function without your constant hard work. How you manage to keep everything running smoothly when we are trying so hard to break it will always be a mystery.

Thank you to the graduate students at KU for their willingness to share their knowledge and experience, especially to the friends I made in the classes before me, who seemed way smarter than I thought I would ever be, particularly Dr. Loren Schieber, Dr. Diana Sperger Davey, Dr. Taryn Bagby, Talia Martin, Dr. Maria Feeney, Dr. Sarah Pyszczynski, and Dr. Elodie Dempah.

I was tremendously lucky to enter graduate school with my fellow Deuces, Josh Woods, Dr. Randy Logan, and Dr. Justin Thomas. Together we survived late nights studying and the even later nights of Rock Band. There is nothing quite like the support you get from the only people that know exactly what you are going through. Our friendship means the world to me and I could not imagine doing this without you guys.

Outside of the lab my sanity was kept intact with the help from my many non-science friends and teammates. From dog park dates, to dance parties, to Ultimate tournaments, and community dinners, you have bolstered my spirit and given me a reason to get my experiments done early.

I would not be where I am today without my wonderful family. If it's a balance of nature and nurture then I lucked out on both. My mom and dad are positive, bright, and caring people that have always encouraged me to follow whatever path was in front of me. They raised me to be the curious and dedicated person that I am, and I thank them for all of the advantages they have given me. That includes my two baby brothers, Nick and Matt, who have been my ridiculous partners in crime for the last quarter of a century.

And at last, thank you Nicolas Frisby, for loving me through it all. After many nebulous years in graduate school, we are both finished! Now that the future is wide open, I cannot think of a better person to have by my side as I figure out what's next.



## Table of Contents

- 1 Chapter One: Thesis Objective and Chapter Summaries – pg 1**
  - 1.1 Introduction – pg 2
  - 1.2 Chapter Summaries – pg 2
    - 1.2.1 Chapter Two – pg 2
    - 1.2.2 Chapter Three – pg 3
    - 1.2.3 Chapter Four – pg 4
    - 1.2.4 Chapter Five – pg 4
    - 1.2.5 Chapter Six – pg 5
- 2 Chapter Two: Recent Advances in the Analysis of Therapeutic Proteins by Capillary and Microchip Electrophoresis – pg 7**
  - 2.1 Introduction – pg 8
  - 2.2 Techniques – pg 9
    - 2.2.1 Capillary Zone Electrophoresis– pg 9
      - 2.2.1.1 Dynamic coatings – pg 10
      - 2.2.1.2 Static coatings – pg 13
      - 2.2.1.3 Evaluation of capillary coating performance – pg 14
    - 2.2.2 Capillary gel electrophoresis – pg 17
    - 2.2.3 Capillary isoelectric focusing – pg 21
    - 2.2.4 Capillary electrochromatography – pg 26
  - 2.3 Detection methods – pg 31
    - 2.3.1 Spectroscopic detection– pg 31
    - 2.3.2 Mass Spectrometry– pg 32
  - 2.4 Applications – pg 37

2.4.1	Glycosylation – pg 37
2.4.2	Biosimilars – pg 42
2.5	Microchip electrophoresis – pg 45
2.5.1	Microchip gel electrophoresis – pg 45
2.5.2	Microchip isoelectric focusing – pg 46
2.5.3	Microchip electrophoresis-mass spectrometry – pg 48
2.6	Conclusions and future perspectives – pg 50
2.7	References – pg 51
<b>3</b>	<b>Chapter Three: Capillary Electrophoresis Separation of the Desamino Degradation Products of Oxytocin– pg 61</b>
3.1	Introduction – pg 62
3.2	Materials and methods – pg 65
3.2.1	Chemicals and reagents – pg 65
3.2.2	Preparation of buffers – pg 65
3.2.2.1	Buffer composition optimization – pg 65
3.2.2.2	Buffer additive optimization – pg 66
3.2.3	Standard preparation – pg 66
3.2.4	Equipment conditions – pg 66
3.2.5	Acid-catalyzed deamidation of oxytocin – pg 67
3.3	Results and discussion – pg 67
3.3.1	Separation optimization– pg 67
3.3.1.1	BGE selection – pg 67
3.3.1.2	CD additives – pg 68
3.3.1.3	Organic modifiers– pg 69
3.3.1.4	Separation voltage – pg 71

3.3.2	Separation parameters – pg 71
3.3.3	Tracking degradation in heat-stressed oxytocin samples – pg 73
3.4	Concluding remarks – pg 76
3.5	References – pg 78
<b>4</b>	<b>Chapter Four: Investigation into the Effect of Chlorobutanol on the Stability of Oxytocin– pg 81</b>
4.1	Introduction – pg 82
4.2	Materials and methods – pg 86
4.2.1	Chemicals and reagents – pg 86
4.2.2	Preparation of oxytocin formulations – pg 86
4.2.3	Accelerated degradation studies – pg 88
4.2.4	LC-UV-MS equipment condition – pg 88
4.3	Results and discussion– pg 89
4.3.1	Q1 scan range optimization– pg 89
4.3.2	Effect of formulation buffering capacity on OT degradation– pg 92
4.3.3	Effect of chlorobutanol on OT degradation– pg 95
4.3.4	Effect of chlorobutanol-like species on OT degradation – pg 98
4.3.4.1	Antimicrobial effect– pg 98
4.3.4.2	Alcohol substitution– pg 98
4.3.4.3	Trichloro group– pg 100
4.3.5	Potential rationale for increased OT stability in the presence of CB and TCE– pg 103
4.4	Concluding remarks – pg 104
4.5	References – pg 105

**5 Chapter Five: Development of Methods for On-site Separation Based Analysis of Small Molecule Pharmaceuticals for use in Developing Countries – pg 107**

5.1 Introduction– pg 108

5.2 Material and methods– pg 114

5.2.1 Chemicals and reagents– pg 114

5.2.2 Background electrolyte preparation– pg 116

5.2.3 Sample preparation– pg 116

5.2.4 Microchip design– pg 117

5.2.4.1 PDMS microchannel fabrication– pg 117

5.2.4.2 Electrode fabrication – pg 117

5.2.4.3 Microchip construction– pg 120

5.2.5 Microchip operation– pg 120

5.2.6 Instrumentation for C<sup>4</sup>D– pg 120

5.3 Results and discussion – pg 122

5.3.1 Rational for BGE composition– pg 122

5.3.2 ME separation performance for EMB from standards  
vs pharmaceutical formulation– pg 128

5.3.3 Analysis of a lab-made counterfeit – pg 130

5.3.4 Identification of an internal standard– pg 130

5.4 Conclusions– pg 135

5.5 References – pg 136

**6 Chapter Six: Conclusions and future directions – pg 139**

6.1 Conclusions– pg 140

6.1.1 Oxytocin project– pg 140

6.1.2 ME-C<sup>4</sup>D portable analysis project– pg 142



6.2 Future Directions– pg 143

6.2.1 CE separation of all oxytocin degradation products– pg 143

6.2.2 Continuing development for on-site ME analysis – pg 143

6.2.2.1 ME-C<sup>4</sup>D for small molecule analysis – pg 143

6.2.2.2 ME-LIF for protein and peptide drug analysis – pg 145

6.3 References– pg 148

**Chapter One:**  
**Thesis Objective and Chapter Summaries**

## **1.1 Introduction**

Both small molecule drugs and biopharmaceuticals are needed around the world to prevent and cure illness. However, there are significant barriers to the effective global distribution of these products. In particular, biopharmaceuticals have limited geographical distribution due to the risk of both chemical and physical degradation when these products are transported in the absence of a cold-chain shipping and storage. To help support regulatory efforts within developing countries, innovative methodologies for protein integrity screening that use preexisting inexpensive instrumentation are needed. For small molecule drugs, the supply chain is threatened by an overabundance of counterfeit products. Counterfeits are present throughout distribution lines in warehouses, pharmacies, and clinics. Analysis of these products needs to be able to be performed on-site to detect them prior to administration. To combat this, the development of new instrumentation and methodologies for portable and high-throughput assessment of drug quality is necessary.

This dissertation explores the use of capillary electrophoresis (CE) and microchip electrophoresis (ME) as low-cost analysis techniques for quantitative testing of the integrity of both small molecule drugs and biopharmaceuticals. The focus of the research described in this dissertation has been the development of novel methodologies and instrumentation for on-site analysis that can be used in the various environmental conditions faced in low-resource areas.

## **1.2 Chapter Summaries**

### **1.2.1 Chapter Two**

This chapter is a thorough review of the recent developments and applications of CE-based separation methods for the characterization of protein and peptide therapeutics. The development of biopharmaceuticals is an expensive and time-intensive process. Biologics, which have become a multi-billion dollar industry, are chemically complex products that require constant observation during each stage of development and production. Post-translational modifications, along with chemical and physical

degradation from oxidation, deamidation, and aggregation, can lead to high levels of heterogeneity that affect drug quality and efficacy.

In particular, this chapter focuses on summarizing research as described in papers accepted for publication over the in the two-year period between January 2012 and December 2013. The separation principles and recent technological advances of CE, capillary gel electrophoresis, capillary isoelectric focusing, capillary electrochromatography and CE-mass spectrometry are discussed, along with exciting new applications of these techniques that are relevant to pharmaceutical analysis. Also included is a short summary of recent ME methods to indicate the direction this field is moving with regards to the development of inexpensive and portable analysis systems for on-site, high-throughput analysis.

### 1.2.2 Chapter Three

CE-UV can be used for fast qualitative analysis of proteins, and operated in developing countries at a fraction of the cost of liquid chromatographic methods. In this chapter the development of a rapid CE method for the separation of oxytocin (OT) from its desamino degradation products is presented. OT is a critical drug for the treatment of post-partum hemorrhage, the leading cause of maternal death in developing countries. Under heat-stress conditions OT undergoes deamidation which leads to reduced therapeutic efficiency. OT has three specific sites of deamidation that leads to the formation of seven structurally similar peptides.

To achieve a separation of the seven desamino OT peptides, the background electrolyte composition was optimized to include sulfobutyl ether  $\beta$ -cyclodextrin (SBE) with MeOH as an organic modifier. The SBE acts as a pseudostationary phase, enhancing the resolution based on affinity between the peptide and the cyclodextrin. A rapid separation was accomplished using CE-UV (214 nm) on a 50 cm capillary (40 cm to window) that could resolve all eight peptides in less than 13 min. The method was then applied to monitor the heat-stress degradation products of OT at 70 °C, where all seven desamino species were observed over a 96 h period.

### 1.2.3 Chapter Four

Chapter four provides the results of a preliminary study investigating the possible protective effects of chlorobutanol (CB) on OT during heat-stress degradation. CB is added to injectable oxytocin formulations as an antimicrobial preservative (AP) at 0.5% w/v. Previous studies investigating the degradation of OT have been performed in the absence of CB. Yet, it has been shown numerous times by other groups that APs can have a significant effect on protein formulation stability. Prior to the development of a CE-based method that can separate and detect all of the known degradation products of OT we first wanted to make sure that the presence of CB did not alter the degradation mechanisms to produce additional products.

To monitor both the degradation products formed as well as the kinetics, LC-UV-MS was used to investigate the degradation of OT in presence of CB and CB-like species. The various CB-like species included structurally similar compounds tert-butol alcohol (TBA), trichloroacetic acid (TCA), and trichloroethanol (TCE); as well as, benzyl alcohol (BA), which has similar antimicrobial properties to CB. This preliminary study showed that OT formulations without additives (as well as those containing TBA, TCA, and BA) degraded quickly and, after 48 h at 70 °C, less than 30% of the parent OT remained in solution. On the other hand, the OT formulations containing the CB or TCE were much more stable and more than 70% of the OT was still present after the 48 h at 70 °C. It has been shown that halogenated alcohols such as TCE can alter the structure of the peptide, which could lead to an increased stability. However, more work is needed on this project to determine the mechanism for how CB and TCE inhibit OT degradation.

### 1.2.4 Chapter Five

This chapter presents a brief review on portable methods for pharmaceutical analysis to transition the focus of the dissertation towards the work that has been done in our lab to develop a ME device for small molecule integrity screening. ME is a fast-growing technology that places the separation

mechanism of capillary electrophoresis on to a miniaturized platform, significantly decreasing the cost and size of the supporting instrumentation. Inexpensive and portable technologies are particularly important for regulation of drugs in developing countries that are working to protect the pharmaceutical supply chain from counterfeit drugs.

Currently, counterfeit drug detection is performed by a variety of available analysis techniques that can provide accurate and specific qualitative analysis to confirm active ingredient identity; however, the quantitative capabilities of these assays is limited. By coupling the ME separation with a simple and universal detection method, capacitively coupled contactless conductivity detection (C<sup>4</sup>D), this system is able to perform quantitative analysis of multiple species simultaneously. This approach is particularly useful for the analysis of formulations that contain multiple active ingredients, or for the detection of counterfeit products with large amounts of impurities and contaminants.

This chapter demonstrates the utility of the ME-C<sup>4</sup>D system for on-site pharmaceutical analysis using two first-line anti-tuberculosis drugs, ethambutol (EMB) and isoniazid (INH). Both EMB and INH were separated on-chip using a low-conductivity buffer of 60 mM HEPES, 0.1 mM lactic acid pH 4.0. The linearity of the method was determined for both drugs over a range of 0.25-5.0 M with R<sup>2</sup> values of greater than 0.997. Further metrics of analytical performance including precision and separation efficiency for EMB in both samples made from both the standard and tablet formulation are presented.

### 1.2.5 Chapter Six

Chapter six summarizes the research presented in this dissertation and discusses potential future directions of both the oxytocin and ME-C<sup>4</sup>D projects.



## **Chapter Two:**

### **Recent advances in the analysis of therapeutic proteins by capillary and microchip electrophoresis**

Published as:

J.S. Creamer, N.J. Oborny, S.M. Lunte, 'Recent advances in the analysis of therapeutic proteins by capillary and microchip electrophoresis', *Analytical Methods*, 2014, 6 (15), 5427-5449



## 2.1 Introduction

The characterization of protein therapeutics presents a unique analytical challenge due to the inherent heterogeneity of recombinant protein expression. Even small changes in the manufacturing process can lead to vastly different active pharmaceutical ingredients. Additionally, numerous physical and chemical degradation pathways can occur during manufacturing and storage that compromise protein integrity, leading to a potentially harmful, unstable product [1]. Thorough characterization of protein therapeutics is necessary at every step of the research and development process, from drug discovery to lot release.

Due to the potential complexity of product degradation during preformulation and formulation studies, additional separation techniques are needed to complement the more widely used column liquid chromatography (LC) methods. To address this issue, capillary electrophoresis (CE) has become a popular choice for the separation and analysis of therapeutic proteins and peptides.

CE provides several distinct advantages over LC. First, due to the faster separation times and the use of multi-capillary arrays, hundreds of samples can be processed by CE per day. Second, CE is capable of achieving very high efficiency separations due to the low diffusion coefficients of biomolecules. Lastly, the small dimensions of the capillary and the low sample volume requirements keep reagent and analyte use to a minimum, reducing the cost-per-test. The benefits of CE for the analysis of therapeutic peptides and proteins have been addressed in several excellent reviews to date [2-5].

This chapter is aimed at highlighting the advances made in the field of CE therapeutic protein analysis during 2012 and 2013 by expanding on a paper that was recently published by Zhao *et al.* [5]. Following brief descriptions of the working principles of the different CE separation and detection methods, recent technological improvements and novel applications are discussed. Two additional sections have been included to further explore the use of CE for the determination of protein glycosylation and the comparison of biosimilars. Finally, a brief introduction into microfluidic approaches to protein analysis is given. Microchip electrophoresis (ME) has the additional advantages of

increased speed, high-throughput capabilities, and portability for on-site analyses. Tables are presented in each section to highlight the relevant CE and ME application-based citations.

## 2.2 Techniques

Historically, capillary zone electrophoresis (CZE) has been the most commonly employed form of CE. Yet, the principles of electrophoretic separations and the benefits of capillary-based techniques are applicable to other CE separation modes as well. Protein analysis based on size can be accomplished by capillary gel electrophoresis (CGE), capillary isoelectric focusing (CIEF) can be used to determine isoelectric points and charge heterogeneity, and capillary electrochromatography (CEC), which combines the high efficiency electrophoretic separation with chromatographic retention, can be used for more selective separations and analysis of neutral species. Depending on the properties of the analyte and requirements of the assay, each of these separation modes can be coupled to a number of detection methods such as UV-Vis absorbance, laser-induced fluorescence (LIF), and mass spectrometry (MS).

### 2.2.1 Capillary zone electrophoresis

Of the electrophoresis-based separation techniques, CZE is most frequently used for the analysis of small molecules, carbohydrates, and peptides. It is simple, easy-to-use, and requires minimal amounts of reagents compared to chromatographic methods. Additionally, in CZE, the separation of analytes is based on their size-to-charge ratio, making it well suited for separations of proteins with post-translational modifications (PTMs) or degradations that affect the charge of the molecule [6, 7] including deamidation, glycosylation, and phosphorylation.

One example of the use of CZE for the investigation of deamidation concerns the stability of oxytocin. Deamidation of Asn and Gln residues is the most common chemical degradation pathway for peptides and proteins [1]. This process leads to the production of an ionizable carboxylic acid from the neutral amide ( $R\text{-CONH}_2 \rightarrow R\text{-COOH}$ ), facilitating a separation by CZE. However, if peptides, such as oxytocin, contain several labile Asn and Gln sites, multiple degradation products of the same size-to-

charge ratio are produced and a straightforward separation becomes impossible. To distinguish between the seven desamino degradation products of heat-stressed oxytocin, Creamer *et al.* utilized sulfolbutyl ether  $\beta$ -cyclodextrin (SBE  $\beta$ -CD) as a pseudo-stationary phase [8]. The negatively charged SBE  $\beta$ -CD forms an inclusion complex with the hydrophobic Tyr<sup>2</sup> residue of oxytocin, affecting the electrophoretic mobility of the peptides. A baseline separation of all eight peptides and a migration time RSD of less than 1.2% was achieved.

Unfortunately, reproducible separations of larger biomolecules using bare fused-silica capillaries are rare due to protein adsorption. Many proteins have large localized regions of positive charge that are electrostatically attracted to the negatively charged silanol groups at the capillary surface. Additional adsorption can be caused by hydrophobic and hydrogen-bonding interactions. This adsorption process prevents CZE from obtaining the  $10^6$  theoretical plates that should be possible due to the very low diffusion coefficients of large proteins. [9, 10].

One strategy for minimizing protein adsorption is to alter either the charge density of the protein or the capillary wall by changing the pH or ionic strength of the background electrolyte (BGE). Another approach is to simply add a modifier to the BGE to reduce protein-wall interactions. The addition of surfactants, small amines, or anionic salts, such as phytic acid, to the BGE is common [11, 12]. In cases where modification of the run buffer does not obviate protein adsorption, dynamic and static capillary coatings have been used to create a barrier between the ionized silanol groups and the protein of interest.

#### 2.2.1.1 Dynamic coatings

Dynamic coatings are buffer additives that adsorb to the surface of the capillary, shielding the silanol groups from analyte adsorption [13]. These noncovalent coatings are popular due to their simplicity, versatility, and ease-of-use. However, because of their impermanent nature, the coatings need to be continuously regenerated. This can be accomplished by refreshing the physically adsorbed layer at the capillary with rinses between runs, or adding a small amount to the BGE to prevent coating degradation

during electrophoresis. A variety of such coatings have been used for protein separations, ranging from small molecules such as ionic liquids (ILs) to larger molecules such as surfactants and polymers [14].

ILs have been previously explored as dynamic coatings for CZE protein separations [15-17]. ILs are salts made up of organic cations and inorganic or organic anions that are liquid at, or around, room temperature. Recently, a new IL, N-methyl-2-pyrrolidonium methyl sulfonate ( $[\text{NMP}]^+\text{CH}_3\text{SO}_3^-$ ), was used to prevent basic protein (pI 9.0-10.7) adsorption to capillary walls during CE separation [18]. The  $[\text{NMP}]^+$  moiety electrostatically adsorbs to the capillary surface, where it is able to form a hydrogen bond for additional stability (Fig. 1). Using this coating, the authors were able to achieve a baseline separation of four basic proteins (Table 1) with an interday migration time RSD of less than 1.5%. The improvement in the separation after addition of only 0.02% w/v IL, compared to that obtained with phosphate buffer alone, is easily seen in Fig. 1D.

Polysaccharides are also attractive candidates for dynamic coatings for protein separations because they are non-toxic, readily abundant, and biocompatible [19-21]. Two novel dynamic coatings based on the chemical substitutions of cellulose have recently been reported [22, 23]. The first, a positively charged quaternized cellulose (QC), was synthesized through a reaction of cellulose with 3-chloro-2-hydroxypropyltrimethylammonium chloride. The positive charge of the QC leads to the electrostatic adsorption of the compound to the capillary surface, reversing the electroosmotic flow (EOF). Addition of 5  $\mu\text{g}/\text{mL}$  QC to the BGE prevented adsorption of model basic proteins leading to higher separation efficiencies [22]. To increase the reverse EOF by 10%, and further improve separation efficiency, additional substitution of the QC was made using hydrophobic hexadecyl groups [23]. Both QCs were evaluated with a separation of five basic proteins (Table 1). In both cases, the modified capillaries produced a migration time reproducibility with RSD of less than 2.7%.

Despite their simplicity, buffer additives and dynamic coatings are not always the best approach to eliminate protein adsorption. If the modifier is highly charged, band broadening can occur due to high separation currents and Joule heating. Additionally, some buffer modifiers can interfere with protein

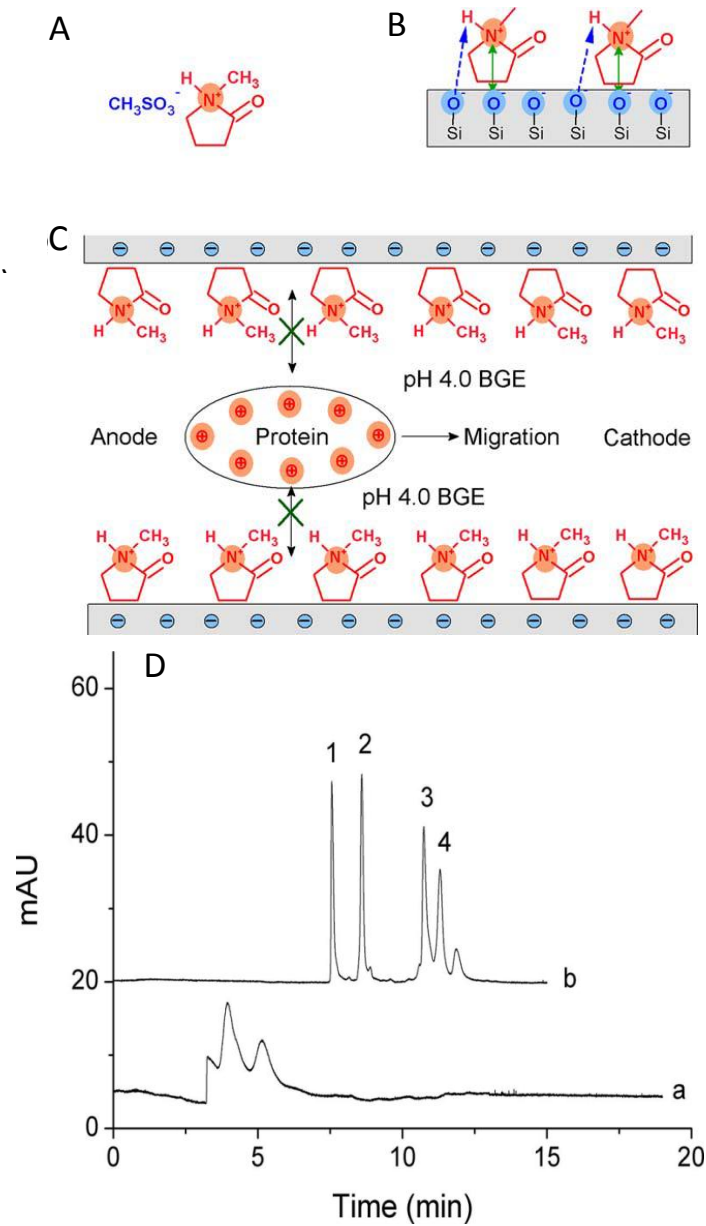


**Fig. 1.** A) The structure of the IL [NMP]<sup>+</sup>CH<sub>3</sub>SO<sub>3</sub><sup>-</sup>, B) the interaction between [NMP]<sup>+</sup> and the silica capillary inner wall, and C) the mechanism of separation of proteins using [NMP]<sup>+</sup> as dynamic coating material, D) Electropherograms of four basic proteins in bare silica capillary (bottom trace) and in the presence of 0.02% w/v IL (top trace). Run buffer: 40 mM pH 4.0 sodium phosphate; voltage: 18 kV; detection: 214 nm; peaks: (1) cytochrome *c*, (2) lysozyme, (3) ribonuclease A, (4)  $\alpha$ -chymotrypsinogen A. Reprinted with permission from ref. 18

binding assays [24], disrupt protein stability [25], or be incompatible with downstream detection methods such as MS. In cases where greater stability and reproducibility are needed, static coatings have been used [13].

#### 2.2.1.2 Static coatings

Static coatings are chemically linked to the capillary wall and do not need to be added to the run buffer to achieve reproducible separations. Therefore, they have the potential for large-scale production and can be made commercially available. Several companies, including GL Sciences (FunCap®), Target Discovery (UltraTrol™), MicroSOLV (CElixer™), and Beckman Coulter (eCAP™), are already selling coated capillaries for protein separations.

Gassner et al. performed a thorough comparison of both commercially available and lab-generated static coatings in 2013 [26]. Eight coatings were selected—four positive: FunCap®-type A, UltraTrol™ HR, Hexadimethrin bromide (polybrene) (PB)-dextran sulfate-PB, and polyethylenimine; and four neutral: FunCap®-type D, UltraTrol™ LN, hydroxypropylcellulose, and polyvinyl alcohol (PVA). The coatings were evaluated for the protein recovery, isoform resolution, and migration time reproducibility of two monoclonal antibodies (mAbs).

For the positively charged coatings, the separation was run in negative polarity. With these capillaries it was determined that the slower the EOF, the better the resolution. Yet, while UltraTrol™ HR had the slowest EOF, it had poor reproducibility (8.9% RSD) and was discarded from the study. For the neutral coatings run in normal polarity, the largest factor for protein adsorption was the presence of residual silanol groups. This was apparent by the fact that some EOF was still generated in the capillary. Of the four neutral coatings in this study, both commercial options, FunCap®-type D and UltraTrol™ LN, generated a small amount of EOF at pH 7.0, indicating that the coating was not uniform and there were still potential sites for protein adsorption. However, it is important to note that the separation performance of each coating was highly dependent on the pH and composition of the BGE. Consequently, care should be taken during method development to fully optimize the BGE for the selected coating.

Due to the varied performance of the commercially available products, new coatings for the separation of basic and hydrophobic proteins are still under development. One particularly attractive choice for static coatings is phospholipid bilayers (PLB) because of the protein resistant nature of the phosphocholine polar headgroup. However, the limiting factor for these coatings are their poor long-term chemical and physical stability. This can be remedied by cross-linking the PLB with bis-SorbPC which produces a stabilized phospholipid bilayer (SPB) at the capillary surface [27]. In a recent report, it was shown that the SPB produced a stable coating over a pH range from 4.0–9.3 [28]. Over the course of 45-days dry storage the migration time reproducibility for both model proteins (Table 1) was marginally affected and the overall RSD for the EOF was only changed by 1.1%.

To reduce the preparation time of static coated capillaries, self-assembled bilayers and photoinitiated polymerization can be used. An example of such a process was described by Yu *et al.* using a photosensitive diazoresin (DR) in combination with either PVA [29] or polyethylene glycol (PEG) [30]. After exposure to 365 nm light, both the DR/PVA and DR/PEG coatings were able to prevent protein adsorption and achieve an efficient separation of several model basic proteins (Table 1) with a migration time precision less than 4% RSD.

### 2.2.1.3 Evaluation of capillary coating performance

Prior to assay development, the determination of capillary coating performance is extremely important. A previous analytical approach to determine protein adsorption in capillaries involves flushing the capillary with the protein of interest to allow adsorption and then measuring desorption on a subsequent rinse [31-33]. However, with this method, only irreversibly bound proteins are measured. As an alternative, de Jong *et al.* recently developed a more direct method using pressure-driven flow [34]. Briefly, a plug of sample is pressure injected into a capillary at a low flow rate (0.5 psi) and the Taylor dispersion of the plug is measured at two different detection points along the capillary. Based on these measurements, the magnitude of the protein adsorption can be estimated (Fig. 2).

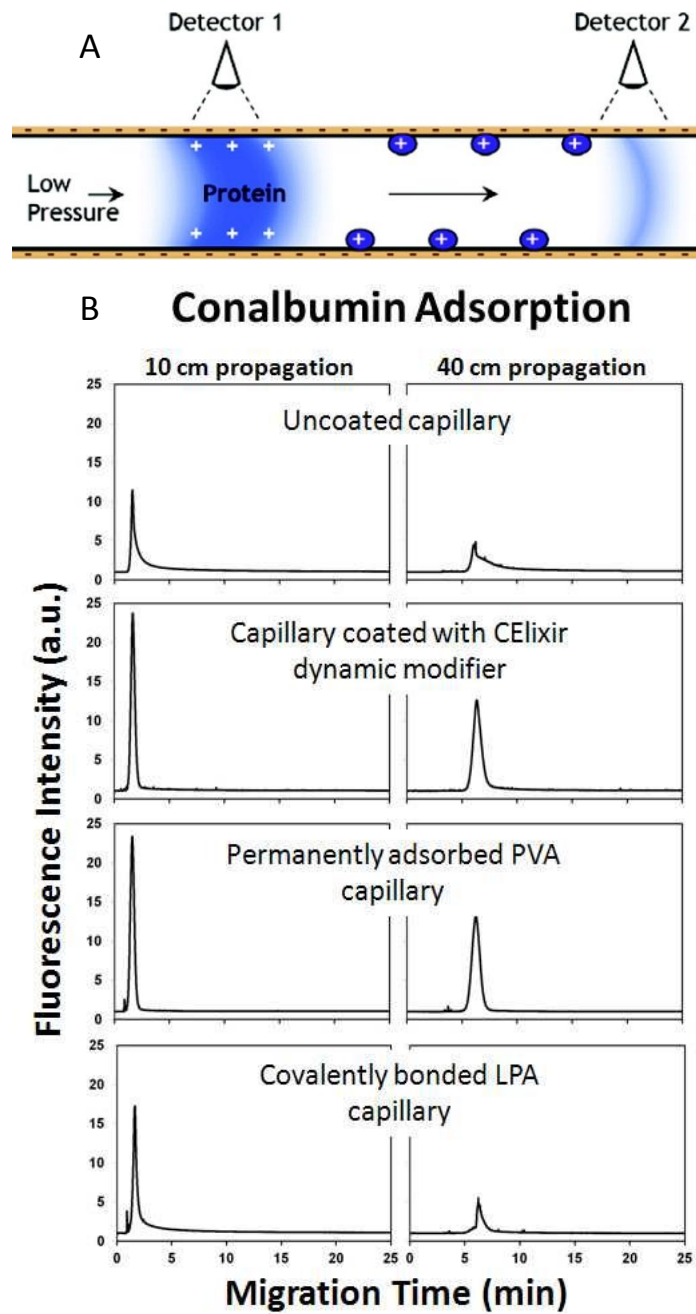


**Fig. 2.** A) Diagram of the set-up for the dual detection pressure-based technique for assessing protein adsorption. B) Pressure-driven propagation of 5.3  $\mu\text{M}$  chromeo-labeled conalbumin detected at 10 and 40 cm. Better protection against adsorption can be seen in both the capillary coated with CELixir dynamic modifier and the capillary with a permanently adsorbed PVA coating. Reprinted with permission from ref.



**Table 1.** CZE and capillary coatings

Analyte	Coating	Capillary	BGE	Voltage	Detection	Notes	Ref.
Therapeutic albumin	Semi-permanent coating with PEO	57 (50) cm, 50 $\mu$ m id	50 mM HEPES, pH 7.5, 0.5 mM SDS	- 25 kV	UV 214 nm	Separation of human serum albumin isoforms	[6]
In-house IgG1 mAbs	Bare fused silica	30.2 (20) cm, 50 $\mu$ m id	20 mM NaAc, 0.3% PEO, 2 mM triethylenetetraamine, pH 6.0	+ 30 kV	UV 214 nm	Rapid method to determine mAb charge variance	[7]
Oxytocin	Bare fused silica	50 (40) cm, 50 $\mu$ m id	50 mM sodium phosphate pH 6.0, 12.5 mM SBE $\beta$ -CD, 10% v/v MeOH,	+ 22 kV	UV 214 nm	Separation of all oxytocin desamino products	[8]
Cytochrome c, lysozyme, ribonuclease A, and $\alpha$ -chymotrypsinogen A	Static coating with ionic liquid [NMP] <sup>+</sup> CH <sub>3</sub> SO <sub>3</sub> <sup>-</sup>	50 (41.5) cm, 75 $\mu$ m id	40 mM sodium phosphate, pH 4.0, 0.3% w/v ionic liquid	+ 15 kV	UV 214 nm	Minimize protein adsorption	[18]
(1,2) Chymotrypsinogen, ribonuclease A, cytochrome c, trypsin inhibitor, lysozyme	(1) QC (2) HMQC	47 (40) cm, 75 $\mu$ m id	25 mM sodium phosphate over a range of pH 3.0-8.0	+ 12 and - 12 kV	UV 214 nm	The hydrophobic QC provided a more effective for coating	QC [22] HMQC [23]
Purchased mAbs	Various commercial and in-house coatings	64.5 (56) cm, 50 $\mu$ m id	Various BGE composition, pH, and additives	+ 30 and - 30 kV	UV 200 nm	Comparison of static capillary coatings	[26]
Enhanced green fluorescent protein and R-phycoerythrin	Polymerize phospholipid bilayer	42 (32) cm, various $\mu$ m id	Various BGEs over a range of pH 4.0-9.3	+ 24 kV	LIF	Best coating stability in capillaries with id of $\leq$ 50 $\mu$ m	[28]
(1,2) Lysozyme, cytochrome c, BSA	(1) PVA or (2) PEG and diazoresin	50 (41) cm, 75 $\mu$ m id	40 mM sodium phosphate over a range of pH 3.0-9.0	+ 15-18 kV	UV 214 nm	Easy to form covalently bonded capillary coatings	PVA [29] PEG [30]
<p>Capillary: actual length (effective length), inner diameter            Bovine serum albumin (BSA), Hydrophobically modified QC (HMQC), N-methyl-2-pyrrolidonium methyl sulfonate IL ([NMP]<sup>+</sup>CH<sub>3</sub>SO<sub>3</sub><sup>-</sup>), Polyethylene glycol (PEG), Polyethylene oxide (PEO), Polyvinyl alcohol (PVA), Quaternized celluloses (QC), Sulfobutyl ether <math>\beta</math>-cyclodextrin (SBE <math>\beta</math>-CD)</p>							

### 2.2.2 Capillary gel electrophoresis

The most commonly used analytical method for size determination, purity assessment, and quality control of therapeutic recombinant proteins is sodium dodecyl sulfate polyacrylamide gel electrophoresis (SDS-PAGE). SDS is used to coat the proteins, resulting in a uniform negative charge proportional to their size. Under an electric field the proteins are then separated through a sieving gel matrix, allowing estimation of protein molecular weight (MW). However, conventional SDS-PAGE can be time-consuming and tedious and yield irreproducible results with limited quantitative abilities [35].

To improve on this important technique, the CGE equivalent, SDS-CGE, has been developed and utilized for the determination of size heterogeneity of therapeutic proteins [36-38] (Table 2). Here the sieving gel is placed inside the capillary through which the negatively charged SDS-coated proteins are separated. SDS-CGE has many advantages over SDS-PAGE, including high efficiency separations, more accurate MW and concentration determination, and the ability to automate the process for high-throughput analysis.

Shi *et al.* demonstrated these advantages of SDS-CGE over SDS-PAGE, along with the improved precision of migration time and peak area, for the analysis of the light chain, nonglycosylated heavy chain, and heavy chain fragments of a mAb [39]. Using the capillary format, the authors were able to achieve RSDs of less than 0.5% for migration time and less than 5% for corrected peak area. However, for quality control of biopharmaceuticals, the precision for a quantitative assay needs to be lower than 2% RSD. By switching to hydrodynamic rather than electrokinetic injection, along with increased sample concentration, the precision of a standard SDS-CGE assay was improved to 0.2% RSD for migration time and between 1 and 2% RSD for peak area ratio [40].

Another method to improve assay precision for the SDS-CGE assay is through automation of the sample preparation process. A large number of samples are generated during the development of high-quality biologics. These samples originate from every step of the development process and are presented for analysis in a variety of matrices. The use of an automatic robotic platform for sample preparation can

help mitigate user error introduced in the multi-step sample preparation process. The PhyNexus Micro-Extractor Automated Instrument uses a ProA resin column to bind mAb samples prior to separation. Once bound, the instrument performs sample concentration normalization, removal of contaminants, desalting, and mixing with appropriate SDS-CGE buffers. With this method, protein recovery of Fc-fusion proteins, and IgG1 and IgG2 mAbs was increased to 90% [41].

UV absorbance and LIF spectroscopy are the dominant detection methods for SDS-CGE. However, for detection of specific mAbs, Western blot immunoassay detection has also been utilized. The ProteinSimple Simple Western™ (or Simon™) automates the immunoassay detection procedure by performing all separation steps and washes in-capillary. Following a SDS-CGE separation, the proteins are photochemically cross-linked to the capillary wall, where they are exposed to a horseradish peroxidase-conjugated secondary antibody for whole-capillary chemiluminescence imaging (Fig. 3). Simon™ also makes quantitative Western blots possible. Using this instrument, a standard curve was generated for a vaccine candidate protein with linearity from 0.45–7 µg/mL and R<sup>2</sup> values of 0.990 or greater for five experiments [42].

Spectroscopic detection using immunoassay methods for CGE are useful because coupling CGE with MS by electrospray ionization (ESI) is difficult due to the presence of nonvolatile BGE. However, SDS-CGE has been coupled successfully to matrix-assisted laser desorption ionization (MALDI) MS by moving a poly(tetrafluoroethylene) membrane past the end of the capillary to collect the peaks as they leave the capillary [43]. CGE-MALDI-MS has been utilized for the direct mass measurement of recombinant proteins [44, 45] and neoglycoproteins [46].

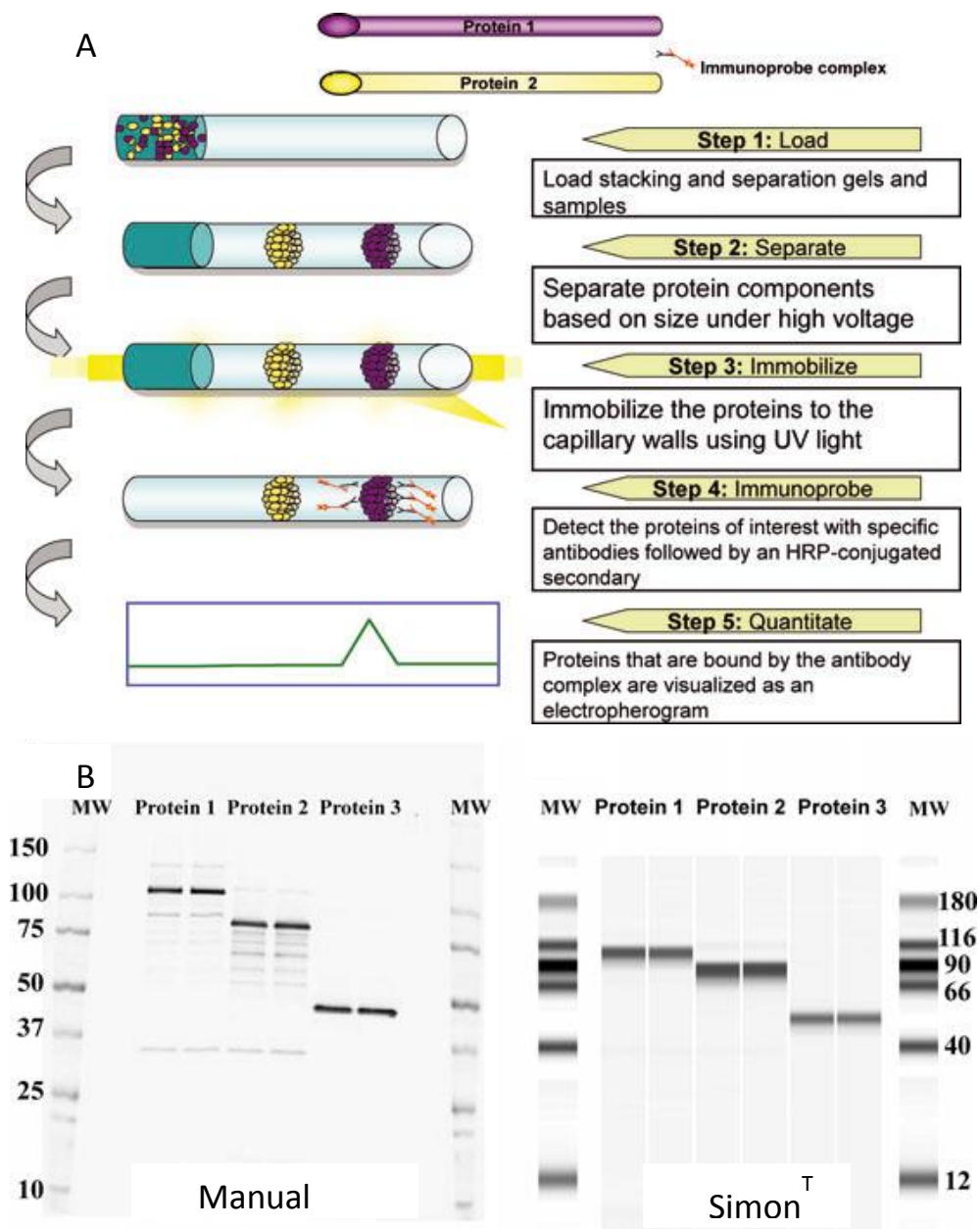


**Fig. 3.** A) Step-by-step overview of the Simon<sup>TM</sup> operational procedure. B) Comparison between the manual Western blot and Simon<sup>TM</sup> for duplicate runs of three proteins. Reprinted with permission from ref. 42

**Table 2. CGE and MGE**

Analyte	Mode	Gel	Capillary	Voltage	Detection	Notes	Ref.
In-house IgG2 $\lambda$ , IgG2k, and IgG1k mAbs	Nonreducing	Beckman Coulter SDS-MW gel buffer	30 (20) cm, 50 $\mu$ m id	15 kV	UV 220 nm	Monitor disulfide reduction during production	[36]
In-house IgG1 mAbs	Reducing and nonreducing	Agilent High Sensitivity Protein 250 Kit	Agilent 2100 Bioanalyzer	NR	LIF	Characterization of size variants	[37]
In-house IgG1 and IgG4 mAbs	Reducing and nonreducing	Beckman Coulter SDS-MW gel buffer	31.2 (20) cm, 50 $\mu$ m id	-15 kV	LIF ex. 488 nm / em. 600 nm	Impurity analysis	[38]
IgG 1 mAb	Reducing	Beckman Coulter SDS-MW gel buffer	30.2 (20) cm, 50 $\mu$ m id	-15kV	PDA	Comparison of SDS-CGE to SDS-PAGE	[39]
Myoglobin, carbonic anhydrase I, ovalbumin, BSA	Nonreducing	Beckman Coulter SDS-MW gel buffer	33 (24.5) cm, 50 $\mu$ m id	-16.5 kV	220 nm	Demonstration of improved precision	[40]
In-house Fc-fusion proteins, and IgG1 and IgG2 mAbs	Reducing and nonreducing	Beckman Coulter SDS-MW gel buffer	30 (20) cm, 50 $\mu$ m id	15 kV	220 nm	Automated sample preparation	[41]
In-house vaccine proteins	Reducing	ProteinSimple separation matrix	12-capillary cartridge; 5 cm, 100 $\mu$ m id	250 V	Chemiluminescence from secondary antibody	Automated separation and Western blot	[42]
Ricin A-chain immunotoxins	Reducing and nonreducing	Bio-Rad CE-SDS run buffer	24 (19.5) cm, 50 $\mu$ m id	5 or 15 kV	UV 220 nm and MALDI-TOF-MS	CGE-MALDI-TOF-MS of ricin proteins	[45]
In-house mAbs and proteins	MGE Reducing and nonreducing	HT Protein Express gel matrix	LabChip GXII	NR	Indirect and direct LIF ex. 620 nm / em. 700 nm	MGE methods for high-resolution and high-sensitivity	[138]
Actin, carbonic anhydrase II, and, lysozyme	MGE Nonreducing	Beckman Coulter SDS-MW gel buffer	2 cm glass microchip	480 kV	Western blot	MGE separation with off-chip Western blot detection	[140]

Capillary: actual length (effective length), inner diameter  
Bovine serum albumin (BSA), Not reported (NR)

### 2.2.3 Capillary isoelectric focusing

Another capillary-based technique that was adapted from its original slab-gel format is capillary isoelectric focusing (CIEF). Like SDS-CGE, performing IEF in a capillary exhibits the benefits of faster analysis times, higher resolutions (up to 0.005 pH units [47]), lower limits of detection, and the capacity for high-throughput analysis [48].

CIEF separates proteins based on their isoelectric point (pI) and can be used to determine charge heterogeneity of biogenic products [49]. The assay is typically performed in a coated capillary to eliminate EOF. A pH gradient is self-assembled under an electric field using a mixture of mobile carrier ampholytes with a distribution of pIs. The anodic end of the capillary is then placed in an acidic solution and the cathodic end in a basic solution. Under the applied electric field, the protein will migrate through the ampholyte solution toward the oppositely charged electrode until the pH environment equals its pI.

UV detection at 280 nm is typically used with CIEF because the ampholytes exhibit strong absorbance at wavelengths below 240 nm [50]. Optical detection for CIEF can be accomplished either by a two-step method that requires mobilization after focusing to bring the analyte bands past a small detection window or using whole-capillary imaging CIEF (iCIEF) within a transparent capillary.

An important application of CIEF for the analysis of biologics is for the characterization of charge heterogeneity, as it is possible to identify proteins based on their unique charge profile [51]. Variations in this charge profile are often used to determine protein stability [52, 53] and identify degradation products and PTMs that change the charge of the protein, such as glycosylation and deamidation [54] (Table 3).

As mentioned earlier, deamidation can be a major pathway of protein and peptide degradation. The rate of deamidation depends on both the primary and secondary structure surrounding the Asn or Gln residue in question [1]. Typically, characterization of deamidation sites is accomplished through peptide mapping and MS analysis. However, this process can be complicated, sometimes impossible, when a fragment contains multiple desamino sites. Shimura *et al.* used CIEF and site-directed mutagenesis to

determine the rates of deamidation in Fab fragments of mouse IgG1- $\kappa$  [54]. The rate of disappearance of the parent peak of each mutant was compared to that of the wild type to obtain the single-residue deamidation rates. By monitoring the CIEF charge profile of the six Fab mutants for the additional acidic peaks, a third, previously unknown, deamidation hotspot for the mouse IgG1- $\kappa$  was identified.

CIEF can be even more powerful when run in combination with an orthogonal separation technique such as SDS-CGE [55] or reversed-phase LC, or in tandem with MS. CIEF has been coupled to MS through both ESI [56, 57] and MALDI interfaces [58, 59]. Due to the presence of the non-volatile ampholytes in the separation buffer, coupling CIEF with ESI can be complicated by ion-suppression and source contamination. To cut down on the intensive sample preparation needed to desalt protein samples from gels, a segmented capillary has been described. In this design, seven segments of PEEK capillary were connected by Nafion joints, each with its own buffer reservoir (Fig. 4) [60]. This allowed analytes in the capillary segments to be selectively mobilized after focusing, creating an online fractionator prior to additional analysis by LC, CE, or MS.

Additional technological advances in CIEF-MS interface development have been reported by Zhong *et al.* [61] and Wang *et al.* [62]. Their work is discussed further in the MS detection section of this chapter. Along with the development of new interfaces, several straightforward BGE buffer modifications have been described in the literature to solve the problems of high backgrounds and ion suppression [63, 64].

As with SDS-CGE, detection of proteins by immunoassay following separation by CIEF can be used to improve detection limits and specificity without the need for MS. For example, Michels *et al.* have described the first multiplexed iCIEF immunoassay for investigation of the charge heterogeneity of mAbs [65]. Once the mAbs were focused, they were then photochemically immobilized to the capillary wall where they were then exposed to a secondary antibody, conjugated with horseradish peroxidase, and detected by chemiluminescence (Fig. 5). The resulting LOD of this assay was 6 ng/mL, which was a 1000-fold increase over UV detection.

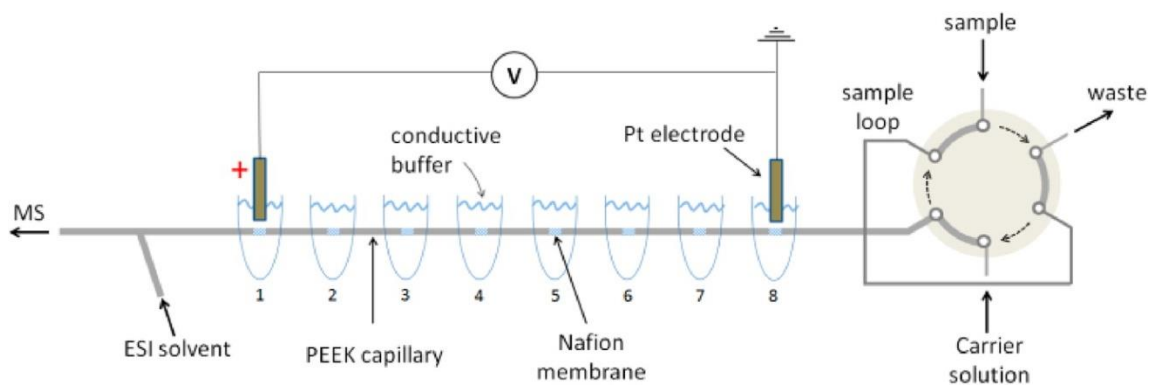


**Fig. 4.** Schematic layout of the on-line multiple junction CIEF setup; the six-port injector is shown in the sample-loop loading position. Reprinted with permission from ref. 60



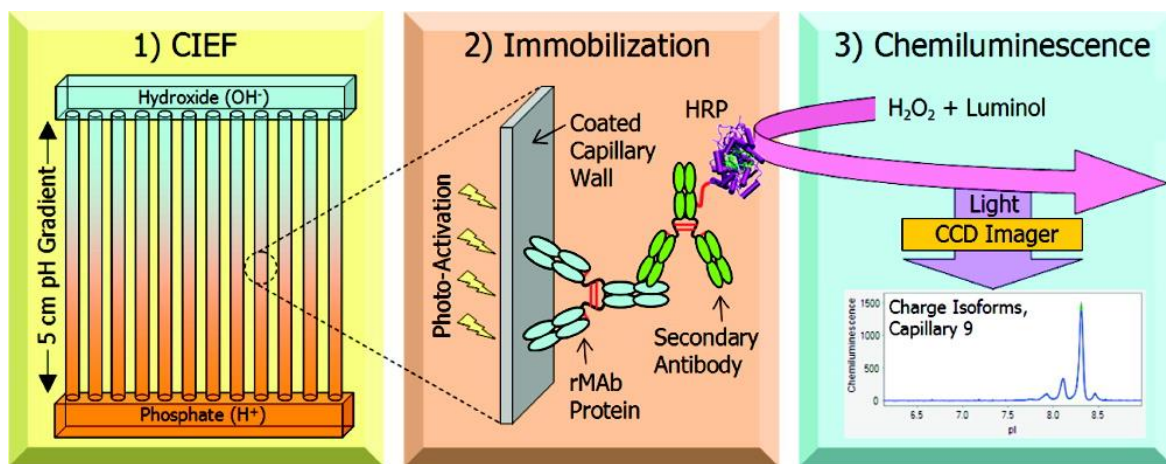


**Fig. 5.** Schematic of the Nanopro three-step process . 1) Separation by CIEF, 2) immobilization of the antibody to the capillary wall, 3) detection with secondary antibody by chemiluminescence. Reprinted with permission from ref. 65

**Table 3.** CIEF and microchip IEF (mIEF)

Analyte	Mode	Capillary coating	Capillary	Detector	Ampholyte	Catholyte	Analyte	Notes	Ref
In-house EPO, Fc-fusion protein, and IgG mAb	iCIEF	Fluorocarbon (ProteinSimple)	iCE280 Analyzer; 50 mm, 100 µm id	UV 280 nm	Pharmalyte pH 3-10, 4-6.5, 5-8, and 8-10.5	0.1 M NaOH in 0.1% MC	0.08 M phosphoric acid in 0.1% MC	Wide range of therapeutic protein applications	[51]
In-house noninfectious virus-like particles	iCIEF	Fluorocarbon (ProteinSimple)	iCE280 Analyzer; 50 mm, 100 µm id	UV 280 nm	Pharmalyte pH 2.5-5 and 3-10	0.1 M NaOH in 0.1% MC	0.08 M phosphoric acid in 0.1% MC	Charge characterization of virus-like particles	[52]
In-house vaccine carrier protein	iCIEF	Fluorocarbon (ProteinSimple)	iCE280 Analyzer; 50 mm, 100 µm id	UV 280 nm	Pharmalyte pH 3-10 and 4-6.5	0.1 M NaOH in 0.1% MC	0.08 M phosphoric acid in 0.1% MC	Characterization of polysaccharide vaccine carrier protein	[53]
In-house IgG2k mAb	CIEF	PDMA	180 mm, 50 µm id	LIF ex. 543.5 nm / em. 590 nm	Pharmalyte pH 3-10, 0.001% BSA	20 mM NaOH	20 mM phosphoric acid	Determination of deamidation rates in mAb	[54]
Trypsinogen, β-lactoglobulin, BSA, and ovalbumin	CIEF	4% acrylamide 0.6% cross-linker	Various capillary lengths and id	LIF ex. 488 nm	BioRad pH 3-10	20 mM NaOH	10 mM phosphoric acid	Microchip interface for 2D CIEF and CGE separations	[55]
β-lactoglobulin A, hemoglobin A, myoglobin, α-chymotrypsinogen A, ribonuclease A, cytochrome c, lysozyme	CIEF		Seven PEEK tubing segments, 1.55 cm, 395 µm id connected by Nafion membrane 0.2 cm, 330 µm id	TOF and Orbitrap	Various MS-compatible carrier ampholytes	Various electrolytes at each Nafion junction modified the local pH of the carrier ampholyte		Segmented capillary for selective mobilization	[60]
Insulin receptor and protein tryptic digests	CIEF	LPA	50 cm, 50 µm id	Sheath flow ESI-Orbitrap-MS	Glutamate, asparagine, glycine, proline, histidine, and lysine	0.1% Formic acid, pH 2.5	0.3% ammonium hydroxide, pH 11	Amino acids used as low MW ampholyte	[64]
In-house IgG mAb	iCIEF	Proprietary photoreactive layer	12-channel cartridge; 50 mm, 100 µm id	Chemiluminescence from secondary antibody	Pharmalyte pH 5-8 (30%) and pH 8-10.5 (70%)	0.1 M NaOH in 0.1% MC	0.08 M phosphoric acid in 0.1% MC	CIEF with immunoassay detection	[65]
Donated mAb products	imIEF	Uncoated quartz	MCE-2010 system, 2.7 cm	UV 280 nm	Protein imple pH 3-10, 5-8, and 8-10.5	300 mM NaOH, 0.4% HPMC	200 mM phosphoric acid, 0.4% HPMC	mIEF of mAb charge variants	[141]
Model Proteins	iMIEF		100 µm id	Immunoblot	Polyprotic carboxylic amino acids	20 mM lysine	20 mM arginine	Integrated microchip for separation and immunoblot	[142]

Capillary: actual length, inner diameter  
 Bovine serum albumin (BSA); Linear polyacrylamide (LPA); Methylcellulose (MC); Polydimethylacrylamide (PDMA); Polyvinyl alcohol (PVA);

#### 2.2.4 Capillary electrochromatography

Capillary electrochromatography (CEC) is a technique that uses both chromatographic retention and electrophoretic migration for the separation of analytes, with bulk fluid flow created by the EOF. This combination enhances the selectivity and efficiency of the separation, drastically lowers the reagent use compared to LC, and enables the separation of neutral species not possible with CZE.

In the first applications of CEC to proteins, capillaries packed with porous particles were utilized because of their similarity to the stationary phase materials used for conventional LC and the commercial availability of particles with a variety of functionalities. However, the packed CEC columns have significant limitations in terms of stability and fabrication reproducibility and are not yet able to match the robust performance of nano-LC [66]. This limits their usefulness for routine protein assays on a larger industrial scale. In its place, the use of nanoparticles (NP) as a pseudostationary phase (PSP), open-tubular CEC (OTCEC), and monolithic columns have gained momentum.

The use of NP as a PSP for CEC has been thoroughly reviewed [67]. In the BGE, the NP can interact with the proteins during the separation, changing their electrophoretic mobility and generating a separation based on the difference in affinity between the analytes for the NP. A wide range of materials have been investigated for PSP-CEC, including polymer NP, carbon nanotubes, gold NP, and silica NP (SNP) [67]. To improve the stability and functionality of SNP, Gao *et al.* synthesized polyamidoamine-grafted SNP (PAMAM-SNP) and utilized them for a separation of basic and acidic proteins [68] (Fig. 6). With 0.01% PAMAM-SNP in the BGE, a complete separation of all four model proteins (Table 4) was possible. Additionally, the PAMAM-SNP were able to effectively reduce the adsorption of basic proteins to the capillary wall.

OTCEC columns are a popular alternative to packed columns because of their ease of fabrication and excellent separation efficiency [69]. These OTCEC columns can be made by either physically bonding the stationary phase to the capillary wall or several layered coatings. In one report, OTCEC columns were fabricated through the immobilization of gold NP (AuNP) on the surface of the capillary that had been

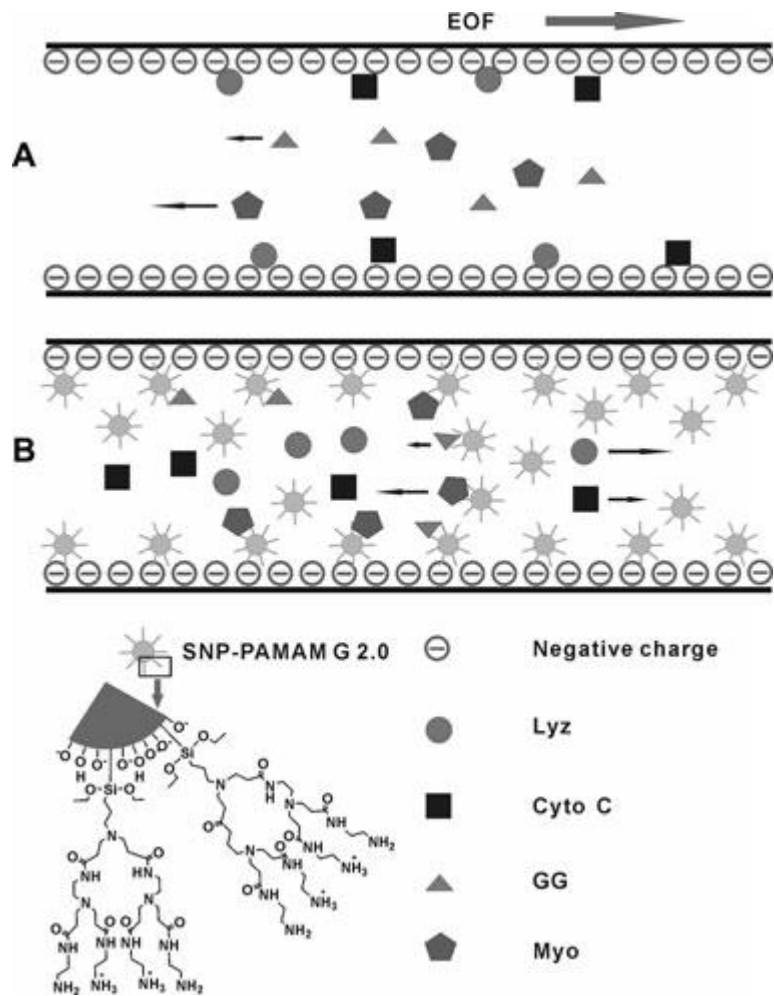


**Fig. 6.** A) Diagram of the separation of four proteins without and B) with the pseudostationary phase effect of the polyamidoamine (PAMAM)-grafted silica nanoparticles (SNP). Reprinted with permission from ref. 68

pretreated with a sol-gel. The gold immobilized in the sol-gel participates in noncovalent interactions with thiol and amino groups of proteins, increasing their capacity factor. Using this technique, Miksik *et al.* were able to separate the peptides generated by the tryptic digestion of native and glycosylated bovine serum albumin (BSA) and human transferrin [70]. Unfortunately, preparation of the AuNP-modified columns required several days and many reaction steps, which limited its utility. To alleviate this problem, a new method for AuNP immobilization to the capillary wall through covalent binding using (3-aminopropyl)triethoxysilane has been described [71]. This procedure creates a stable coating that could be reused over 900 times with migration time RSDs less than 1.7% for model proteins (Table 4).

Another novel OTCEC column was described by Qu *et al.* and was produced by immobilizing graphene (G) and graphene oxide (GO) sheets to the capillary wall to act as the stationary phase. It was found that between the two coatings, only the GO exhibited a reproducible EOF over the pH range of 3–9 and separated a mixture of egg white proteins [72]. The separation was achieved due to the reverse-phase-like interaction between the GO coated surface and the proteins. To improve the stacking of GO at the capillary wall, a layer-by-layer technique to produce the GO-modified OTCEC column was reported. In this case, GO nanosheets were adsorbed on a poly(diallyldimethylammonium chloride)-treated capillary by electrostatic interaction. This created a stable coating for over 200 runs [73]. Both methods for column fabrication produced excellent run-to-run, day-to-day, and column-to-column reproducibility with less than 3% RSD for the EOF.

Often, OTCEC separations suffer from low capacity factors because of the small active surface area and fewer available functional sites. This also can lead to poor separation efficiency and co-eluting peaks. In an attempt to improve peak capacity, a new porous layer for OTCEC has been described that uses the in situ polymerization of a mixture of monomers in the presence of porogen for higher separation efficiencies [74]. A column generated from the porogen, 1-propanol, was able to generate a high abundance of micropores and mesopores, resulting in a large specific surface area. This generated an efficient separation of the two model proteins, BSA and cytochrome-*c*.

Another widely explored approach for the implementation of CEC is the use of monolithic columns. Monoliths have high permeability, a fast mass transfer rate, and high loading capacity. Many commercially available monoliths are made from silica, leading to a risk of band broadening and sample loss due to protein adsorption. Therefore, to minimize protein adsorption during CEC and improve separation efficiencies, neutral and cationic monoliths have been developed.

A series of neutral nonpolar monolithic columns were manufactured and tested for the separation of both intact proteins and peptides from protein tryptic digest. To produce the monoliths, various ratios of monomers C8-methacrylate, C12-methacrylate, and C16-methacrylate were mixed with the crosslinking polymer pentaerythritol (PETA) [75]. In these experiments, it was determined that when the ratio of monomer to PETA was kept constant, the C8 monolith gave the best separations for intact proteins. The C16 column exhibited the best efficiencies for smaller peptides. In their report, Puangpila *et al.* claim that, even in the absence of a charged surface, there is EOF generated by adsorption of BGE ions to the monolith, and it can be controlled by changes in the pH and ACN content of the mobile phase.

Cationic monolithic columns can also be used to reduce electrostatic interaction of basic proteins to the monolithic and capillary surface. Wang *et al.* developed a novel monolithic IL column that was made by a simple “one pot” approach using thermal free radical copolymerization [76]. Using this method, several counterions (bromide, tetrafluoroborate, hexafluorophosphate, and bis-trifluoromethanesulfonylimide ( $\text{NTf}_2^-$ )) were tested with the cation 1-vinyl-3-octylimidazolium ( $\text{ViOcIm}^+$ ) to create an IL monolith capillary columns [77]. Each IL monolith was capable of generating a consistent reverse EOF over the pH range 2.9–12.0. However, only the  $\text{ViOcIm}^+\text{NTf}_2^-$  was able to achieve baseline resolution for all proteins in a standard mix (Table 4).

**Table 4.** CEC

Analyte	Column type	Column material	Capillary	BGE	Voltage	Detection	Notes	Ref.
Cytochrome c, myoglobin, gamma globulin, and lysozyme	Pseudostationary phase	Polyamidoamine-grafted SNP	48 (38) cm, 75 $\mu$ m id	12.5 mM tetraborate/ phosphate, pH 9.1, 0.01% SNP	+ 15 kV	UV 214 nm	Improved SNP stability	[68]
Tryptic digests of BSA and human transferrin	Open-tubular	Bare AuNP on sol-gel modified surface	47 (40) cm, 50 $\mu$ m id	100 mM sodium phosphate, pH 2.5	+ 10 kV	UV 214 nm	AuNP OT column for tryptic digests of native and glycosylated proteins	[70]
Bradykinin, LHRH, oxytocin, angiotensin I, met-enkephalin, and HSA tryptic digest	Open-tubular	AuNP on (3-aminopropyl) triethoxysilane modified surface	41.2 (31) cm, 75 $\mu$ m id	20 mM potassium phosphate, pH 8.0	+ 12 kV	UV 214 nm	New preparation of AuNP OT column with improved stability	[71]
Egg white proteins	Open-tubular	Graphene oxide and graphene	60 (50) cm, 75 $\mu$ m id	5 mM sodium phosphate, pH 7.0	+ 20 kV	UV 214 nm	Separation was only possible with the GO column	[72]
Egg white proteins	Open-tubular	Ionic adsorption of GO to surface modified with PDDA	60 (50) cm, 75 $\mu$ m id	5mM sodium phosphate, pH 7.5	+ 20 kV	UV 214 nm	Improved assembly and stability of GO OT columns	[73]
Cytochrome c and BSA	Open-tubular	Mixture of four monomers in the presence of 1-propanol as sole porogen	35 (25) cm, 75 $\mu$ m id	5 mM sodium borate, 45% ACN, pH 9.04 and 10 mM Tris-HCl, 0.4% PVP, pH 8.86	- 10 kV	UV 214 nm	Improve retention of proteins in OTCEC	[74]
Many model proteins and tryptic digests of cytochrome c	Monolith	C-8, -12, and -16 methacrylate with pentaerythritol triacrylate	27 (20) cm, 100 $\mu$ m id	1-10 mM sodium phosphate, ACN, pH 7.0	+ 15 kV	UV 214 nm	Neutral monoliths to reduce adsorption	[75]
Cytochrome c, equine myoglobin, lysozyme, and BSA	Monolith	Cationic ionic liquid ViOclm <sup>+</sup> with various anions: Br <sup>-</sup> , BF <sub>4</sub> <sup>-</sup> , PF <sub>6</sub> <sup>-</sup> , and NTf <sub>2</sub> <sup>-</sup>	32 (20) cm, 100 $\mu$ m id	20% ACN, 30 mM sodium phosphate/citric acid buffer, pH 2.5-4.0	- 10 kV	UV 210 nm	Only the anion NTf <sub>2</sub> <sup>-</sup> was able to achieve separation of proteins	[77]

Capillary: Actual length (effective length), inner diameter  
1-vinyl-3-octylimidazolium (ViOclm<sup>+</sup>), Bovine serum albumin (BSA), Gold nanoparticles (AuNP), Graphene oxide (GO), Human serum albumin (HSA), Ionic liquid anions (bromide, Br<sup>-</sup>; tetrafluoroborate, BF<sub>4</sub><sup>-</sup>; hexafluorophosphate, PF<sub>6</sub><sup>-</sup>; and bis-trifluoromethanesulfonylimide, NTf<sub>2</sub><sup>-</sup>) Open-tubular (OT), Luteinizing-hormone-releasing hormone (LHRH), Poly(diallyldimethylammonium chloride) (PDDA), Polyvinylpyrrolidone (PVP), Silica nanoparticles (SNP)

## 2.3 Detection methods

### 2.3.1 Spectroscopic detection

Spectroscopy is the most common detection method for proteins and peptides separated by CE. UV absorbance tends to be favored over fluorescence spectroscopy due to a natural absorbance of the amide bonds and aromatic residues in the near UV (214 and 280 nm). However, this approach suffers from poor limits of detection due to the micrometer pathlengths characteristic of CE and high background from the UV source. Additionally, BGE composition, pH, and ionic strength can have a significant effect on background. Approaches such as increasing the pathlength through modification of the detection window using Z-shaped capillaries and bubble-cells have been successful in decreasing the LOD by an order of magnitude or greater [78, 79].

Fluorescence detection of proteins can be accomplished based on the native fluorescence of tryptophan, phenylalanine, and tyrosine residues in proteins using a deep UV light source [80-82]. However, with native fluorescence based detection, the signal is dependent on the number of excitable residues as well as their accessibility within the tertiary structure of the protein. Therefore, the applicability of this technique varies from protein to protein. To improve the LODs for native fluorescence detection of erythropoietin (EPO), Wang *et al.* utilized a magnetic bead-based extraction system for pre-concentration. Using this procedure, it was possible to obtain an LOD of 10 nM, two orders of magnitude lower than what was possible with UV absorbance at 214 nm [83].

Low limits of detection achievable by LIF can also be obtained through derivatization of the protein or peptide of interest with a fluorophore [84]. The most common derivatization sites for proteins are the primary amines and cysteine residues. These can be tagged with a variety of agents including Alexa Fluor-based dyes, naphthalene-2,3-dicarboxaldehyde, fluorescein isothiocyanate, and many others. A major disadvantage of pre-separation derivatization for proteins is the complexity of the derivatization process. This approach requires not only that the tag is specific for the functional group on the analyte of interest but also that it does not interfere with the separation by introducing additional fluorescent by-



products. Proteins typically have several reactive sites that can be labeled, which leads to multiple peaks for one analyte, complicating data analysis [85].

### 2.3.2 Mass spectrometry

CE-MS is a powerful combination of high efficiency separation with selective and sensitive detection. This technique can provide important information on identity, glycoforms, degradation, and impurities of protein therapeutics [86, 87]. It is possible to couple CE to MS using different ionization techniques, as has been described in several excellent reviews [88, 89]. For this chapter, only the recent advances regarding the development and application of the ESI interfaces will be highlighted. CE was first interfaced with MS by ESI in 1987 [90] and it remains the most popular ionization method due to its broad applicability and commercialization.

ESI is a robust soft-ionization technique that produces multiply charged ions for proteins in the gas phase. However, there are many considerations that must be taken into account when coupling it with CE. Primarily, the use of run buffers containing non-volatile salts and additives can lead to their deposition within the instrument, and subsequent contamination of the source. While formic acid and acetate buffers have been used as BGEs for the separation of proteins by CE, they are not always ideal because of inadequate resolution and possible protein instability at low pH. Additionally, the voltages typically applied to the capillary for separation are 2–3 orders of magnitude higher than what is used for ESI. Toward this end, researchers have developed three general approaches for coupling CE to MS with ESI: sheath-liquid, sheathless, or junction-at-the-tip interfaces.

The most widely used and commercially available option is the sheath-liquid interface. This is accomplished by placing the outlet of the CE capillary coaxially within a tube. The tube delivers a MS-compatible sheath liquid (Fig. 7A) that provides easy electrical connections and a flow rate to the ESI of  $\mu\text{L}/\text{min}$ . This is beneficial because the EOF of the CE is generally much slower ( $\text{nL}/\text{min}$ ) than what is compatible for a stable spray.

The compatibility of separation and detection parameters for CE-ESI-MS with a sheath-liquid interface was evaluated for eight model proteins and several EPO isoforms [91]. It was found that the BGE composition and capillary coating play the largest role in the quality of the separation. For all analytes the best signal was obtained with a sheath flow rate between 2-5  $\mu\text{L}/\text{min}$  and a sheath flow liquid composed of 1% acetic acid in 1:1 organic:water; in this study, 2-propanol was chosen over MeOH or ACN. The optimal gas pressure was determined to be 0.2 bar, since anything lower lead to a loss of analyte intensity and anything higher was shown to affect the resolution of the separation. As an added benefit, the nebulizer gas pressure can create suction at the capillary outlet, increasing the CE flow rate for separations performed in neutral capillaries (Table 5).

An obvious disadvantage of the sheath-liquid interface is the loss in detector sensitivity from dilution of the eluting peaks. To improve detection limits, a sheathless interface was developed. The largest downside of this approach is the difficulty in properly completing the electrical circuits for the CE and the ESI. While many attempts have been made, these interfaces were limited by stability and ease of application [89, 92].

Recently, Moini and Whitt developed a sheathless interface based on a porous junction [93, 94]. In this interface, the end of the capillary was made porous to small ions by drilling a well into the polyamide coating and etching the remaining material with hydrofluoric acid. The capillary was then placed within an existing ESI needle filled with BGE, allowing electrical connection to both the CE and ESI (Fig. 7B). The tip of the capillary could then be used for electrospray when voltage is applied. The only drawback to this technique was the difficulty in reproducibly etching the capillary end. To improve the applicability and availability of the Moini and Whitt sheathless interface, Beckman Coulter developed a prototype that has been successfully applied to the analysis of intact proteins [95], protein glycoforms [96], and protein tryptic digests [97, 98] (Table 5).

In a recent report, both CE- and LC-MS were compared for the analysis of a particular therapeutic mAb [98]. With LC-MS, 11 small peptides eluted in the void volume and could not be detected, including

two fragments that were critical for the identification of the binding domain of the mAb. The same digest was analyzed by CE-MS employing both a traditional sheath-liquid interface and the Beckman Coulter sheathless interface using a BGE consisting of 10% acetic acid at pH 2.3. Sixty of 61 peptides were detected with the sheath-liquid interface, while all 61 peptides were detected with the sheathless system with higher separation efficiencies and better sensitivity.

Another alternative to the sheath-liquid interface is the junction-at-the-tip design developed by Chen's group. In this interface, the capillary end is placed within a hollow needle that forms a "flow-through microvial" [99] (Fig. 7C). The hollow needle is filled with a chemical modifier that provides the necessary electrical contacts for the separation and ESI voltages. Similar to a sheath-liquid interface, this modifier increases the CE BGE compatibility with the ESI. However, because the flow rates are much lower ( $< 1 \mu\text{L}/\text{min}$ ), the dilution factor is not significant. Chen's group has extensively characterized the performance of this interface in several publications [100-102].

Perhaps the most exciting new use of these interfaces is in coupling MS to more complex CE modes, such as CIEF and capillary isotachopheresis (CITP) which require high concentrations of non-volatile components to achieve a separation. In 2011, Zhong *et al.* described a CIEF-MS approach for the analysis of several model peptides and proteins using the junction-at-the-tip interface with coated and uncoated capillaries [61]. Unfortunately, the ampholytes used for the separation were still able to reach the detector, leading to high backgrounds and ion suppression. To prevent this from occurring, a new sheathless interface was developed by Wang *et al.* that uses a large bore separation capillary for sample loading and a sheathless interface with a porous emitter for its application with CITP [62] (Fig. 7D). This system was then utilized for the analysis of test peptides spiked into tryptic digests of BSA (Table 5). They were able to obtain a linear range over 4.5 orders of magnitude and a five-fold sensitivity improvement compared to the sheath-liquid interface for two test peptides, kemptide and angiotensin II.

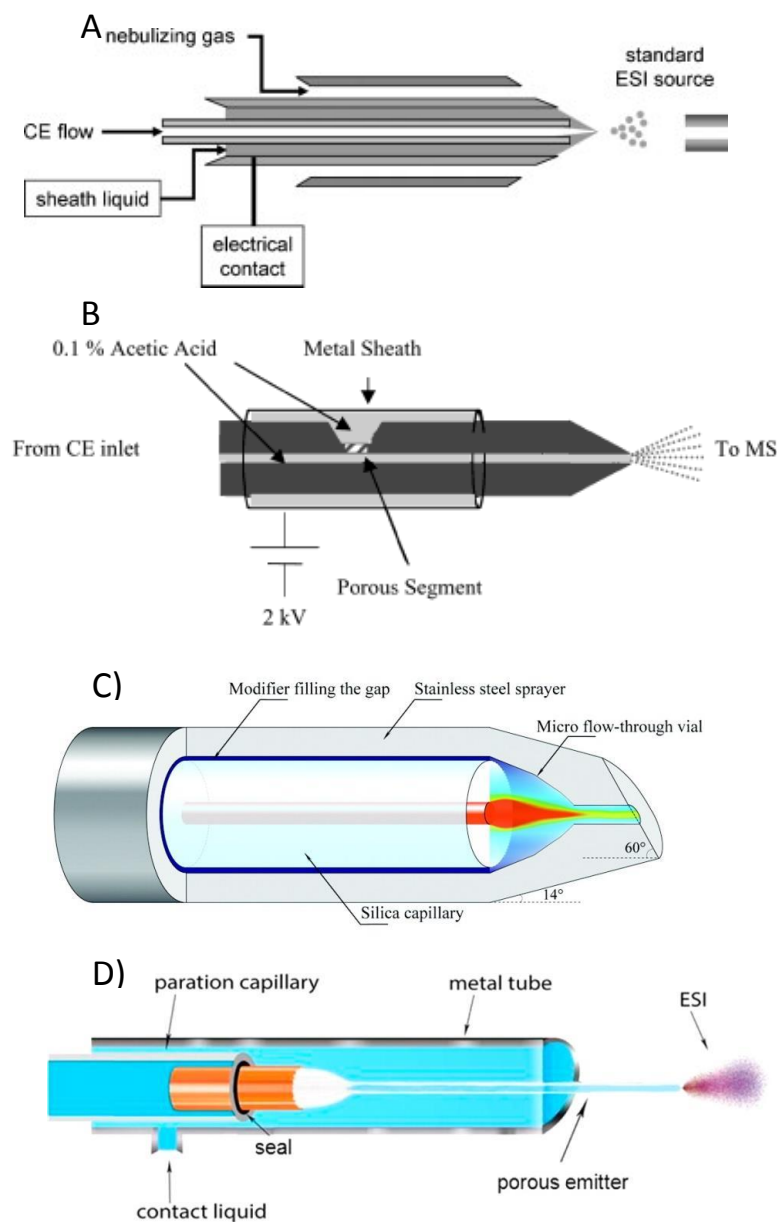


**Fig. 7.** Diagrams of four CE-ESI-MS interfaces. A) Sheath-flow, B) Moini and Whitt sheathless flow, C) Chen junction-at-the-tip, D) sheathless interface for CITP/CZE-nanoESI-MS. Reprinted/adapted with permission from ref. 89, 94, 102, 62, respectively

**Table 5. CE-MS and ME-MS**

Analyte	Mode	Interface	Sheath flow	BGE	Capillary coating	MS	Notes	Ref.
Lysozyme, $\beta$ -lactoglobulin A, cytochrome c, RNase A, myoglobin, RNase B, trypsin inhibitor, carbonic anhydrase, and EPO glycoforms	CZE	Agilent sheath-liquid	2-propanol /water (1:1), 1% acetic acid	0.5-2 M acetic acid	Various coating solutions and permanently coated capillaries	TOF	Comparison of coatings. Emphasis on intact protein analysis	[91]
EPO and interferon- $\beta$ glycoforms	CZE	Beckman Coulter sheathless		0.5 mM - 2.0 M acetic acid	Beckman Coulter neutral bilayer	TOF	Glycoprofiling of pharmaceutical products	[96]
Tryptic digest of Trastuzumab	CZE	Beckman Coulter sheathless		10% acetic acid	Bare fused silica	TOF	Rapid characterization of therapeutic mAbs	[97]
Tryptic digests of in-house mAbs	CZE	(1) Agilent sheath-liquid (2) Beckman Coulter sheathless	(1) 0.1% acetic acid	10% acetic acid	(1) PVA-coated and bare silica (2) Bare fused silica	TOF	Improving detection of small peptides from tryptic digests	[98]
Bradykinin, angiotensin I, neurotensin, fibrinopeptide, substance P, kemptide, leu-enkephalin, angiotensin II, melittin, and renin spiked in tryptic digests of BSA	CITP	In-house sheathless		0.1 M acetic acid (90%), MeOH (10%) LE: 25 mM ammonium acetate, pH 4	HPMC	TQ	Five fold sensitivity improvement from the sheath-liquid interface	[62]
Tryptic digest of in-house IgG2 mAb	LC-ME	Microchip		50% ACN, 0.1% formic acid	APTES	TOF	UPLC followed by MCE and on-chip ESI-MS interface	[146]

Capillary: Actual length (effective length), inner diameter  
Aminopropyltriethoxysilane (APTES), Bovine serum albumin (BSA), Capillary isotachopheresis (CITP), Hydroxypropyl cellulose (HPMC), Leading electrolyte (LE), Polyvinyl alcohol (PVA), Triple quadrupole (TQ)

## 2.4 Applications

In addition to assessing protein pharmaceutical products based on their size and charge heterogeneity and the presence of impurities, the analysis of biologics poses two additional analytical challenges: 1) how to characterize and better understand the complicated cellular process of glycosylation, and 2) preparing for the onset of biosimilar drugs to the market and how to best prove their similarity to the innovator product.

### 2.4.1 Glycosylation

Glycosylation is one of the most prevalent PTMs of therapeutic proteins. *In vivo*, glycosylation plays several important roles, including protection against degradation and non-specific interactions as well as orientation for the binding domain. The two major types of glycosylation that occur involve N-linked and O-linked carbohydrates. N-linked glycans are attached to the protein backbone at the amine side of Asn and are found in the well-defined amino acid sequence of Asn-X-Ser/Thr, where X is any amino acid but proline. O-linked glycans are not sequence-specific and are found attached to the protein backbone at the OH group of Ser or Thr.

Monoclonal antibody-based therapeutics of the IgG1 sub-type make up a 100 billion dollar annual market [103]. These mAbs consist of 2–3% carbohydrate by mass. Most of the glycosylation occurs as N-linked glycans located on the Asp<sup>297</sup> in the C<sub>H</sub>2 domain of the Fc region of each heavy chain. A number of factors can affect the composition, structure, and frequency of these glycans, posing an interesting challenge for the manufacturing of a homogeneous product. To ensure a homogeneous product and avoid potentially immunogenic glycans, each step of biotherapeutic production from clone selection to lot release needs to be well characterized. This characterization requires fast, high-throughput analytical methods to accurately screen the numerous samples generated per day.

The size and charge characterization of glycoproteins can be accomplished by the various electrophoretic separation techniques mentioned in the previous sections of this chapter. Several methods

and protocols for CZE, SDS-CGE, and CIEF separations of glycoproteins have been compiled by Rustandi *et al.* [104]. A typical downside to CE-based methods is the characteristic migration time irreproducibility. To address this, freely available software, glyXalign, was developed based on a set of rapid algorithms that enables automatic correction of distortions in CGE-LIF data to improve peak identification [105].

For further understanding of the nature, location, and composition of the glycans, methods for the removal and analysis of the sugars themselves are also needed. The majority of these carbohydrate analyses are performed by LC. In particular, hydrophilic interaction chromatography (HILIC) coupled to LIF and MS detection has been useful for the sensitive analysis of glycans [106].

CE-LIF is an excellent orthogonal technique to HILIC-LIF for separation of glycans, and in a comparative study it was shown that they were able to detect an equal number of glycans removed from an IgG [107]. An advantage of CE-LIF for glycan analysis is that it can be used to distinguish both lineage and positional isomers [108, 109]. Using CZE-LIF, carbohydrate sequencing can be performed by both top-down digestion and bottom-up identification using a series of sugar-specific exoglycosidases. Typically, glycans are enzymatically removed, fluorescently labeled, and separated by size or charge. There are several charged fluorescent reagents commercially available for tagging glycans. The most common reagent used in conjunction with CE-LIF is 8-aminopyrene-1,3,6-trisulfonic acid (APTS). However, recently, Kuo *et al.* published a rapid method for labeling aldoses with 2,3-naphthalenediamine to produce highly fluorescent naphthimidazole derivatives [110]. Using this reagent, it was possible to perform composition analysis and enantioseparation of the glycans using CE with cyclodextrin in the BGE.

An important advantage of CE-LIF over HILIC-LIF is the ability to multiplex 48- and 96-capillary arrays for high-throughput analysis. Callewaert *et al.* were the first to perform glycan analysis using a commercially available multiplexed CE-based DNA analyzer [111]. Later, this same technique was used along with a 48-capillary array to perform high-throughput analysis of glycans from IgG. In this

application, glycans were removed by digestion and labeled with APTS in 96-well plates and then subjected to simultaneous analysis by capillary array. This approach made it possible to run 3000 samples in a single day [112] (Table 6).

In the research and development of mAbs, a particular area of interest is the study of immunogenic non-human glycans. The frequency and type of non-human glycans attached to the therapeutic protein during production differ from cell line to cell line [113]. It is well known that the non-human oligosaccharides galactose- $\alpha$ -1,3-galactose ( $\alpha$ 1,3-Gal) and N-glycolylneuraminic acid (Neu5Gc) can illicit an immune response. In fact, in response to enteric bacteria, approximately 1% of all human antibodies are against the  $\alpha$ 1,3-Gal epitope [114].

Detection of both  $\alpha$ 1,3-Gal and Neu5Gc non-human glycans was performed by partial filling affinity CE. In this method, a plug of either anti-Neu5Gc antibody or  $\alpha$ -galactosidase (dissolved in BGE) was injected on capillary prior to injection of the APTS-labeled glycans (removed from the target antibody) [115]. Once the electric field was applied, the higher mobility sugars in the sample pass through the antibody or enzyme plug, causing a reaction. This reaction produced additional product peaks upon LIF detection, allowing specific detection and quantification of the two immunogenic sugars.

In another study, six commercially available mAb pharmaceuticals produced in nonhuman mammalian cell lines were analyzed by CZE-LIF, in parallel with LC-ESI-TOF-MS, to determine the presence of nonhuman N-glycans [116]. By CZE, forty-six fluorescently labeled N-glycans were separated using a tris-borate BGE containing 5% PEG to slow the EOF. Of the six mAb pharmaceuticals, three were found to contain nonhuman N-glycan residues. To obtain additional information regarding the attachment of nonhuman N-glycans to therapeutic proteins, CZE-LIF with exoglycosidase digestion and fluorescent tagging was used to achieve LODs of 1  $\mu$ g allowing characterization of the low-abundance  $\alpha$ 1,3-Gal epitope [117].

CE-MS can also be used in conjunction with CGE-LIF [118] to obtain additional structural information and identify unknown glycans [2]. For example, Bunz et al. described both alkaline and



acidic BGE systems that could be used for the determination of APTS-labeled mAb glycans by CE-TOF-MS [119, 120] (Table 6). The CE-MS methods were then compared against to two CGE-LIF methods commonly used for routine glycan analysis. While both CE-MS and CGE-LIF were able to resolve and detect the glycans, because of the difference in the separation mechanisms they had different migration orders, making it difficult to directly compare the two electropherograms obtained for a complex sample.

The downside of glycan analysis by MS is the likelihood of unwanted fragmentation of sugars during the ionization process. This can lead to large amounts of difficult-to-interpret data and misidentification [121]. For this reason, it is important not only to insure careful optimization during MS method development but to provide orthogonal analyses such as CZE-LIF or CGE-LIF to validate the findings.

**Table 6.** CE-based analysis of protein glycosylation

Analyte	Mode	Capillary	BGE	Detection	Label	Notes	Ref.
N-glycans of mAb1	CGE	48 capillary array, 50 cm each	Applied Biosystems Pop-7™	LIF ex. 473 nm / em. 520 nm	APTS	High-throughput glycan analysis	[112]
(1) Neu5Gc and (2) $\alpha$ 1,3-Gal containing N-glycans	Partial-filling CE	40 (30) cm, 50 $\mu$ m id DB-1 capillary	100 mM Tris-acetic acid, 0.05% HPC, pH 7.0	LIF ex. 488 nm / em. 520 nm	APTS	Reaction with (1) anti-Neu5Gc or (2) $\alpha$ -galactosidase inject prior to sample	[115]
Non-human N-glycans	CGE	40 (30) cm, 100 $\mu$ m id DB-1 capillary	100 mM Tris-borate, 5% PEG, pH 8.3	LIF ex. 325 nm / em. 405 nm	2-AA	Analysis of commercially available mAbs	[116]
$\alpha$ 1,3-Gal containing N-glycans	CGE	60 (50) cm, 50 $\mu$ m id eCAP NCHO coated	Beckman Coulter Carbohydrate Separation Gel Buffer-N	LIF ex. 488 nm / em. 520 nm	APTS and AMAC	Ultrasensitive detection method	[117]
N-glycans of mAb	CGE	50 (40) cm, 50 $\mu$ m id PVA coated	Beckman Coulter Carbohydrate Separation Buffer Or 40 mM EACA-acetate, 0.2% HPMC	LIF ex. 488 nm / em. 520 nm	APTS	Glycans of mAbs from NS0 cells	[118]
N-glycans of fusion protein	CE	90, 60, or 43 cm	0.7 M ammonia and 0.1 M EACA in 70% MeOH	TOF-MS	APTS	Alkaline CE-MS method	[119]
N-glycans	(1) CGE (2) CE	Various capillary lengths and coatings	(1) Beckman glycan separation buffer or POP-7 polymer (2) 40 mM EACA, 131 mM acetic acid, pH 4	(1) LIF ex. 488 nm / em. 512 nm (2) TOF-MS	APTS	CGE-LIF and CE-MS methods compared to the CE-MS method in ref [119]	[120]
N-glycans of mAbs	CE	50 (40) cm, 50 $\mu$ m id N-CHO coated	Beckman Coulter Carbohydrate Separation Gel Buffer	LIF ex. 488 nm / em. 520 nm	APTS	CE-LIF as an orthogonal technique to MS	[121]

Capillary: Actual length (effective length), inner diameter, coating  
 2-aminoacridone (AMAC), 2-aminobenzoic acid (2-AA), 9-aminopyrene-1,3,6-trisulfonic acid (APTS),  $\epsilon$ -aminocaproic acid (EACA), Gal $\alpha$ 1-3Gal ( $\alpha$ 1,3-Gal), Hydroxypropyl cellulose (HPC), Hydroxypropylmethylcellulose (HPMC), N-Glycylneuraminic acid (Neu5Gc), Polyvinyl alcohol (PVA), Poly(ethylene glycol) (PEG),

## 2.4.2 Biosimilars

Follow-on biologics, also known as biosimilars or biobetters, is the term for the “generic” biopharmaceuticals that have recently entered the market. The European Medicines Agency published regulatory guidelines for biosimilars in 2005, and by 2012 there were 14 products approved for sale in Europe [122]. In 2013 the first mAb biosimilar, Hospira’s Inflectra, hit the European market, and more than a half-dozen prospective biosimilars are in the pipeline. In 2015, as the majority of the leading biologics go off patent, there will be ample opportunity for established and start-up companies to begin producing biosimilars.

While production of biosimilars is an inherently less risky venture, due to the established market and tested safety of the innovator product, proving comparability to regulatory agencies still poses a significant challenge. Unlike chemical synthesis of small molecule generics, the composition of biologics is highly dependent on the manufacturing process. Small changes in production can have significant implications on the quality. In particular, the addition of impurities, aggregation products, and/or PTMs such as glycans can cause the protein to be immunogenic. Without detailed knowledge of how the innovator was produced, it can be very difficult to create an identical product.

Fortunately, dozens of analytical techniques exist to verify the physicochemical and functional comparability of the biosimilar to the innovator [123]. As discussed in the previous sections of this chapter, electrophoretic techniques are widely used for characterization of size and charge heterogeneity, product degradation, and PTMs. The appropriate method is generally chosen based on protein complexity, which varies from small non-glycosylated proteins like insulin and HGH to large, heterogeneous glycoproteins and mAbs [124].

EPO is a glycoprotein with approved biosimilars making up 12% of its market [122]. EPO has three complex N-glycosylation sites and one O-glycosylation site, which introduce a high level of heterogeneity into the protein. To be able to differentiate between the various formulations of EPO, or prove similarity between innovator and biosimilar, Taichrib *et al.* evaluated two multivariate statistical approaches for the

analysis of CE-MS data [125] (Table 7). The data were generated using a CE-ESI-TOF-MS method developed previously that exhibited high separation efficiencies and high selectivity for 14 commercially available preparations of EPO [91]. Both statistical approaches proved useful for analyzing the similarity or difference between large sets of glycosylated biologics that were generated under different production conditions, cell lines, and various batch numbers.

With the upcoming mAb biologic patent cliff, much of the biosimilar research has focused on the comparability of antibodies from various sources. Towards this end, CZE [126] and SDS-CGE [127] techniques can be used to determine charge heterogeneity of mAbs. Using CZE, rituximab (Kikuzubam® and Reditux®) and trastuzumab biosimilars were analyzed with respect to existing commercial products, Mabthera® and Herceptin®, respectively [126] (Table 7). The CZE methods were then compared to existing CIEF and chromatographic methods (HILIC and cation exchange chromatography). They found that, not surprisingly, a single method was not sufficient to resolve and characterize a protein, putting the emphasis on orthogonal techniques. However, they did report that CZE and CIEF gave better resolution of the mAbs than either HILIC and cation exchange chromatography, especially when using coated capillaries, since protein adsorption tends to lead to band broadening.

With the multitude of assays that exist, reproducibility and ruggedness is essential for widespread biosimilar production and regulation. The innovator, the biosimilar manufacturer, and the regulatory agency need to be certain that, despite the various laboratory conditions, the experimental results are comparable. To help facilitate this, Salas-Solano *et al.* evaluated an iCIEF method in 12 different laboratories across the world using several analysts, a variety of ampholytes, and multiple instruments [128]. The combined precision for the 12 labs was 0.8% RSD for the pI determination and 11% RSD for the percent peak area values for the charge variants of a therapeutic mAb. This study compared these values to those obtained using conventional CIEF, where the RSDs for pI and peak area were of 0.8% and 5.5%, respectively [129].

**Table 7. CE-based analysis of biosimilars**

Analyte	Mode	Capillary	Coating	BGE	Detection	Notes	Ref.
EPO glycoforms	CZE	60 cm, 50 µm id	UltraTroI™ LN	1 M acetic acid	TOF-MS	Multivariate statistical approach for glycoform analysis	[125]
(1) Rituximab, trastuzumab, and ranibizumab	CZE	40.2 (30.2) cm, 50 µm id	Polyacrylamide	(1) 200 mM EACA-acetic acid, 30 mM lithium acetate, 0.05% HPMC, pH 4.8 (2) 150 mM EACE-acetic acid, 20 mM lithium acetate, 0.05% HPMC, pH 5.5	UV 214 nm	CZE methods tested against orthogonal techniques for mAb characterization	[126]
(2) Infliximab and bevacizumab							
Rituximab	CGE	NR	NR	NR	UV 214 nm	Size heterogeneity of mAbs	[127]
Anti-α1-antitrypsin mAb	iCIEF	50 mm, 100 µm id	Fluorocarbon (ProteinSimple)	Pharmalyte pH 5-8	UV 280 nm	Interlaboratory study for robustness	[128]

Capillary: Actual length (effective length), inner diameter  
ε-aminocaproic acid (EACA), Hydroxypropylmethyl cellulose (HPMC), Not reported (NP)

## 2.5 Microchip electrophoresis

Many aspects of CE, such as low sample volume requirements, speed, efficiency, and the ability to use physiologically appropriate BGEs, make it an attractive method for the analysis of biopharmaceuticals. The advantages CE offers over chromatography are a function of the small inner diameter of the capillary. Consequently there has been an effort to further miniaturize bench-top CE instrumentation to a microfluidic format. This has decreased samples sizes needed for analysis from mL to  $\mu\text{L}$ , reduced analysis times from minutes to seconds, increased separation efficiencies, decreased costs, and added the ability for portable point-of-care analysis. Additionally, multiplex ME systems can be designed to handle high-throughput analysis on a greater scale than CE systems, making them an attractive technology for drug discovery and analysis [130, 131].

While most CE separation modes can be transferred to ME, the majority of the current published assays have dealt with analysis of biomarkers and small molecule drugs. Recent advances in N-glycan profiling by ME have also been made for clinical chemistry applications [132-134]. However, as the field of protein analysis on-chip grows, so does the possibility that the use of these devices will soon be accepted by the FDA as a validated method, allowing them to be incorporated into industry protocols.

### 2.5.1 Microchip gel electrophoresis

The LabChip® GXII, a commercially available microchip gel electrophoresis (MGE) system from PerkinElmer, is used frequently in the pharmaceutical industry [135, 136]. The commercial procedure, which uses indirect fluorescence and a HT Protein Express gel matrix [137], was compared against two new SDS-MGE methods, one for “high-sensitivity” and the other for “high-resolution” [138]. In the “high-sensitivity” method, direct LIF detection of fluorescently labeled proteins was investigated. Two labeling schemes were compared, and it was reported that performing the labeling step prior to protein denaturation improved the signal up to 50-fold for a loading concentration LOD of 1 ng/mL. In the “high-resolution” method, the sieving effect of the commercial gel was increased by the addition of a 6% poly(N,N-dimethylacrylamide) (PDMA) solution. With an optimal ratio of 2:1, gel:PDMA, the assay

achieved resolution between Fab heterodimers without increasing the separation time. Additional high-throughput analysis is available to process 96 samples in less than an hour.

SDS-MGE has also been integrated with Western blot immunoassay detection [139]. The separation of a series of test proteins with a MW range of 11–155 kDa (Table 2) was performed on-chip by Jin *et al.* [140]. Following the separation, the sample was eluted from the chip onto the Western blot membrane. In order to maintain the discrete zones accomplished during the separation, the chip was held in place vertically while the membrane moved below the outlet on an X-Y stage for spotting (Fig. 8). By carefully controlling the membrane spotting rate and the flow from the SDS-MGE chip, separation efficiencies of 40,000 theoretical plates were possible. With this set-up, the throughput capabilities were improved with a total analysis time of less than 32 min for the separation and immunoassay. This is a dramatic improvement over the traditional Western assay that takes several hours to complete.

### 2.5.2 Microchip isoelectric focusing

ME-based systems have also been used to verify the charge heterogeneity of mAbs with microchip isoelectric focusing (MIEF). Using a commercially available MCE-2010 system with whole-channel imaging from Shimadzu, Kinoshita *et al.* were able to analyze the charge variants of several mAbs [141]. The microchip consisted of two sample wells, one containing an anolyte and the second containing a catholyte, separated by a 2.7 cm channel. Following the separation, the whole channel was imaged with UV detection. To reduce the EOF, 0.2% hydroxypropylmethylcellulose was added to the BGE allowing greater focusing while preventing the non-specific adsorption of protein to the capillary wall. Using the optimized conditions, the authors were able to separate charge variants of three commercially available mAbs (bevacizumab, trastuzumab, and cetuximab) within 200–300 s. These separations were very reproducible (< 0.5% RSD) and were roughly 10 times faster than the corresponding CIEF assay (Table 3).

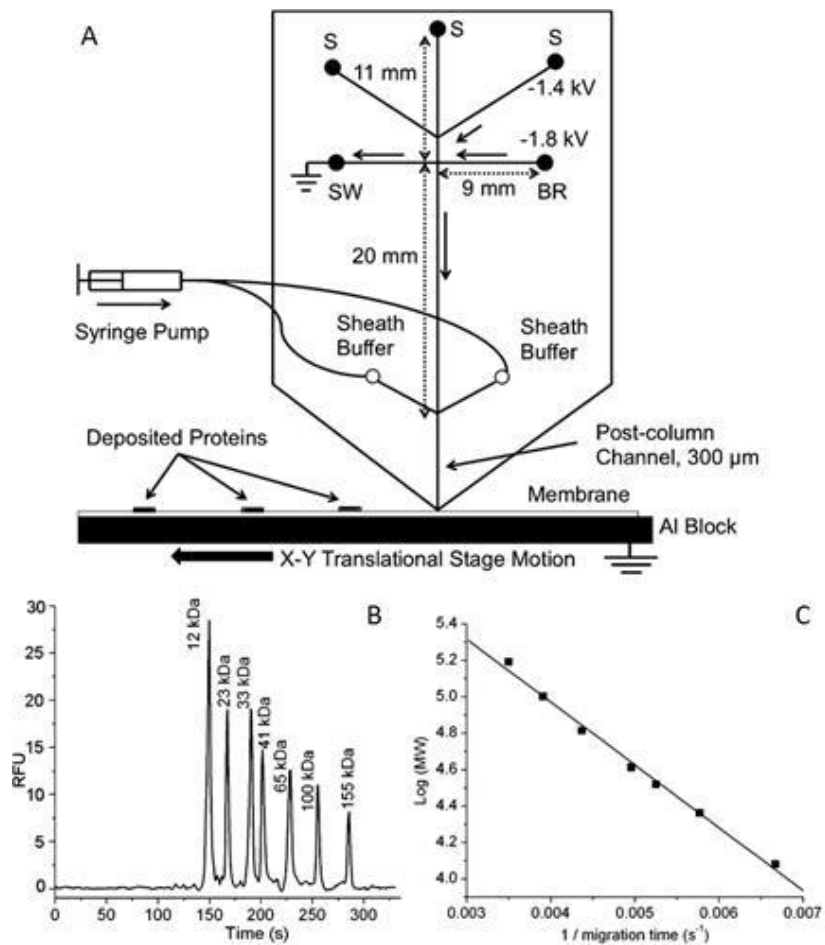


**Fig. 8.** (A) Microchip overview. Samples are loaded in different sample reservoirs (S). Samples are injected by floating the buffer reservoir (BR) and sample waste (SW) with voltage applied between the desired sample reservoir and the Al block at the exit. During separation, flow from the sample reservoir is gated to the sample waste reservoir (SW) using the voltages as shown. During these operations, other sample reservoirs are floating. Sieving media is pumped through the sheath channels to give stable current. Channel lengths are indicated by double arrow lines and direction of flow during separation is indicated by solid, single arrows. B) Size-dependent separation of FITC-labeled protein ladder in microchips. Detection window was set at the end of separation channel, 300 μm away from the chip outlet. Electric field during separation was 240 V/cm. C) Relationship of MW to migration time. Reprinted with permission from ref. 140



To further improve the utility and throughput of MIEF assay a single-channel microchip device where separation, immobilization, and subsequent immunoblot rinse steps could all be performed has been reported [142]. Once the proteins were separated within the pH gradient they were exposed to UV light and covalently cross-linked to a light-activated volume-accessible gel present in the microchip. This technique gave similar capture efficiencies ( $\approx 0.01\%$ ) to previous reports where proteins were immobilized on the inner surface of the capillary [42, 143]. Wash steps were performed by electrophoretic transport on the immobilized protein without concern of sample loss. Using this technique it was possible to complete an isoform assay in less than 120 min, up to 15x faster than the conventional slab-gel followed by Western blot (Table 5). Such rapid purity assays illustrate the significant advantage ME has over CE and other techniques.

### 2.5.3 Microchip electrophoresis-mass spectrometry

As with CE, even more specific and selective detection of analytes is possible by coupling ME to MS. The most common ionization interface for ME with MS is ESI, but MALDI is also possible [144]. The major benefit of ME-ESI-MS is that the flow rate on-chip is compatible with ESI and can therefore be seamlessly interfaced without disrupting the electrophoretic separation. When constructing an ME-MS interface, the geometry of the outlet and flow rate through the capillary must be taken into account given their monolithic construction and integration.

An advantage of ME over CE is that sample preparation and multiple separation methods can be integrated onto a single device prior to the ESI interface. Therefore, the excess dead volumes that are characteristic of conventional systems are eliminated, reducing the band broadening and sample dilution. The Ramsey group reported a fully integrated LC/CE microchip that terminated in an ESI source off the corner of the device in 2011 [145]. The potential combination of LC and ME for a more selective and specific separation is very powerful. In addition, the microchip flow rates are compatible with the ESI. However, a major disadvantage of fully integrated microchips is that the increased complexity of the device makes them difficult to fabricate.

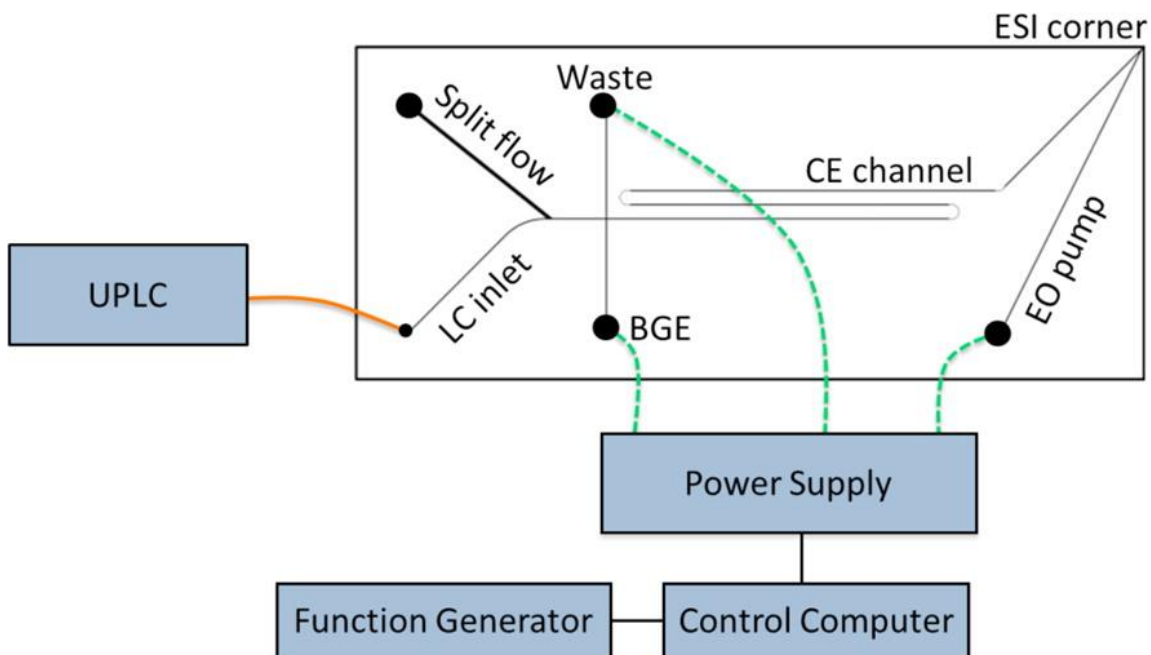


**Fig. 9.** Schematic of the hybrid capillary LC microchip CE-ESI experimental setup. The orange line represents a transfer capillary connecting the LC column to the microfluidic device. The dashed green lines represent electrical connections between the high voltage power supply and the microfluidic reservoirs. Reprinted with permission from ref. 146

As noted in a subsequent Ramsey paper, the fully integrated chip described above could not handle pressures over 200 bar. Therefore, to improve on the earlier design, a glass microchip that could be integrated with an off-chip UPLC was designed (Fig. 9). This allowed higher pressures to be reached than were possible with the LC on-chip [145]. The new device produced significant improvements in reproducibility and peak capacity when evaluated for the analysis of digested N-glycosylated proteins (Table 5). Additionally, the authors point out the utility of the new design in its ability to integrate to existing LC equipment that is already ubiquitous in industry.

## **2.6 Conclusions and future perspectives**

The development of protein and peptide therapeutics is a complex and high-risk venture, as products produced by recombinant expression are inherently heterogeneous. However, with advances in analytical techniques, thorough protein characterization is possible. In particular, CE-based separation techniques such as CZE, CGE, CIEF, and CEC provide versatile, efficient, and fast analyses of proteins. Additionally, CE-based techniques have the potential for high-throughput analysis using capillary arrays. The wide range of capillary-based separations can assess many aspects of protein stability, process impurities, and PTMs such as glycolysis, each of which is essential in providing a safe, effective, and quality product.

Microchip-based formats have the potential for increased speed, higher throughput, and portability of CE. While the development of ME devices is still primarily an academic research area, there is considerable promise for this miniaturized technique in the future of on-site pharmaceutical analysis. Pharmaceutical applications of ME and CE to therapeutic protein analysis will be further expanded through the development and commercialization of specialty capillaries, BGEs, and detection techniques. This is especially true for CE-MS and ME-MS interfaces. With numerous reviews already existing on this topic alone, coupling of MS with these techniques show great promise in the future for therapeutic protein analysis.

## 2.7 References

- [1] Manning, M. C., Chou, D. K., Murphy, B. M., Payne, R. W., Katayama, D. S., *Pharm Res* 2010, 27, 544-575.
- [2] Fekete, S., Gassner, A.-L., Rudaz, S., Schappler, J., Guillaume, D., *TrAC, Trends Anal. Chem.* 2013, 42, 74-83.
- [3] Little, M. J., Paquette, D. M., Roos, P. K., *Electrophoresis* 2006, 27, 2477-2485.
- [4] Staub, A., Guillaume, D., Schappler, J., Veuthey, J.-L., Rudaz, S., *J. Pharm. Biomed. Anal.* 2011, 55, 810-822.
- [5] Zhao, S. S., Chen, D. D. Y., *Electrophoresis* 2014, 35, 96-108.
- [6] Marie, A.-L., Przybylski, C., Gonnet, F., Daniel, R., Urbain, R., Chevreux, G., Jorieux, S., Taverna, M., *Anal. Chim. Acta* 2013, 800, 103-110.
- [7] Shi, Y., Li, Z., Qiao, Y., Lin, J., *J. Chromatogr. B: Anal. Technol. Biomed. Life Sci.* 2012, 906, 63-68.
- [8] Creamer, S. T. Krauss, and S. M. Lunte, *Electrophoresis*, 2014, 35, 563-569
- [9] Jorgenson, J. W., Lukacs, K. D., *Science* 1983, 222, 266-272.
- [10] Lukacs, K. D., Jorgenson, J. W., HRC CC, *J. High Resolut. Chromatogr. Chromatogr. Commun.* 1985, 8, 407-411.
- [11] Corradini, D., *J. Chromatogr. B: Biomed. Sci. Appl.* 1997, 699, 221-256.
- [12] Watzig, H., Degenhardt, M., Kunkel, A., *Electrophoresis* 1998, 19, 2695-2752.
- [13] Stutz, H., *Electrophoresis* 2009, 30, 2032-2061.
- [14] Lucy, C. A., MacDonald, A. M., Gulcev, M. D., *J. Chromatogr. A* 2008, 1184, 81-105.
- [15] Corradini, D., Nicoletti, I., Bonn, G. K., *Electrophoresis* 2009, 30, 1869-1876.

- [16] Li, J., Han, H., Wang, Q., Liu, X., Jiang, S., *Anal. Chim. Acta* 2010, 674, 243-248.
- [17] Wu, X., Wei, W., Su, Q., Xu, L., Chen, G., *Electrophoresis* 2008, 29, 2356-2362.
- [18] Guo, X.-F., Chen, H.-Y., Zhou, X.-H., Wang, H., Zhang, H.-S., *Electrophoresis* 2013, 34, 3287-3292.
- [19] Cao, F., Luo, Z., Zhou, D., Zeng, R., Wang, Y., *Electrophoresis* 2011, 32, 1148-1155.
- [20] Fu, X., Huang, L., Gao, F., Li, W., Pang, N., Zhai, M., Liu, H., Wu, M., *Electrophoresis* 2007, 28, 1958-1963.
- [21] Kato, M., Imamura, E., Sakai-Kato, K., Nakajima, T., Toyo'oka, T., *Electrophoresis* 2006, 27, 1895-1899.
- [22] Zhao, L., Zhou, J., Xie, H., Huang, D., Zhou, P., *Electrophoresis* 2012, 33, 1703-1708.
- [23] Zhao, L., Zhou, J., Zhou, H., Yang, Q., Zhou, P., *Electrophoresis* 2013, 34, 1593-1599.
- [24] de Jong, S., Epelbaum, N., Liyanage, R., Krylov, S. N., *Electrophoresis* 2012, 33, 2584-2590.
- [25] Cooper, B. T., Sanzgiri, R. D., Maxey, S. B., *Analyst (Cambridge, U. K.)* 2012, 137, 5777-5784.
- [26] Gassner, A.-L., Rudaz, S., Schappler, J., *Electrophoresis* 2013, 34, 2718-2724.
- [27] Mansfield, E., Ross, E. E., Aspinwall, C. A., *Anal. Chem.* 2007, 79, 3135-3141.
- [28] Adem, S. M., Mansfield, E., Keogh, J. P., Hall, H. K., Aspinwall, C. A., *Anal. Chim. Acta* 2013, 772, 93-98.
- [29] Yu, B., Liu, P., Cong, H., Tang, J., Zhang, L., *Electrophoresis* 2012, 33, 3066-3072.
- [30] Yu, B., Cui, W., Cong, H., Jiao, M., Liu, P., Yang, S., *RSC Adv.* 2013, 3, 20010-20015.
- [31] Castelletti, L., Verzola, B., Gelfi, C., Stoyanov, A., Righetti, P. G., *J. Chromatogr. A* 2000, 894, 281-289.
- [32] Verzola, B., Gelfi, C., Righetti, P. G., *J. Chromatogr. A* 2000, 874, 293-303.

- [33] Verzola, B., Gelfi, C., Righetti, P. G., *J. Chromatogr. A* 2000, 868, 85-99.
- [34] de Jong, S., Krylov, S. N., *Anal. Chem.* 2012, 84, 453-458.
- [35] Zhu, Z., Lu, J. J., Liu, S., *Anal. Chim. Acta* 2012, 709, 21-31.
- [36] Hutterer, K. M., Hong, R. W., Lull, J., Zhao, X., Wang, T., Pei, R., Le, M. E., Borisov, O., Piper, R., Liu, Y. D., Petty, K., Apostol, I., Flynn, G. C., *MAbs* 2013, 5, 608-613.
- [37] Lu, C., Liu, D., Liu, H., Motchnik, P., *MAbs* 2013, 5, 102-113.
- [38] Michels, D. A., Parker, M., Salas-Solano, O., *Electrophoresis* 2012, 33, 815-826.
- [39] Shi, Y., Li, Z., Lin, J., *Anal. Methods* 2012, 4, 1637-1642.
- [40] Cianciulli, C., Hahne, T., Waetzig, H., *Electrophoresis* 2012, 33, 3276-3280.
- [41] Le, M. E., Vizek, A., Hutterer, K. M., *Electrophoresis* 2013, 34, 1369-1374.
- [42] Rustandi, R. R., Loughney, J. W., Hamm, M., Hamm, C., Lancaster, C., Mach, A., Ha, S., *Electrophoresis* 2012, 33, 2790-2797.
- [43] Lu, J. J., Zhu, Z., Wang, W., Liu, S., *Anal. Chem.* 2011, 83, 1784-1790.
- [44] Na, D. H., Park, E. J., Kim, M. S., Cho, C. K., Woo, B. H., Lee, H. S., Lee, K. C., *Bull. Korean Chem. Soc.* 2011, 32, 4253-4257.
- [45] Na, D. H., Park, E. J., Kim, M. S., Lee, H. S., Lee, K. C., *Chromatographia* 2012, 75, 679-683.
- [46] Kerekgyarto, M., Fekete, A., Szirmai, Z., Kerekgyarto, J., Takacs, L., Kurucz, I., Guttman, A., *Electrophoresis* 2013, 34, 2379-2386.
- [47] Shen, Y., Xiang, F., Veenstra, T. D., Fung, E. N., Smith, R. D., *Anal. Chem.* 1999, 71, 5348-5353.
- [48] Koshel, B. M., Wirth, M. J., *Proteomics* 2012, 12, 2918-2926.
- [49] Righetti, P. G., Sebastiano, R., Citterio, A., *Proteomics* 2013, 13, 325-340.

- [50] Wehr, T., Rodriguez-Diaz, R., Zhu, M., *Capillary Electrophoresis of Proteins*, Marcel Dekker, New York 1998.
- [51] Anderson, C. L., Wang, Y., Rustandi, R. R., *Electrophoresis* 2012, 33, 1538-1544.
- [52] Rustandi, R. R., Wang, F., Hamm, C., Cuciniello, J. J., and Marley, M. L., *Electrophoresis*, 2014, 35, 1072-1078
- [53] Rustandi, R. R., Peklansky, B., and Anderson, C. L., *Electrophoresis*, 2014, 35, 1065-1071
- [54] Shimura, K., Hoshino, M., Kamiya, K., Enomoto, M., Hisada, S., Matsumoto, H., Novotny, M., Kasai, K.-i., *Anal. Chem.* 2013, 85, 1705-1710.
- [55] Lu, J. J., Wang, S., Li, G., Wang, W., Pu, Q., Liu, S., *Anal. Chem.* 2012, 84, 7001-7007.
- [56] Tang, Q., Harrata, A. K., Lee, C. S., *Anal. Chem.* 1995, 67, 3515-3519.
- [57] Tang, Q., Harrata, A. K., Lee, C. S., *J. Mass Spectrom.* 1996, 31, 1284-1290.
- [58] Foret, F., Mueller, O., Thorne, J., Goetzinger, W., Karger, B. L., *J. Chromatogr. A* 1995, 716, 157-166.
- [59] Zhang, Z., Wang, J., Hui, L., Li, L., *Electrophoresis* 2012, 33, 661-665.
- [60] Chingin, K., Astorga-Wells, J., Pirmoradian, N. M., Lavold, T., Zubarev, R. A., *Anal. Chem.* 2012, 84, 6856-6862.
- [61] Zhong, X., Maxwell, E. J., Ratnayake, C., Mack, S., Chen, D. D. Y., *Anal. Chem.* 2011, 83, 8748-8755.
- [62] Wang, C., Lee, C. S., Smith, R. D., Tang, K., *Anal. Chem.* 2013, 85, 7308-7315.
- [63] Kuroda, Y., Yukinaga, H., Kitano, M., Noguchi, T., Nemati, M., Shibukawa, A., Nakagawa, T., Matsuzaki, K., *J. Pharm. Biomed. Anal.* 2005, 37, 423-428.
- [64] Zhu, G., Sun, L., Yang, P., Dovichi, N. J., *Anal. Chim. Acta* 2012, 750, 207-211.

- [65] Michels, D. A., Tu, A. W., McElroy, W., Voehringer, D., Salas-Solano, O., *Anal. Chem.* 2012, 84, 5380-5386.
- [66] Fanali, C., D'Orazio, G., Fanali, S., *Electrophoresis* 2012, 33, 2553-2560.
- [67] Nilsson, C., Birnbaum, S., Nilsson, S., *Electrophoresis* 2011, 32, 1141-1147.
- [68] Gao, J., Latep, N., Ge, Y., Tian, J., Wu, J., Qin, W., *J. Sep. Sci.* 2013, 36, 1575-1581.
- [69] Cheong, W. J., Ali, F., Kim, Y. S., Lee, J. W., *J. Chromatogr. A* 2013, 1308, 1-24.
- [70] Miksik, I., Lacinova, K., Zmatlikova, Z., Sedlakova, P., Kral, V., Sykora, D., Rezanka, P., Kasicka, V., *J. Sep. Sci.* 2012, 35, 994-1002
- [71] Hamer, M., Yone, A., Rezzano, I., *Electrophoresis* 2012, 33, 334-339.
- [72] Qu, Q., Gu, C., Hu, X., *Anal. Chem.* 2012, 84, 8880-8890.
- [73] Qu, Q., Gu, C., Gu, Z., Shen, Y., Wang, C., Hu, X., *J. Chromatogr. A* 2013, 1282, 95-101.
- [74] Liu, H., Li, X., Huang, L., Zhang, L., Zhang, W., *Anal. Biochem.* 2013, 442, 186-188.
- [75] Puangpila, C., Nhujak, T., El, R. Z., *Electrophoresis* 2012, 33, 1431-1442.
- [76] Wang, Y., Deng, Q.-L., Fang, G.-Z., Pan, M.-F., Yu, Y., Wang, S., *Anal. Chim. Acta* 2012, 712, 1-8.
- [77] Liu, C.-C., Deng, Q.-L., Fang, G.-Z., Liu, H.-L., Wu, J.-H., Pan, M.-F., Wang, S., *Anal. Chim. Acta* 2013, 804, 313-320.
- [78] Hempel, G., *Electrophoresis* 2000, 21, 691-698.
- [79] Swinney, K., Bornhop, D. J., *Electrophoresis* 2000, 21, 1239-1250.
- [80] de Kort, B. J., de Jong, G. J., Somsen, G. W., *Electrophoresis* 2012, 33, 2996-3001.
- [81] Sarazin, C., Delaunay, N., Costanza, C., Eudes, V., Mallet, J.-M., Gareil, P., *Anal. Chem.* 2011, 83, 7381-7387.



- [82] de Kort, B. J., de Jong, G. J., Somsen, G. W., *Anal. Chim. Acta* 2013, 766, 13-33.
- [83] Wang, H., Dou, P., Lue, C., Liu, Z., *J. Chromatogr. A* 2012, 1246, 48-54.
- [84] Walt, D. R., *Anal. Chem.* 2013, 85, 1258-1263.
- [85] Ramsay, L. M., Dickerson, J. A., Dovichi, N. J., *Electrophoresis* 2009, 30, 297-302.
- [86] Haselberg, R., de Jong, G. J., Somsen, G. W., *LC GC Asia Pac.* 2012, 15, 13-18.
- [87] Pioch, M., Bunz, S.-C., Neusuess, C., *Electrophoresis* 2012, 33, 1517-1530.
- [88] Haselberg, R., de Jong, G. J., Somsen, G. W., *Electrophoresis* 2013, 34, 99-112.
- [89] Hommerson, P., Khan, A. M., de Jong, G. J., Somsen, G. W., *Mass Spectrom. Rev.* 2011, 30, 1096-1120.
- [90] Olivares, J. A., Nguyen, N. T., Yonker, C. R., Smith, R. D., *Anal. Chem.* 1987, 59, 1230-1232.
- [91] Taichrib, A., Pioch, M., Neusuess, C., *Electrophoresis* 2012, 33, 1356-1366.
- [92] Bonvin, G., Schappler, J., Rudaz, S., *J. Chromatogr. A* 2012, 1267, 17-31.
- [93] Moini, M., *Anal. Chem.* 2007, 79, 4241-4246.
- [94] Whitt, J. T., Moini, M., *Anal. Chem.* 2003, 75, 2188-2191.
- [95] Haselberg, R., Ratnayake, C. K., de Jong, G. J., Somsen, G. W., *J. Chromatogr. A* 2010, 1217, 7605-7611.
- [96] Haselberg, R., de Jong, G. J., Somsen, G. W., *Anal. Chem.* 2013, 85, 2289-2296.
- [97] Gahoual, R., Burr, A., Busnel, J.-M., Kuhn, L., Hammann, P., Beck, A., Francois, Y.-N., Leize-Wagner, E., *MAbs* 2013, 5, 479-490.
- [98] Whitmore, C. D., Gennaro, L. A., *Electrophoresis* 2012, 33, 1550-1556.
- [99] Maxwell, E. J., Zhong, X., Zhang, H., van, Z. N., Chen, D. D. Y., *Electrophoresis* 2010, 31, 1130-1137.

- [100] Maxwell, E. J., Zhong, X., Chen, D. D. Y., *Anal. Chem.* 2010, 82, 8377-8381.
- [101] Zhao, S. S., Zhong, X., Chen, D. D. Y., *Electrophoresis* 2012, 33, 1322-1330.
- [102] Zhong, X., Maxwell, E. J., Chen, D. D. Y., *Anal. Chem.* 2011, 83, 4916-4923.
- [103] Researchmoz.us, <http://www.researchmoz.us/global-and-china-monoclonal-antibody-industry-report-2013-2017-report.html> 2013.
- [104] Rustandi, R. R., Anderson, C. L., Hamm, M., *Glycosylation Engineering of Biopharmaceuticals*, Springer New York 2013.
- [105] Behne, A., Muth, T., Borowiak, M., Reichl, U., Rapp, E., *Electrophoresis* 2013, 34, 2311-2315.
- [106] Wuhrer, M., de, B. A. R., Deelder, A. M., *Mass Spectrom. Rev.* 2009, 28, 192-206.
- [107] Mittermayr, S., Bones, J., Doherty, M., Guttman, A., Rudd, P. M., *J. Proteome Res.* 2011, 10, 3820-3829.
- [108] Guttman, A., *TrAC, Trends Anal. Chem.* 2013, 48, 132-143.
- [109] Mittermayr, S., Bones, J., Guttman, A., *Anal. Chem.* 2013, 85, 4228-4238.
- [110] Kuo, C.-Y., Wang, S.-H., Lin, C., Liao, S. K.-S., Hung, W.-T., Fang, J.-M., Yang, W.-B., *Molecules* 2012, 17, 7387-7400.
- [111] Callewaert, N., Geysens, S., Molemans, F., Contreras, R., *Glycobiology* 2001, 11, 275-281.
- [112] Reusch, D., Habeger, M., Kailich, T., Heidenreich, A.-K., Kampe, M., Bulau, P., Wuhrer, M., *MAbs* 2013, 6, 185-196.
- [113] Croset, A., Delafosse, L., Gaudry, J.-P., Arod, C., Glez, L., Losberger, C., Begue, D., Krstanovic, A., Robert, F., Vilbois, F., Chevalet, L., Antonsson, B., *J. Biotechnol.* 2012, 161, 336-348.
- [114] Galili, U., Rachmilewitz, E. A., Peleg, A., Flechner, I., *J. Exp. Med.* 1984, 160, 1519-1531.

- [115] Yagi, Y., Kakehi, K., Hayakawa, T., Ohyama, Y., Suzuki, S., *Anal. Biochem.* 2012, *431*, 120-126.
- [116] Maeda, E., Kita, S., Kinoshita, M., Urakami, K., Hayakawa, T., Kakehi, K., *Anal. Chem.* 2012, *84*, 2373-2379.
- [117] Szabo, Z., Guttman, A., Bones, J., Shand, R. L., Meh, D., Karger, B. L., *Mol. Pharmaceutics* 2012, *9*, 1612-1619.
- [118] Hamm, M., Wang, Y., Rustandi, R. R., *Pharmaceuticals* 2013, *6*, 393-406.
- [119] Bunz, S.-C., Cutillo, F., Neusuess, C., *Anal. Bioanal. Chem.* 2013, *405*, 8277-8284.
- [120] Bunz, S.-C., Rapp, E., Neusuess, C., *Anal. Chem.* 2013, *85*, 10218-10224.
- [121] Wang, Y., Santos, M., Guttman, A., *J. Sep. Sci.* 2013, *36*, 2862-2867.
- [122] Initiative, G. a. B., <http://www.gabionline.net/Reports/Biosimilars-marketed-in-Europe> 2012.
- [123] Falconer, R. J., Jackson-Matthews, D., Mahler, S. M., *J. Chem. Technol. Biotechnol.* 2011, *86*, 915-922.
- [124] Beck, A., Diemer, H., Ayoub, D., Debaene, F., Wagner-Rousset, E., Carapito, C., Van, D. A., Sanglier-Cianferani, S., *TrAC, Trends Anal. Chem.* 2013, *48*, 81-95.
- [125] Taichrib, A., Pioch, M., Neusuess, C., *Anal. Bioanal. Chem.* 2012, *403*, 797-805.
- [126] Espinosa-de, I. G. C. E., Perdomo-Abundez, F. C., Padilla-Calderon, J., Uribe-Wiechers, J. M., Perez, N. O., Flores-Ortiz, L. F., Medina-Rivero, E., *Electrophoresis* 2013, *34*, 1133-1140.
- [127] Visser, J., Feuerstein, I., Stangler, T., Schmiederer, T., Fritsch, C., Schiestl, M., *BioDrugs* 2013, *27*, 495-507.
- [128] Salas-Solano, O., Kennel, B., Park, S. S., Roby, K., Sosic, Z., Boumajny, B., Free, S., Reed-Bogan, A., Michels, D., McElroy, W., Bonasia, P., Hong, M., He, X., Ruesch, M., Moffatt, F., Kiessig, S., Nunnally, B., *J. Sep. Sci.* 2012, *35*, 3124-3129.

- [129] Salas-Solano, O., Babu, K., Park, S. S., Zhang, X., Zhang, L., Susic, Z., Boumajny, B., Zeng, M., Cheng, K.-C., Reed-Bogan, A., Cummins-Bitz, S., Michels, D. A., Parker, M., Bonasia, P., Hong, M., Cook, S., Ruesch, M., Lamb, D., Bolyan, D., Kiessig, S., Allender, D., Nunnally, B., *Chromatographia* 2011, 73, 1137-1144.
- [130] Culbertson, C. T., Mickleburgh, T. G., Stewart-James, S. A., Sellens, K. A., Pressnall, M., *Anal. Chem.* 2014, 86, 95-118.
- [131] Neuzi, P., Giselbrecht, S., Laenge, K., Huang, T. J., Manz, A., *Nat. Rev. Drug Discovery* 2012, 11, 620-632.
- [132] Mitra, I., Snyder, C. M., Alley, W. R., Novotny, M. V., Jacobson, S. C., American Chemical Society 2013, pp. ANYL-279.
- [133] Mitra, I., Alley, W. R., Goetz, J. A., Vasseur, J. A., Novotny, M. V., Jacobson, S. C., *J. Proteome Res.* 2013, 12, 4490-4496.
- [134] Zhuang, Z., Starkey, J. A., Mechref, Y., Novotny, M. V., Jacobson, S. C., *Anal. Chem.* 2007, 79, 7170-7175.
- [135] Han, H., Livingston, E., Chen, X., *Anal. Chem.* 2011, 83, 8184-8191.
- [136] Primack, J., Flynn, G. C., Pan, H., *Electrophoresis* 2011, 32, 1129-1132.
- [137] Chen, X., Tang, K., Lee, M., Flynn, G. C., *Electrophoresis* 2008, 29, 4993-5002.
- [138] Han, H., Chen, X., *Electrophoresis* 2012, 33, 765-772.
- [139] Pan, W., Chen, W., Jiang, X., *Anal. Chem.* 2010, 82, 3974-3976.
- [140] Jin, S., Anderson, G. J., Kennedy, R. T., *Anal. Chem.* 2013, 85, 6073-6079.
- [141] Kinoshita, M., Nakatsuji, Y., Suzuki, S., Hayakawa, T., Kakehi, K., *J. Chromatogr. A* 2013, 1309, 76-83.
- [142] Hughes, A. J., Herr, A. E., *Proc. Natl. Acad. Sci. U. S. A.* 2012, 109, 21450-21455

[143] O'Neill, R. A., Bhamidipati, A., Bi, X., Deb-Basu, D., Cahill, L., Ferrante, J., Gentalen, E., Glazer, M., Gossett, J., Hacker, K., Kirby, C., Knittle, J., Loder, R., Mastroieni, C., MacLaren, M., Mills, T., Nguyen, U., Parker, N., Rice, A., Roach, D., Suich, D., Voehringer, D., Voss, K., Yang, J., Yang, T., Vander Horn, P. B., *Proc. Natl. Acad. Sci. U. S. A.* 2006, *103*, 16153-16158.

[144] He, X., Chen, Q., Zhang, Y., Lin, J.-M., *TrAC, Trends Anal. Chem.* 2014, *53*, 84-97.

[145] Chambers, A. G., Mellors, J. S., Henley, W. H., Ramsey, J. M., *Anal. Chem.* 2011, *83*, 842-849.

[146] Mellors, J. S., Black, W. A., Chambers, A. G., Starkey, J. A., Lacher, N. A., Ramsey, J. M., *Anal. Chem.* 2013, *85*, 4100-4106.

**Chapter Three:**

**Capillary electrophoresis separation of the desamino degradation products of oxytocin**

Published as:

J.S. Creamer, S.T. Krauss, S.M. Lunte, 'Capillary electrophoresis separation of the desamino degradation products of oxytocin', *Electrophoresis*, 2014, 35, 563-569

### 3.1 Introduction

Oxytocin (OT) is a cyclic nonapeptide hormone secreted from the pituitary gland of the hypothalamus. Traditionally, OT is used therapeutically in maternal health to induce and augment labor as well as prevent death from postpartum hemorrhage. However, low concentrations of endogenous OT have also been implicated in behavioral disorders such as depression, anxiety, and autism [1]. As research progresses in this field, new therapeutic uses for OT and its analogs will be discovered. To ensure safety and efficacy, inexpensive and fast analytical methods are needed to determine the integrity and stability of OT.

As a biopharmaceutical drug, OT is susceptible to both chemical and physical degradation during purification, shipping, storage, and delivery. Yet, prior to 2009, there were few reports on the specific degradation pathways of OT. In 1981, Nachtmann et al. compiled the then current knowledge of the physical, chemical, and pharmaceutical characteristics of OT, noting the importance of formulation pH on the rate of degradation [2]. In the following years, several methods were published in which LC-UV was used to determine OT quality in pharmaceutical dosage forms [3-6], including the US and EU Pharmacopoeias [7, 8]. In these stability-indicating methods, OT was resolved from its pH-, heat-, light-, and oxidative-stress degradation products. However, none of these reports identified the degradation products formed. Hawe et al. were the first to publish a systematic discussion of the formation of specific degradation products and the degradation kinetics of OT using LC-MS [9].

Deamidation is the most common chemical degradation pathway for proteins and peptides [10]. It is not surprising then that OT undergoes deamidation under both acidic and basic conditions and that the rate of deamidation increases with exposure to heat [9]. Proper functionality of OT at the uterine receptor requires that both the receptor binding region (Ile<sup>3</sup>, Gln<sup>4</sup>, Pro<sup>7</sup>, and Leu<sup>8</sup>) and the active site (Asn<sup>5</sup> and Tyr<sup>2</sup>) be intact [11]. Both of these sites rely on amino acids with amide functional groups (Gln<sup>4</sup> and Asn<sup>5</sup>). Different combinations of deamidation at those sites, and at the amidated C-terminus, lead to a total of

seven possible desamino-OT species (Figure 1). It has also been shown that deamidation at each site significantly diminishes the peptide's biological activity [12-14].

To evaluate the extent of OT deamidation, we employed a CE-based method for analysis. CE has several benefits over LC for peptide analysis. CE requires very little reagent use for the preparation of the run buffer (mL), allowing the use of expensive and exotic additives without significantly increasing the cost-per-test or waste generated by this technique. Additionally, CE is known for high efficiency separations of both proteins and peptides. The size-to-charge based separation is particularly useful for the identification of deamidation products [15, 16]. This is because deamidation yields an ionizable side group from a neutral amide ( $R\text{-CONH}_2 \rightarrow R\text{-COOH}$ ), which alters the electrophoretic mobility of the peptide depending on the pH of the background electrolyte.

To the best of our knowledge, there is only one report that uses CE to address OT degradation. In that report, the separation of the degradation products was performed with an acidic background electrolyte inside positively charged, noncovalently coated capillaries [17]. At this low pH the desamino side chains are protonated and are, therefore, neutral, producing a +1 charge for all species due to the protonated N-terminus. Because of this, only partial resolution of OT from the desamino species was possible. For identification of the products, the authors relied on MS to collect extracted-ion electropherograms to identify the degradants. Additionally, the authors did not identify which specific site(s) of the peptide had undergone deamidation, instead distinguishing only between mono- and bis-deamidated OT.

In this chapter, a CE method is described that utilizes a modified charged  $\beta$ -cyclodextrin as a pseudo-stationary phase and the organic modifier MeOH in a phosphate buffer (pH 6.0) to achieve a separation of the seven desamino degradation products from OT. All seven of these desamino species are detected after a 96 h heat-stressed degradation study of OT. This fast and cost-effective analysis method makes it possible to determine the extent of OT deamidation in 12 minutes without requiring the use of expensive, high-resolution MS.



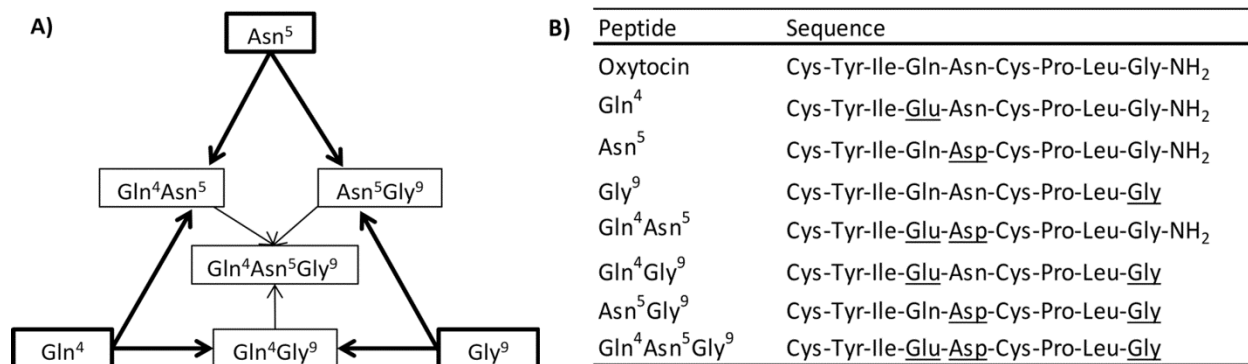


**Figure 1:** A) Progression of desamino-OT species starting with the individual mono-desamino products and ending with the tris-desamino peptide. B) Amino acid sequences of oxytocin and seven desamino-oxytocin species with specific sites of deamidation underlined.

## 3.2 Materials and methods

### 3.2.1 Chemicals and reagents

OT acetate salt was obtained from Bachem (Torrance, CA, USA). OT desamino standards of mono-desamino at Gln<sup>4</sup> (Gln<sup>4</sup>), mono-desamino at Asn<sup>5</sup> (Asn<sup>5</sup>), mono-desamino at Gly<sup>9</sup>-NH<sub>2</sub> (Gly<sup>9</sup>), bis-desamino at Gln<sup>4</sup> and Asn<sup>5</sup> (Gln<sup>4</sup>Asn<sup>5</sup>), bis-desamino at Gln<sup>4</sup> and Gly<sup>9</sup>-NH<sub>2</sub> (Gln<sup>4</sup>Gly<sup>9</sup>), bis-desamino at Asn<sup>5</sup> and Gly<sup>9</sup>-NH<sub>2</sub> (Asn<sup>5</sup>Gly<sup>9</sup>), and tris-desamio at Gln<sup>4</sup>, Asn<sup>5</sup>, and Gly<sup>9</sup>-NH<sub>2</sub> (Gln<sup>4</sup>Asn<sup>5</sup>Gly<sup>9</sup>) were synthesized by Shanghai Mocell Biotech Co. (Shanghai, China).  $\beta$ -cyclodextrin, o-phosphoric acid, monobasic sodium phosphate, dibasic sodium phosphate, HEPES, mesityl oxide (MO), acetonitrile, methanol, dimethyl sulfoxide, concentrated HCl, and NaOH were obtained as analytical grade reagents from Sigma Aldrich (St. Louis, MO, USA). Sulfobutyl ether  $\beta$ -cyclodextrin (SBE) was donated by Cydex Pharmaceuticals (Lenexa, KS, USA).

### 3.2.2 Preparation of buffers

#### 3.2.2.1. Buffer composition optimization

Several background electrolytes were investigated over a pH range of 4.0-9.0; each was prepared at a concentration of 50 mM. The phosphate buffers (pH 4.0, 5.0, 6.0, 7.0, 8.0, and 9.0) were prepared by mixing the appropriate amounts of acid and conjugate base as calculated by the Henderson-Hasselbalch equation, and the pH was adjusted as needed with either 1 M NaOH or 1 M o-phosphoric acid. The HEPES buffer (pH 7.0) was prepared by simply adding the correct amount of HEPES to water and adjusting the pH as needed with 1 M NaOH or 1 M HCl. All buffers were prepared with 18 M $\Omega$  deionized water (Millipore, Billerica, MA, USA) and filtered through 0.2  $\mu$ m pore nylon filters before use (GE Water and Process Technologies, Trevose, PA, USA).

### 3.2.2.2. Buffer additive optimization

Phosphate buffer stock (pH 6.0) was prepared at 100 mM and diluted daily to 50 mM with selected buffer additives with DI water to prepare the background electrolyte (BGE).  $\beta$ -cyclodextrin stock was prepared at 10 mM in 50 mM pH 6.0 phosphate buffer and diluted with buffer to 1, 5, and 10 mM. SBE stock was prepared at 100 mM in water and was added to BGE at 1-12 mM (in increments of 1 mM). The organic solvents ACN and MeOH were added to the BGE at concentrations 1-20 % v/v (in increments of 5 %), while DMSO was evaluated at 1 and 5 % v/v. Any pH change due to the addition of organic solvents was not corrected for (ie. 10% MeOH can increase the pH up to 0.2 units). All measurements of the EOF were done with a 0.3% v/v solution of MO into BGE.

### 3.2.3 Standard preparation

For all BGE optimization and spiking studies, standard solutions of OT and the desamino peptides were made daily by dissolving a measured amount of the lyophilized peptide into 50 mM phosphate buffer, pH 2.0. The 50 mM phosphate buffer was prepared at pH 2.0 by combining the appropriate amounts of o-phosphoric acid (15 M) and monobasic sodium phosphate.

### 3.2.4 Equipment conditions

Separations were performed on a Beckman Coulter P/ACE MDQ (Brea, CA, USA) with UV detection (214 nm). The system was controlled using 32-Karat software. Subsequent data analysis was performed using this software and Origin 8.6 (Northampton, MA, USA). A 50 cm fused silica capillary (50 mm id  $\times$  360 mm od) from Polymicro Technologies (Phoenix, AZ, USA) was used for the separation, and a small window was burned into the polyimide coating 10 cm from the capillary end for detection. Each day, prior to use, the capillary was conditioned by rinsing for 5 min with 0.1 M HCl, water, methanol, water, 0.1 N NaOH, water, and for 10 min with BGE. To expedite equilibration of the buffer within the capillary, a 20 kV potential was applied across the capillary for 25 min following the conditioning. To maintain separation efficiency, the capillary was rinsed for 3 min with 0.1 M HCl, water,

0.1 N NaOH, water, and BGE between every run. Pressure injections were performed at 1 psi for 5.0 s. A separation voltage of 20–30 kV was applied.

### 3.2.5 Acid-catalyzed deamidation of oxytocin

Lyophilized OT acetate was dissolved at 0.1 mg/mL in 50 mM phosphate buffer (pH 2.0) and sealed in borosilicate glass vials with TFE-lined caps (Fisher Scientific, Fairlawn, NJ, USA). To track the degradation, the sealed vials were placed in a water bath at 70 °C, and aliquots were removed at regular intervals. The extent of degradation was monitored by measuring the OT peak height using CE-UV. The pH of the blank (50 mM phosphate buffer, pH 2.0) was monitored at the start and end of every experiment and was found to fluctuate within  $\pm 0.2$  pH units.

## 3.3 Results and discussion

### 3.3.1 Separation optimization

#### 3.3.1.1. BGE selection

Initially, phosphate buffer was investigated over a pH range of 4-9 as a potential background electrolyte (BGE) for the analysis of OT and its desamino degradation products. To evaluate the usefulness of phosphate as a BGE, migration time reproducibility, separation current, and separation efficiency were determined for triplicate runs of the OT standard. At the low pH (4-5) the EOF was significantly reduced, causing increased migration times and poor separation efficiency. The reproducibility increased with the pH from 6-7 with minimal improvements past pH 7, while the efficiency of the separation improved continually from pH 6-9. However, the separation current also increased significantly over this pH range.

To avoid high currents which can lead to band broadening, HEPES, a low conductivity buffer, was also tested. However, this BGE resulted in large system peaks, possibly due to difference in conductivity between the BGE and the sample. For this reason HEPES was excluded from further buffer studies. It was

concluded that 50 mM phosphate buffer at pH 6.0 provided the best separation efficiency while maintaining a relatively low current, and it was implemented for further optimization.

With 50 mM phosphate buffer at pH 6.0 as the BGE, the initial separation of OT and the seven desamino-OT standards gave four distinct peaks. From spiking studies, the peaks were identified as OT, the three mono-desamino OT species, the three bis-desamino OT species, and finally the tris-desamino OT species. Given the similar size of the analytes, it is not surprising that species migrated based on their overall charge (+1, 0, -1, and -2, respectively). Additional optimization of buffer additives was performed to increase the resolution of these species.

#### 3.3.1.2. CD additives

Under the free zone electrophoresis conditions mentioned above, it was not possible to resolve the multiple mono- and bis-desamino species from one another due to their identical size-to-charge ratios. In order to improve the separation, cyclodextrins were investigated due to their ability to act as a pseudo-stationary phase. The cyclodextrins form inclusion complexes with hydrophobic peptide residues, such as the Tyr<sup>2</sup> residue of OT, thereby increasing the apparent size of the peptide and changing its mobility. However, the addition of neutral  $\beta$ -cyclodextrin to the BGE yielded no noticeable improvement in resolution because, based on hydrophobicity alone, the selectivity for peptide inclusion would be identical for each species.

To introduce more selectivity for the separation, sulfobutyl ether-modified  $\beta$ -cyclodextrin (SBE) was evaluated. When the peptide associates with the SBE, both its size and overall negative charge increase, significantly reducing the electrophoretic mobility. Positively charged OT has the highest affinity for the SBE and, as the concentration of SBE in the BGE was increased, the migration time of OT increased. This is illustrated in the plot of the migration time of the analytes, relative to the EOF maker MO, versus SBE concentration shown in Figure 2a.

The mono-desamino species have a weaker interaction with the SBE than OT does. The additional negative charge from the deamidated side group creates an electrostatic repulsion with the negatively charged cyclodextrin, lowering the binding constant. However, a significant improvement in selectivity was introduced by the addition of the SBE. Fig. 2 shows that by increasing the concentration of SBE from 0 to 11 mM it was possible to completely separate all three mono-desamino species (peaks 1, 2, and 6). This is extremely useful since they are neutral species at this pH and, without the negatively charged SBE, they would be impossible to separate with only free-zone electrophoresis. The enhanced selectivity most likely comes from the relative position of the mono-desamino site to the Tyr<sup>2</sup> residue.

As OT deamidation progresses, increasing the peptide's overall negative charge, a less dramatic shift in relative migration time was observed with the bis-desamino species due to decreased interaction with the SBE. At 11 mM SBE, Gln<sup>4</sup>Asn<sup>5</sup> (peak 3) is resolved from Asn<sup>5</sup>Gly<sup>9</sup> and Gln<sup>4</sup>Gly<sup>9</sup> which remain co-migrated (peak 4/5). However, when all the standards were run together, Gln<sup>4</sup>Asn<sup>5</sup> was found to co-migrate with the mono-desamino Gln<sup>4</sup> (peak 2/3) as shown in Figure 2b.

At all concentrations of SBE, Gln<sup>4</sup>Asn<sup>5</sup>Gly<sup>9</sup> migrates last (peak 8), showing a small difference in migration time with respect to the EOF. This indicates a minimal interaction with the SBE due to electrostatic repulsion from the three deamidated sites.

### 3.3.1.3. Organic modifiers

To further resolve the co-migrating species (Gln<sup>4</sup>/Gln<sup>4</sup>Asn<sup>5</sup> and Asn<sup>5</sup>Gly<sup>9</sup>/Gln<sup>4</sup>Gly<sup>9</sup>), the organic solvents DMSO, ACN, and MeOH were evaluated as modifiers to the BGE. The organic solvent in the BGE alters the hydrophobic affinity of the cyclodextrin for the peptide, changing the binding constant and therefore affecting the relative electrophoretic mobilities. Neither DMSO nor ACN exhibited an appreciable benefit to the separation at any concentration. ACN increased the EOF, which in turn increased the separation efficiency; however, the resolution of all species was lost as a result. DMSO at 1 % v/v did not change the separation in any way; yet increasing the concentration to 5 % v/v resulted in an

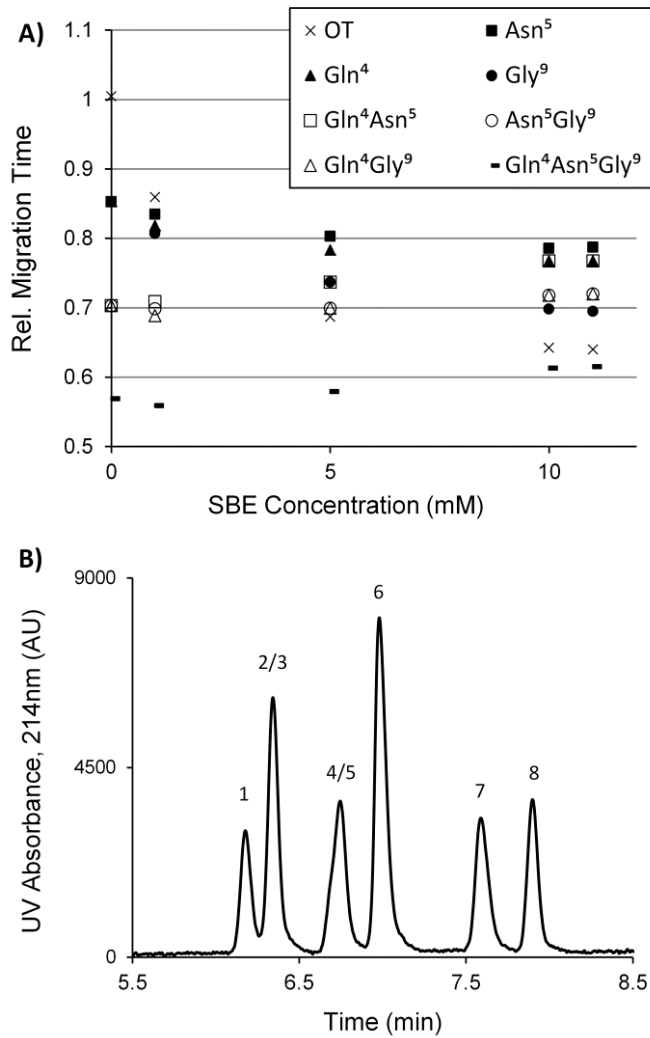


**Figure 2:** A) Effect of SBE concentration on relative migration time. BGE: 50 mM phosphate buffer, pH 6.0 with varying concentrations of SBE. Migration times are based on the average of triplicate runs, relative to the neutral marker MO. B) Separation of peptides with optimized SBE. BGE: 50 mM phosphate buffer, pH 6.0 and 11 mM SBE. Peptides are 0.05 mg/mL in 50 mM phosphate buffer, pH 2.0. Peaks: 1 Asn<sup>5</sup>; 2 Gln<sup>4</sup>; 3 Gln<sup>4</sup>Asn<sup>5</sup>; 4 Asn<sup>5</sup>Gly<sup>9</sup>; 5 Gln<sup>4</sup>Gly<sup>9</sup>; 6 Gly<sup>9</sup>; 7 OT; 8 Gln<sup>4</sup>Asn<sup>5</sup>Gly<sup>9</sup>.

electropherogram with zero peaks, probably due to a significant decrease in the EOF. MeOH not only changed the polarity of the BGE, it also slightly decreased the EOF, increasing the resolution. With 10 % v/v MeOH, it was possible to achieve a complete separation of all seven desamino species from OT. Figure 3a demonstrates the change in migration time (relative to the EOF) versus the concentration of MeOH.

#### 3.3.1.4. Separation voltage

The effect of voltage on the separation efficiency was investigated by increasing the separation voltage from 20–30 kV, in increments of 2 kV, and calculating the theoretical plates and resolution of the peptides in the resulting electropherograms. Based on these experiments, 22 kV was chosen for the greatest separation efficiency without loss of resolution due to Joule heating. An electropherogram demonstrating the fully optimized separation of all eight species is shown in Figure 3b.

#### 3.3.2 Separation parameters

The linear range of this assay is 2.5-100  $\mu\text{M}$  for all analytes, except  $\text{Gln}^4$ , which exhibited a linear range of 5-100  $\mu\text{M}$ . For all peptide calibration curves the  $R^2$  value was greater than 0.9995 ( $n = 3$  for five concentrations). The LOD ( $S/N = 3$ ) and LOQ ( $S/N = 10$ ) are provided in Table 1. It should be noted that a common concentration for OT in maternal health therapeutics is 10 IU/mL (approximately 20  $\mu\text{M}$ ). While this concentration falls well within the linear range of the assay, the LOQ for OT on the current system is not ideal for research or quality control settings. However, it would be possible to improve the low sensitivity with improved CE-UV technology such as a bubble cell or Z-shaped capillaries [18].

Migration time can be a helpful tool for peak identification. However, CE is notorious for irreproducible migration times due to changes in the EOF over time and slight differences in BGE additive concentration. To improve the %RSD for the migration times of all species, the desamino peak



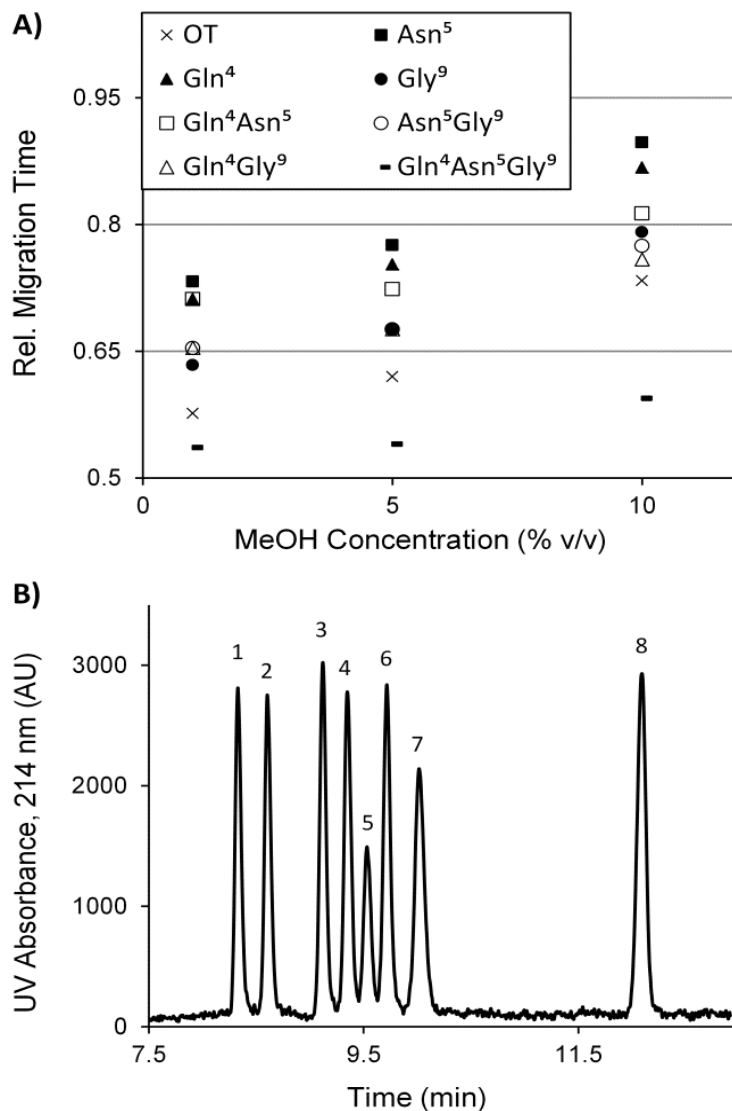


**Figure 3:** A) Effect of MeOH concentration on relative migration time. BGE: 50 mM phosphate buffer, pH 6.0, 11 mM SBE with varying concentrations of MeOH. Migration times are based on the average of triplicate runs, relative to the neutral marker MO. B) Optimized separation of peptides. BGE: 50 mM phosphate buffer, pH 6.0, 11 mM SBE, 10 % v/v MeOH. Peptides are 0.05 mg/mL in 50 mM phosphate buffer, pH 2.0. Peaks: 1 Asn<sup>5</sup>; 2 Gln<sup>4</sup>; 3 Gln<sup>4</sup>Asn<sup>5</sup>; 4 Gly<sup>9</sup>; 5 Asn<sup>5</sup>Gly<sup>9</sup>; 6 Gln<sup>4</sup>Gly<sup>9</sup>; 7 OT; 8 Gln<sup>4</sup>Asn<sup>5</sup>Gly<sup>9</sup>.

migration times were taken relative to the OT peak. Table 1 provides the %RSD values for the migration time and relative migration times of the desamino peaks.

### 3.3.3 Tracking degradation in heat-stressed oxytocin samples

The heat-stressed degradation of OT was monitored using the optimized separation described above. OT was prepared at 0.1 mg/mL in acidic conditions (pH 2.0) to ensure that the primary degradation pathway was acid-catalyzed deamidation. Three samples were degraded concurrently at 70 °C over the course of 5 days, sampling every 12 hours.

The degradation of OT was determined by monitoring the peak heights of all species as a function of time. Using the method described in this paper, it was possible to monitor the appearance and disappearance of OT and all seven desamino species over the 5 day period. In Figure 4a, electropherograms from five different time points (time points 10, 34, and 58 h excluded for clarity) are stacked to illustrate the extent of degradation over time.  $t = 0$  h shows one peak in the electropherogram corresponding to OT. All subsequent peaks of the degradation products were identified by migration time relative to OT and by spiking studies.

At  $t = 24$  h, the OT peak height was diminished slightly, giving rise to the three mono-desamino species. The concentration of both  $\text{Gln}^4$  and  $\text{Gly}^9$  (peaks 2 and 4) increased over time, cresting at the 72 h time point, seen more clearly in Figure 4b. However, the height of the  $\text{Asn}^5$  peak (peak 1) stayed at a fairly constant low concentration from 10-72 h. This could be indicative of the relative reactivity between the deamidation sites due to the secondary structure of the peptide. Structural studies of OT have shown hydrogen bond formation between the hydroxyl group of the  $\text{Tyr}^2$  and the carboxamide of  $\text{Asn}^5$ , which would decrease the likelihood of deamidation at this site [19].

As the sample continued to degrade at 70 °C, the mono-desamino species gave rise to the bis-desamino species. Due to the low reactivity of  $\text{Asn}^5$ , both  $\text{Gln}^4\text{Asn}^5$  and  $\text{Asn}^5\text{Gly}^9$  (peaks 3 and 5) were

Table 1  
 Separation parameters of OT and the desamino-OT standards (n=9)

Peptide	LOD ( $\mu$ M) S/N = 3	LOQ ( $\mu$ M) S/N = 10	Theoretical Plates plates/meter	Ave. Migration Time min. (% RSD)	Ave. Rel. Migration Time min. (% RSD)
Asn <sup>5</sup>	0.83	2.5	240,000	7.92 (2.5)	0.840 (0.46)
Gln <sup>4</sup>	2.6	8	240,000	8.16 (2.5)	0.866 (0.38)
Gln <sup>4</sup> Asn <sup>5</sup>	3.7	11	260,000	8.73 (2.5)	0.916 (0.14)
Gly <sup>9</sup>	4	12	220,000	8.84 (2.7)	0.937 (0.20)
Asn <sup>5</sup> Gly <sup>9</sup>	8.6	26	190,000	9.11 (2.6)	0.955 (0.10)
Gln <sup>4</sup> Gly <sup>9</sup>	2	5.9	240,000	9.23 (2.6)	0.972 (0.20)
OT	3	8.9	150,000	9.35 (3.6)	1
Gln <sup>4</sup> Asn <sup>5</sup> Gly <sup>9</sup>	1.5	4.4	230,000	11.42 (3.9)	1.20 (0.95)

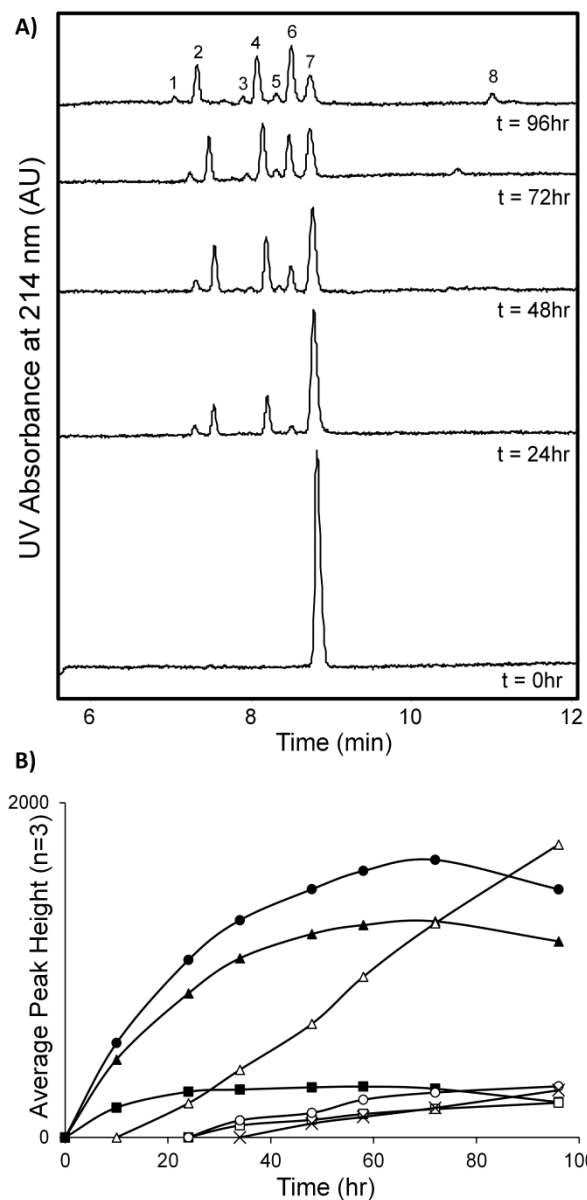


**Figure 4:** A) Degradation time points of heat-stressed oxytocin. BGE: 50 mM phosphate buffer, pH 6.0, 11 mM SBE, 10 % v/v MeOH. Peaks: 1 Asn<sup>5</sup> (■); 2 Gln<sup>4</sup> (▲); 3 Gln<sup>4</sup>Asn<sup>5</sup> (□); 4 Gly<sup>9</sup> (●); 5 Asn<sup>5</sup>Gly<sup>9</sup> (○); 6 Gln<sup>4</sup>Gly<sup>9</sup> (△); 7 OT; 8 Gln<sup>4</sup>Asn<sup>5</sup>Gly<sup>9</sup> (x). B) Formation of desamino-OT products over time at 70 °C. Initial OT concentration was 0.1 mg/mL in 50 mM phosphate buffer, pH 2.0.

first seen at 34 h and remained in low concentrations over the course of the study. The more reactive sites of Gln<sup>4</sup> and Gly<sup>9</sup> led to a steady increase in the presence of Gln<sup>4</sup>Gly<sup>9</sup> (peak 6) from 24-96 h.

The Gln<sup>4</sup>Asn<sup>5</sup>Gly<sup>9</sup> species was first observed as a small peak in the t = 48 h time point, and its peak height steadily increased until the end of the study. Notably, using the LC-MS method, the appearance of Gln<sup>4</sup>Asn<sup>5</sup>Gly<sup>9</sup>, Asn<sup>5</sup>, and Gln<sup>4</sup>Asn<sup>5</sup> was either not observed or not at high enough concentrations to be detected by the method [9].

From this degradation study, the kinetics for the disappearance of OT (n = 3) were calculated to be pseudo-first order with a  $k_{\text{obs}}$  of 0.465 days<sup>-1</sup> (3.4% RSD) and a  $t_{1/2}$  of 1.5 days (3.9% RSD). This half-life is similar to that reported by Hawe et al., 1.1 days with a less than 5% RSD [9]. At each time point, all of the peaks were accounted for by mass balance (104% ± 5), by adding up the peak heights and comparing them to the initial OT peak. This indicates no sample loss by adsorption on the capillary wall or by precipitation in the sample vial during degradation.

### 3.4 Concluding remarks

A CE-UV method to separate the desamino degradation products of OT has been described. Deamidation creates seven desamino-OT species with structures very similar in size and charge, making resolution with free zone electrophoresis a challenge. To resolve the many desamino degradation species with identical size-to-charge ratios, it was necessary to include the pseudo-stationary phase SBE as well as the organic modifier MeOH in the BGE. Using this approach, the heat-stressed degradation of OT in acidic buffer was monitored over time. All seven desamino degradation products were detected over a 96 h heat-stress period at 70 °C in acidic conditions.

For this study, formulation in a pH 2.0 buffer was chosen to force deamidation to be the major degradation pathway of OT. However, as reported by both Hawe et al. and Hasselberg et al., OT degradation is pH dependent and deamidation is not the major pathway at higher pHs [9, 17]. At the

pharmaceutically relevant pH 4.5, both papers report minimal deamidation, with the formation of both dimers and tri- and tetrasulfide as the primary degradation species.

Preliminary results from analysis of heat-stressed OT at pH 4.5 with the assay described in this paper, corroborate the previous reports showing little deamidation after 96 h under 70 °C heat-stress conditions. Additional work is ongoing to modify the current assay and create a comprehensive CE-UV method for the determination of all degradation species of OT.

Having a low-cost and fast CE-UV method for OT analysis will enhance the field of study by allowing more labs to participate in research without having to invest in expensive LC-MS instrumentation. Additionally, CE has the potential for miniaturization through method transfer to microchip electrophoresis (ME), reducing the cost-per-test and analysis time even further. ME allows portability, which increases the range of the assay to places like developing countries, where traditional laboratory equipment is not readily available.

### 3.5 References

- [1] Miller, G., *Science*. 2013, 339, 267-269.
- [2] Nachtmann, F., Krummen, K., Maxl, F., Riemer, E., *Analytical Profiles of Drug Substances* 1981, 10, 563-600.
- [3] Ohta, M., Fukuda, H., Kimura, T., Tanaka, A., *J. Chromatogr.* 1987, 402, 392-395.
- [4] Dudkiewicz-Wilczynska, J., Snycerski, A., Tautt, J., *Acta Pol. Pharm.* 2000, 57, 403-406.
- [5] Wang, G., Miller, R. B., Melendez, L., Jacobus, R., *J. Liq. Chromatogr. Relat. Technol.* 1997, 20, 567-581.
- [6] Chaibva, F. A., Walker, R. B., *J. Pharm. Biomed. Anal.* 2007, 43, 179-185.
- [7] *European Pharmacopoeia 5th Edition* 2005, 2174-2175.
- [8] Callahan, L. N., *Pharmacopeial Forum* 2007, 29, 1946.
- [9] Hawe, A., Poole, R., Romeijn, S., Kasper, P., van, d. H. R., Jiskoot, W., *Pharm. Res.* 2009, 26, 1679-1688.
- [10] Cornell, M. M., Chou, D. K., Murphy, B. M., Payne, R. W., Katayama, D. S., *Pharm. Res.* 2010, 27, 544-575.
- [11] Walter, R., Schwartz, I. L., Darnell, J. H., Urry, D. W., *Proc. Nat. Acad. Sci. U. S.* 1971, 68, 1355-1359.
- [12] Photaki, I., du, V. V., *J. Am. Chem. Soc.* 1965, 87, 908-913.
- [13] Branda, L. A., Du, V. V., *J Biol Chem* 1966, 241, 4051-4054.
- [14] Ferrier, B. M., Vigneaud, V. d., *J. Med. Chem.* 1966, 9, 55-57.
- [15] Lai, M., Skanchy, D., Stobaugh, J., Topp, E., *J. Pharm. Biomed. Anal.* 1998, 18, 421-427.
- [16] Mandrup, G., *J. Chromatogr.* 1992, 604, 267-281.

[17] Haselberg, R., Brinks, V., Hawe, A., de, J. G. J., Somsen, G. W., *Anal. Bioanal. Chem.* 2011, 400, 295-303.

[18] Hempel, G., *Electrophoresis* 2000, 21, 691-698.

[19] Urry, D. W., Walter, R., *Proc. Nat. Acad. Sci. U. S.* 1971, 68, 956-958.





## **Chapter Four:**

### **Investigation into the Effect of Chlorobutanol on the Stability of Oxytocin**

## 4.1 Introduction

Capillary electrophoresis (CE) provides a distinct cost advantage over high performance liquid chromatography (HPLC) as a separation method for quantitative analysis in developing countries. Most background electrolytes (BGEs) used for CE are composed of inexpensive aqueous buffers and, when more expensive additives are necessary, the low volume requirements and minimal reagent use keep the cost-per-test low. Additionally, the instrumentation cost for CE is significantly lower than HPLC. CE-UV instrumentation for use in developing countries is available for \$10,000 [1] and has been used for counterfeit pharmaceutical detection of small molecule drugs using previously published methods [2]. However, inexpensive CE based methods for the analysis of biopharmaceuticals are still needed. The overall aim of this project is to develop a CE-based method for the separation and detection of oxytocin (OT) and all of its degradation products formed in pharmaceutical preparations under heat-stress conditions. Building on the work described in chapter three of this dissertation, where the desamino degradation products of OT are separated by CE [3], chapter four investigates the other degradation products formed in OT pharmaceutical formulations.

OT is an important biopharmaceutical used to induce labor and treat post-partum hemorrhage (PPH). In developing countries PPH is the leading cause of maternal death, killing approximately 250,000 women per year. These deaths can largely be attributed to the lack of effective obstetric care and treatment, including access to OT. The challenge to achieving widespread distribution of OT is due in part to the inconsistent availability of cold-chain shipping and storage in low-resource areas. Peptide drugs are known to undergo a variety of chemical and physical degradation pathways at elevated temperatures [4], and World Health Organization (WHO) studies have shown that both solid dose and injectable OT rapidly degrade in “tropical climates” [5]. Currently, these complex degradation pathways lead to a variety of compounds that are not easily distinguishable from OT itself without the use of expensive HPLC instrumentation to separate the different products.

Historically, HPLC with UV detection has been the primary tool for analysis of OT. Many LC-based methods have been reported to measure the quantity of OT in pharmaceutical preparations [6-8]. LC-based stability indicating methods also exist that make it possible to resolve OT from degradation products generated during oxidation, acid, base, and thermal stress [9, 10]. However, it was not until 2009 that the identification of the specific degradation products formed during heat-stress (Table 1) was accomplished by Hawe et al. using LC-MS [11]. Additional studies regarding the mechanism of degradation of OT were published last year by Wisniewski et al. (Figure 1) [12].

In the degradation studies performed by Hawe and Wisniewski, OT was formulated in phosphate buffers over a range of pH 2.0, 4.5, 7.0 and 9.0. This was done to control the pH, which plays a significant role in OT degradation kinetics and product formation. However, the injectable form of OT is not formulated in phosphate buffer. According to the package insert, Pitocin, a synthetic injectable OT, is formulated in water that has been pH adjusted to a value between pH 3 and 5 with acetic acid, and contains 0.5% w/v chlorobutanol (CB) as a preservative (Watson Labs, Teva Pharmaceuticals). In this pH range, acetic acid can act as a buffer; however, at low concentrations its buffer capacity is poor. Therefore, it is possible that a different set of degradation products will be formed.

In this chapter, OT degradation is investigated in a solution similar that of the pharmaceutical preparation. This study was carried out using LC-UV-MS to monitor the degradation kinetics of OT as well as the appearance of known degradation products of OT, in the presence and absence of several CB and CB-like additives. The effect of CB on the degradation was of specific interest because the presence of antimicrobial preservatives (APs) has been shown by others to influence the stability of a wide range of biopharmaceuticals [13]. Previous reports have shown that the stability of insulin is profoundly improved by the addition of phenol or m-cresol through formation of additional helical segment of the N-terminus of the B-chain [14]. In contrast, the addition of both alkyl and aromatic alcohol APs lead to increased aggregation of cytochrome *c* by promoting partial protein unfolding [15]. To the best of our knowledge there are no reports that specifically address the effects of CB on the stability of OT.

Table 1. Previously Published Degradation Products

Peak Number	Peptide	Mass	Charge
1	Desamino oxytocin	1008.42	1+
2	Oxytocin	1007.42	1+
3	Trisulfide	1039.41	1+
4	Tetrasulfide	1071.38	1+
5	Dimer	975.44	2+
6	Dimer	975.44	2+
7	Higher order aggregates	--	--
*	Unidentified species	--	--

Adapted from Hawe et al with permission

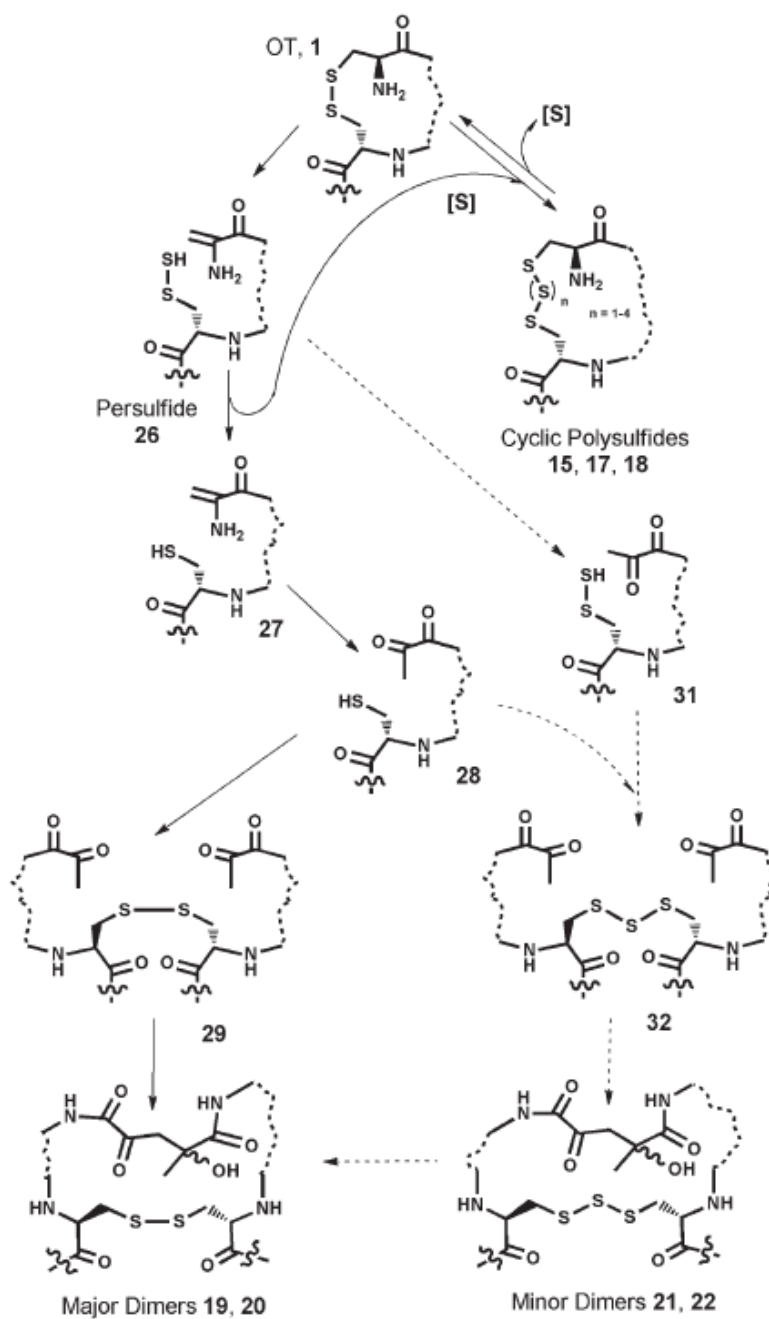


Figure 1: Proposed mechanism of degradation for oxytocin in solution. The solid arrows follow the major pathway of degradation. For simplicity the parts of the molecules that do not participate in the outlined mechanism are represented by a dashed line. Reprinted with permission from Wisniewski et al.

## 4.2 Materials and methods

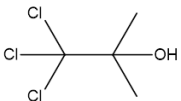
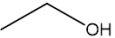
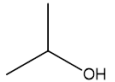
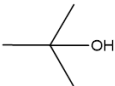
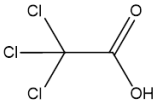
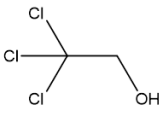
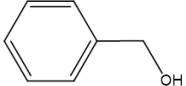
### 4.2.1 Chemicals and reagents

OT acetate powder was obtained from Bachem (Torrance, CA). Analytical grade reagents 2,2,2-trichloroethanol (TCE), ammonium acetate, benzyl alcohol (BA), CB (trichloro-2-methyl-2-propanol), dibasic sodium phosphate, ethanol, glacial acetic acid, isopropyl alcohol, monobasic sodium phosphate, *o*-phosphoric acid, sodium hydroxide, *tert*-butanol (TBA), and trichloroacetic acid (TCA) were received from Sigma Aldrich (St. Louis, MO). Optima LC/MS grade ACN was purchased from Fisher Scientific (Fair Lawn, NJ).

### 4.2.2 Preparation of oxytocin formulations

The stock solution of 50 mM pH 4.5 phosphate buffer was prepared by mixing the necessary amount of mono- and dibasic sodium phosphate with any further pH adjustment performed as needed by the addition of 1 M NaOH or 1 M *o*-phosphoric acid. The unbuffered water solution was prepared by adjusting the pH of nanopure water to 4.0 with 99.9% glacial acetic acid ( $\approx 0.9$  mM). The APs were then added to appropriate solution at 0.5% w/v as shown in Table 2. For formulation H, after the addition of TCA to unbuffered water/acetic acid, the solution pH dropped below 2.0 and required further pH adjustment with the addition ammonium acetate (final concentration 40 mM ammonium acetate with 4.8% w/v TCA) to reach pH 4.0. All solutions were prepared with 18 M $\Omega$  nanopure water (Millipore, Billerica, MA) and filtered through 0.45  $\mu$ m pore nylon filters before use (FisherBrand, Fisher Scientific). The solutions were stored at 4 °C for no more than one week prior to use. Due to the low solubility of CB, all solutions were brought to room temperature and sonicated for 15 min prior to the addition of OT.

Table 2. Formulations used for Degradation Studies

	Solution	Additive	Structure
A	50 mM phosphate buffer, pH 4.5		
B	50 mM phosphate buffer, pH 4.5	Chlorobutanol (CB)	
C	Water and acetic acid, pH 4.0		
D	Water and acetic acid, pH 4.0	CB	
E	Water and acetic acid, pH 4.0	Ethanol	
F	Water and acetic acid, pH 4.0	Isopropyl alcohol	
G	Water and acetic acid, pH 4.0	Tert-butanol (TBA)	
H	Water and acetic acid, pH 4.0	Trichloroacetic acid (TCA)	
I	Water and acetic acid, pH 4.0	2,2,2-Trichloroethanol (TCE)	
J	Water and acetic acid, pH 4.0	Benzyl alcohol (BA)	



#### 4.2.3 Accelerated degradation studies

OT acetate was dissolved at 0.1 mg/mL in 2 mL of the appropriate solution (Table 1). This sample was then sealed in a 4 mL borosilicate glass vial with a TFE-lined cap (Fisher Scientific). The sealed vials were placed in a 70 °C water bath and 150 microliter aliquots were removed at specified time points. No special effort was made to control exposure to air in the vial headspace during the course of these experiments.

#### 4.2.4 LC-UV-MS equipment and conditions

The extent of OT degradation was monitored by LC-UV-MS. The eluent from the LC column was split 30:70 to the UV and ESI-MS detectors, respectively. UV detection was used to quantitate peak area and MS was used to monitor the appearance of specific OT degradation products as found in Table 1 [11]. Analyst 1.5.1 software was used to control the LC-UV-MS system and perform subsequent data analysis.

An ABI Sciex 3200 QTRAP MS (Foster City, CA, USA) with a Shimadzu Prominence UFLC (Shimadzu Corporation, Japan) on the front end was used for all studies. The LC system included two LC-20AD pumps and solvent mixer, a CMB-20A controller, SIL-20AC autosampler, and CT-O-20A column oven. A Shimadzu UV/Vis SPD-10A absorbance detector set at 214 nm was used to monitor all degradation products. The RP-LC method was adapted from a previous method [11] using an Alltima C18 RP-column with 5µm particle size, 4.6 mm inner diameter, and 150 mm length (Alltech, Ridderkerk, Netherlands). Twenty microliter samples were injected and all chromatography was performed at a flow rate of 1 mL/min. For the LC separation, mobile phase A consisted of 10 mM ammonium acetate buffer at pH 5.0 containing 15% CAN, and mobile phase B consisted of 10 mM ammonium acetate pH 5.0 with 60% ACN. In the gradient program, mobile phase B was linearly increased from 11% to 33% from 0-15 min and then to 100% at 20 min. The gradient was kept at 100% B for 1 min to wash the column and then dropped back to 11% B in 0.5 min and allowed to re-equilibrate for 10 min before the next injection.

All 3200 QTRAP MS experiments were conducted using ESI in the positive ion mode. All parameters were optimized using the automated tune function in the Analyst software. This program checked for a response from the compound of interest in a standard solution of 0.1 mg/mL OT in 50:50 ACN:H<sub>2</sub>O. Optimization for the most intense Q1 signal was then performed by increasing and decreasing the voltages that control the path of the ion through the MS. Optimization of the compound-specific parameters was accomplished by direct infusion, while the optimization of curtain gas, ion source gas 1, and ion source gas 2, as well as the source temperature, was performed with flow injection analysis to account for the composition of the mobile phase and LC flow rate.

### **4.3 Results and discussion**

This chapter describes the results of a pilot study done with the goal to explore the effect of CB and CB-like additives on the degradation of OT under heat-stress conditions. Each formulation was tested with an n=1 so no statistically significant conclusions can be drawn. However, the results described below provide a starting point and indicate the potential directions for further research should this project be continued in the future.

#### **4.3.1 Q1 scan range optimization**

The 3200 QTRAP can function as either a triple quadrupole MS or as a sensitive ion trap MS for qualitative analysis. Triple quadrupole mass analyzers are best suited for compound identification based on detection of the product ions formed from the unique fragmentation pattern of the molecule of interest. A quadrupole analyzer (Q) is made up of four parallel metal rods used to create an oscillating electric field through which the ions from the ESI pass (Figure 2i). Based on the voltages applied to the rods, only ions with specific mass-to-charge ratios will reach the detector plate. A triple quadrupole has three of these Q analyzers in series. The samples enter the instrument and pass through the Q1 where specific masses are focused and sent to Q2, also referred to as the collision cell. In this second quadrupole, the precursor ions are bombarded by a neutral collision gas, typically nitrogen or argon. Selected product ions are then isolated and focused in Q3 before being sent to the detector plate (Figure 2ii). This ion selection

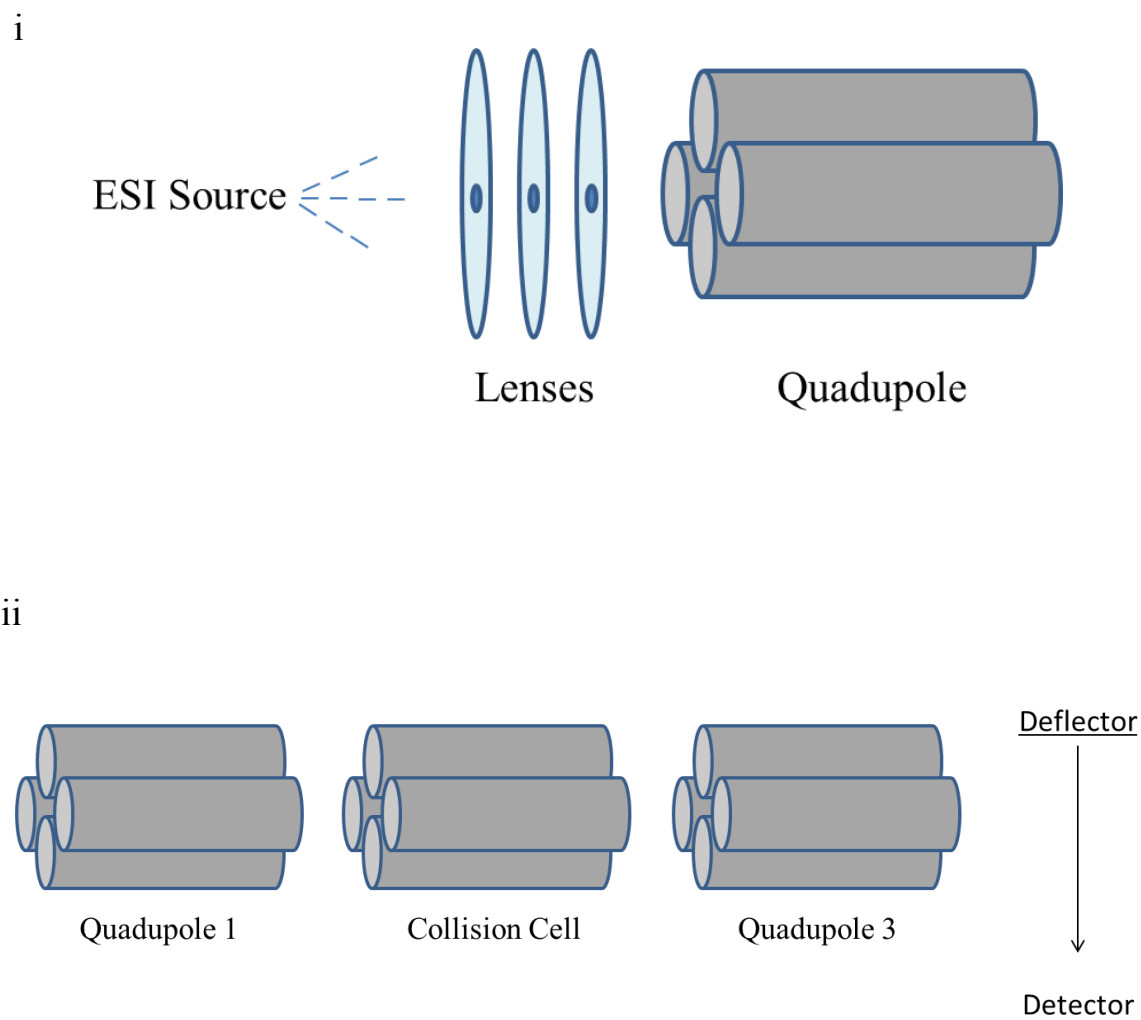


Figure 2: Cartoon schematics of the i) ESI source and quadrupole analyzer and ii) arrangement of quadrupole analyzers in a triple quadrupole mass spectrometer.

process is referred to as multiple reaction monitoring (MRM). The best sensitivity is gained in MRM where the MS selects for the specified ions, lowering the baseline by effectively filtering out unwanted signal from the sample [16].

For the purposes of this exploratory study, the 3200 QTRAP was used qualitatively to scan for peptides of specific masses in an attempt to monitor the formation of known degradation products. These results were then compared to the previously published study [11] to identify similarities or differences in the degradation mechanism of OT in the presence of the formulation additives. Ideally, the Q1 scan would have been performed over a wide enough mass range to monitor all degradation products formed under heat-stress conditions. However, due to the sensitivity limitations of the MS while scanning a large mass range, the background noise was such that it was impossible to obtain a signal from low-abundance degradation products. Initial experiments to optimize the S/N were performed using a degraded sample of 0.1 mg/mL OT that was formulated in phosphate buffer pH 4.5 and was heat-stressed at 50 °C for 99 hours.

For a Q1 scan over the mass range of 400-1200 Da, a high background signal was observed ( $1.0E7$  cps), with a noise of 150 cps. With these settings the limits of detection were so high that it was impossible to quantitate OT or any of its degradation products. By decreasing the mass scan range to 900-1100 Da, it was possible to generate much cleaner spectra with a fifty-fold decrease in the background ( $2.0E5$  cps). Following this trend, the background could be decreased further by scanning over several short mass ranges. The final optimized method involved scanning the mass ranges 974-976 m/z for doubly charged dimer products, 1006-1011 m/z for OT and the desamino degradation products, 1030-1032 m/z for OT trisulfide, and 1070-1072 m/z for OT tetrasulfide. With this method, the background was lowered another order of magnitude ( $1.0E4$  cps). With these settings a S/N of 5000 for 5  $\mu$ M OT was possible.

The LC-UV-MS method was used to monitor the relative abundance of the expected degradation products in the various formulations during heat stress (Table 2). Unfortunately, using this approach, information was lost regarding the molecular weight of new degradation products. However, this was necessary to improve the LODs for this study. In the future it should be possible to rerun these samples using MRM to investigate the identity of any new species.

#### 4.3.2 Effect of formulation buffering capacity on OT degradation

As previously mentioned, injectable OT is not formulated in a buffered solution. However, the previous literature reports of OT degradation have been performed in phosphate buffer to control the pH near that of the pharmaceutical preparation [11, 17]. Therefore, a comparison of the stability of OT formulated in a phosphate buffer solution pH 4.5 (formulation A), to a formulation prepared with unbuffered water, pH adjusted to 4 with acetic acid (formulation C), was performed first (Table 2). Using the data obtained via LC-UV, the kinetics of the disappearance of OT in the pH 4.5 buffered formulation appeared to be pseudo first order with a calculated half-life of 1.5 days. This value is similar to what was reported by Hawe et al (1.9 days, 15% RSD). The unbuffered formulation also followed pseudo first order kinetics but the half-life was 0.71 days, indicating much more rapid degradation (Figure 3i). The difference in the rate of disappearance of oxytocin as a function of time can also be seen in the plot in Figure 3ii that shows the % of OT remaining after 48 h of heat-stress degradation at 70° C for both formulations.

All of the predicted degradation products were produced in both the buffered and unbuffered formulations as determined by LC-MS. However, due to poor ionization in the electrospray source, the dimer products gave a disproportionately low signal compared to the other degradation products (Figure 4). This was not the case for the LC-UV analysis at 214 nm, as each peptide has approximately the same molar absorptivity at 214 nm due to the unchanged peptide backbone and presence of the tyrosine residue [18]. Therefore, the response obtained using LC-UV was used for both quantitative analysis by peak area, and as comparative tool for qualitative analysis between samples.

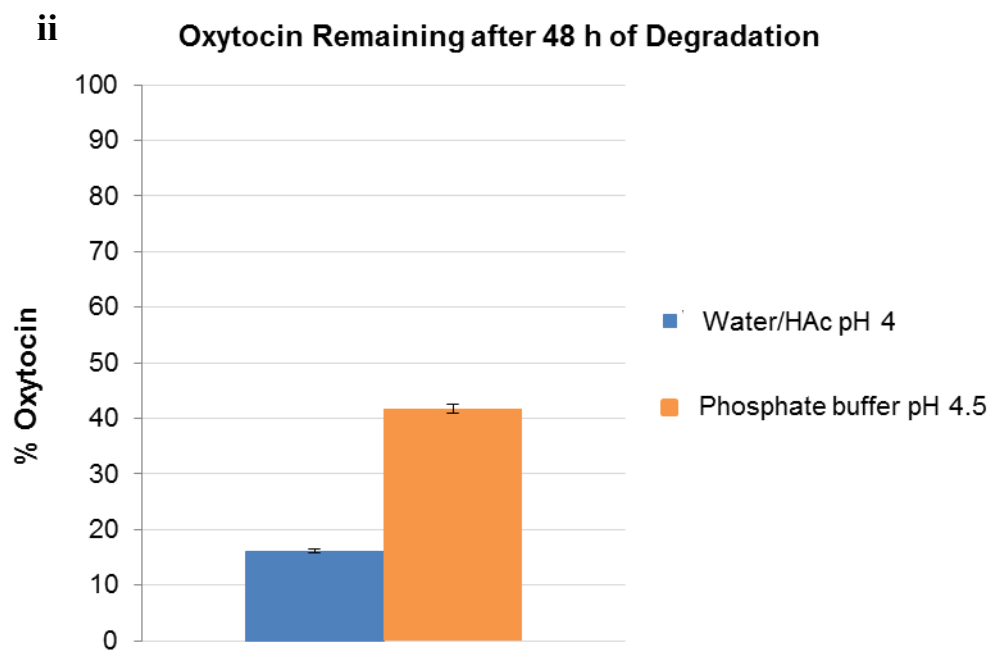
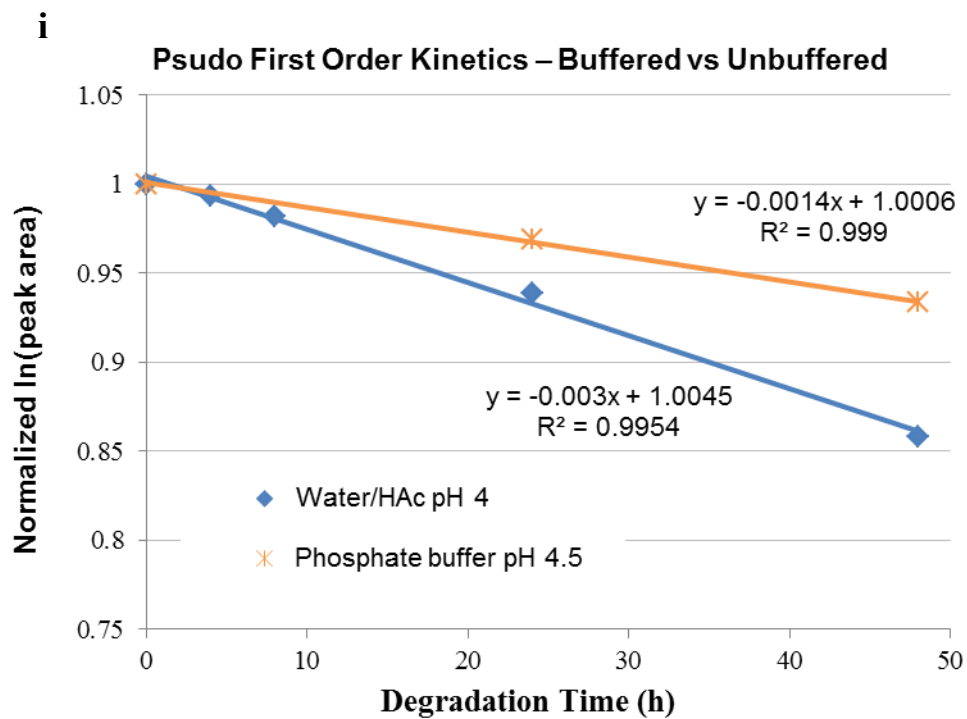


Figure 3: Comparison of the i) pseudo first order degradation kinetics of OT and ii) amount of oxytocin remaining after 48 h 70 °C heat-stress in unbuffered water at pH 4 and phosphate buffer pH 4.5.

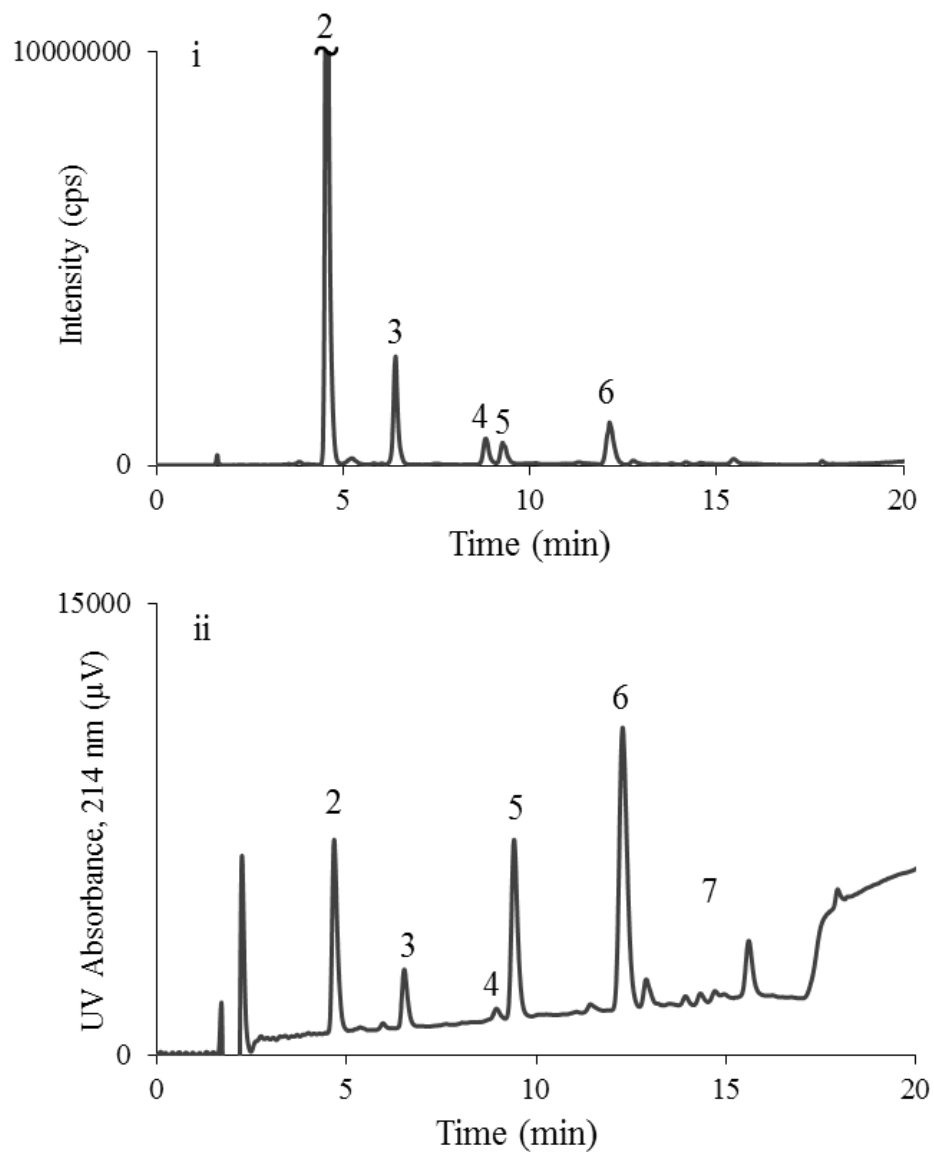


Figure 4: Comparison of the signal intensities of the degradation products of the i) MS and ii) UV chromatograms of 48 h heat-stressed oxytocin formulated in unbuffered water pH 4. Peak assignments: 1) monodesamino OT, 2) OT, 3) trisulfide OT, 4) tetrasulfide OT, 5) dimer, 6) dimer, 7) higher order aggregates.

### 4.3.3 Effect of chlorobutanol on OT degradation

To create a solution that was similar in composition to the pharmaceutical formulation, 0.5% w/v CB was added to the pH 4 unbuffered water solution (formulation D). In order to compare these results to section 4.3.2 of this chapter, CB was also added to pH 4.5 phosphate buffer (formulation B) (Table 2). The LC-UV and LC-MS results indicated that the stability of OT was significantly improved in both formulations with the addition of CB. However, the presence of CB in the unbuffered formulation showed the greatest protective effect, with 81% OT remaining in solution after 48 h at 70 °C (Figure 5ii).

In both the buffered and unbuffered samples, the kinetics of OT degradation was noticeably changed with the addition of CB as compared to the results in section 4.3.2 (Figure 5i). When the data was plotted according to first order kinetics, instead of exhibiting a linear decay during 0-48 h of degradation, both curves appear to level off. After the first 4 h there is no notable OT degradation in the unbuffered solution with CB. This indicates that perhaps equilibrium is reached within the solution. Further investigations are needed to provide a mechanistic rationale for these results.

A comparison of the two LC-UV chromatograms makes it possible to see the differences in the degradation profiles of formulations with CB compared to those without. As shown in Figure 6ii, it is possible to see the formation cyclic polysulfide products in the unbuffered formulation with CB, yet, there are no dimer products formed. In both formulations containing CB, a new unidentified peak was present that elutes between the tri- and tetra sulfide compounds. Identification of this peak by LC-MS MRM could provide useful information as to what reactions are occurring in the sample.



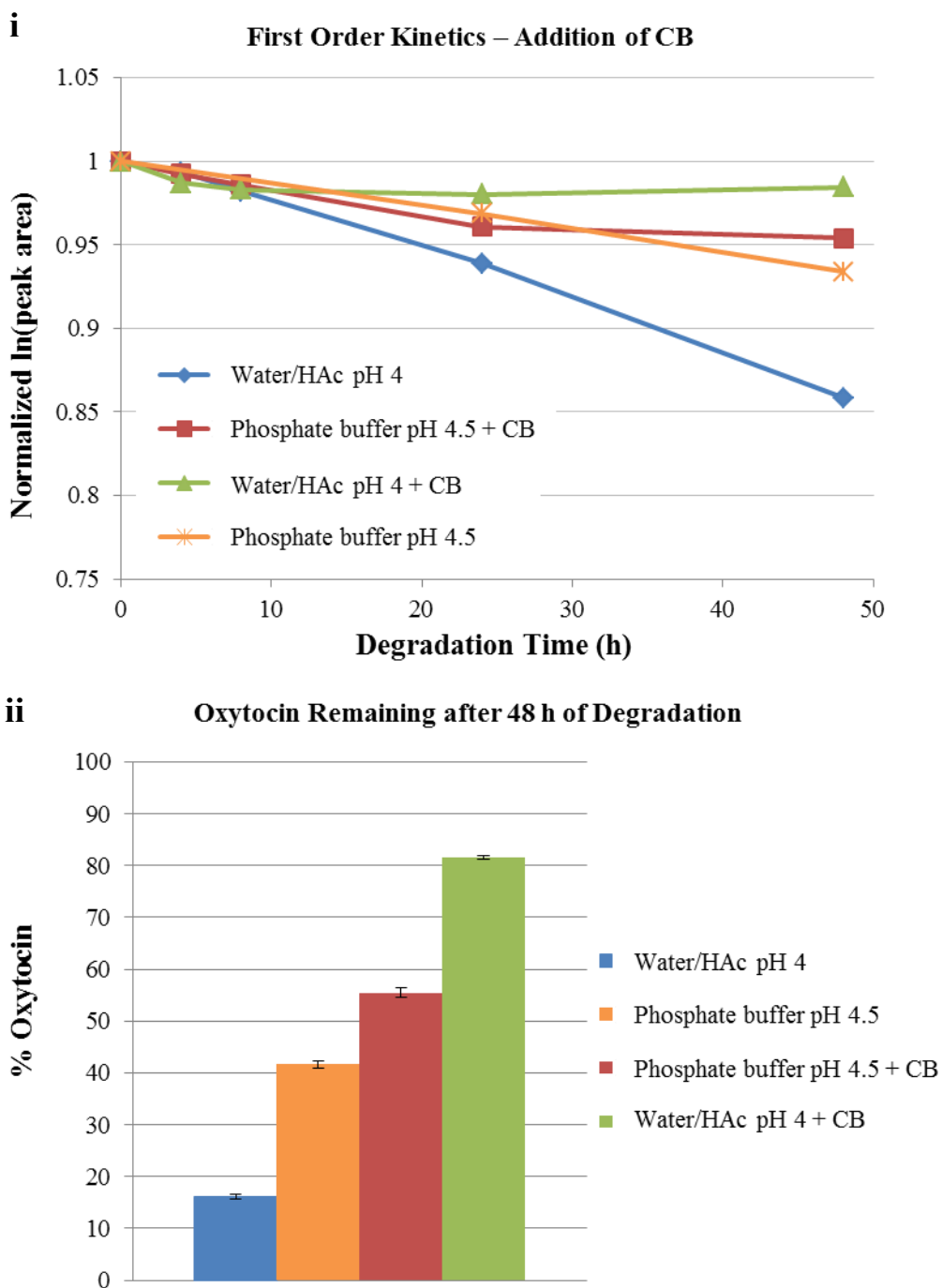


Figure 5: Comparison of the i) pseudo first order degradation kinetics and ii) amount of oxytocin remaining after 48 h 70 °C heat-stress in buffered and unbuffered formulations, with and without CB.

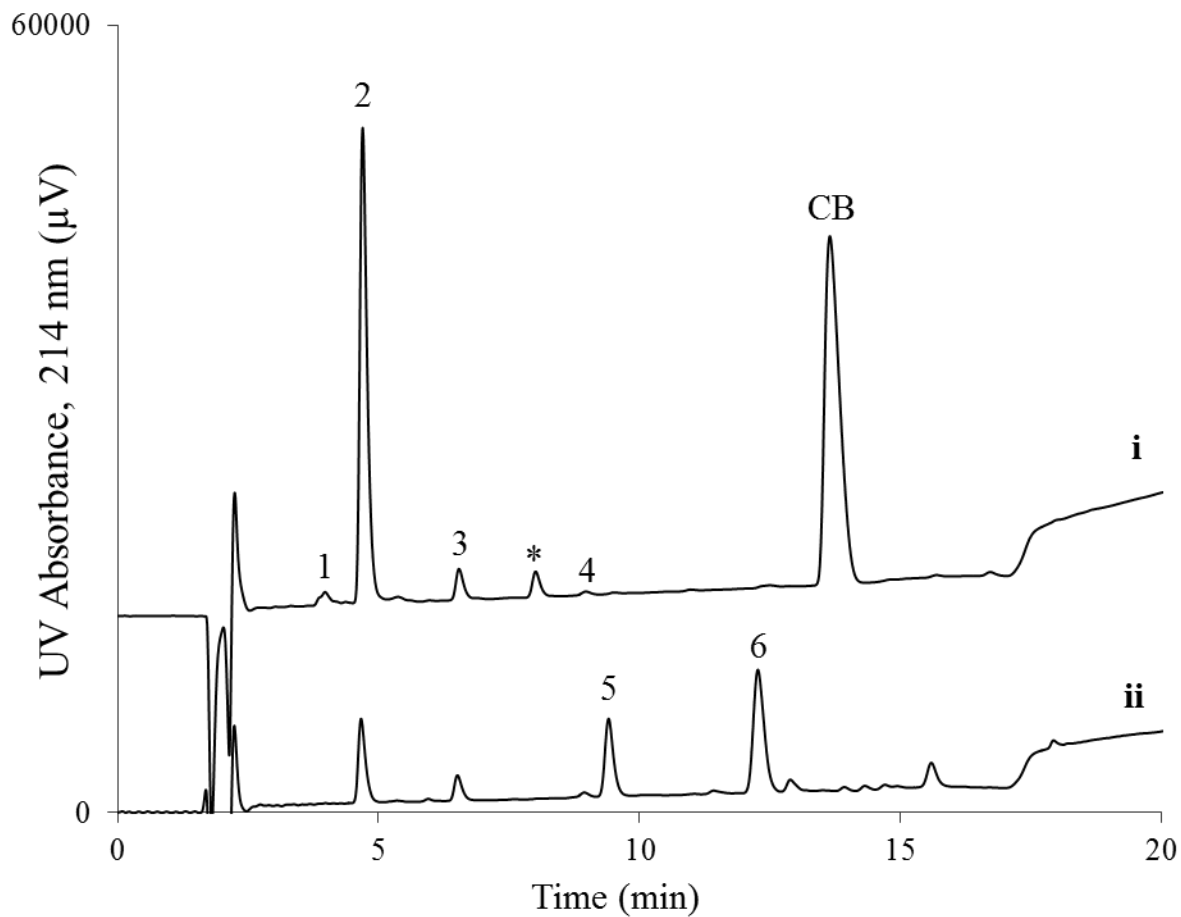


Figure 6: Comparison of the degradation products formed after 48 h at 70 °C oxytocin formulated in i) water pH 4 and ii) water pH 4 with 0.5% w/v chlorbutanol. Peak assignments: 1) monodesamino OT, 2) OT, 3) trisulfide OT, 4) tetrasulfide OT, 5) dimer, 6) dimer, 7) higher order aggregates, \*unidentified species.

#### 4.3.4 Effect of chlorobutanol-like species on OT degradation

As described above, CB has a significant effect on the stability of OT under heat-stressed conditions. To investigate the mechanism of this enhanced stability, several species with antimicrobial or structural similarity to CB were tested with OT in accelerated degradation studies.

##### 4.3.4.1. Antimicrobial effect

To ensure that the prolonged stability of OT in the presence of CB was not simply due to an antimicrobial effect, a formulation with the common antimicrobial agent, benzyl alcohol (BA), was tested (formulation K, Table 2). No protective effect was seen by the addition of BA. A plot of the pseudo first order kinetics was once again linear with a calculated half-life of 0.53 days. Additionally, in the LC-UV chromatogram, all of the previously reported degradation products were present (Figure 7iii), indicating a similar degradation mechanism to the unbuffered formulation with no additives. If anything, the rate of the degradation of oxytocin appeared to increase rather than decrease in the presence of BA. One possible explanation could be that BA has been known to result in increased formation of aggregation products in protein formulations [19, 20].

##### 4.3.4.2. Alcohol substitution

The CB molecule has two distinct functional groups that could interact with peptides. These are the trichloro group and the tertiary alcohol. To investigate the effect of the alcohol moiety on the stability of OT, ethanol (primary), isopropyl alcohol (secondary), and TBA (tertiary) were all tested (formulations F-H, Table 2). None of these formulations appeared to change OT degradation as compared to the unbuffered formulation with no additives. For example, the degradation for the formulation containing TBA was plotted according to pseudo first order kinetics and was linear between 0-48 hours with a calculated half-life of 0.68 days (similar to the 0.71 day half-life of unbuffered OT with no additives). The LC-UV chromatogram for the 48 h degradation sample containing TBA shows all of the expected degradation products with no additional peaks (Figure 7ii).

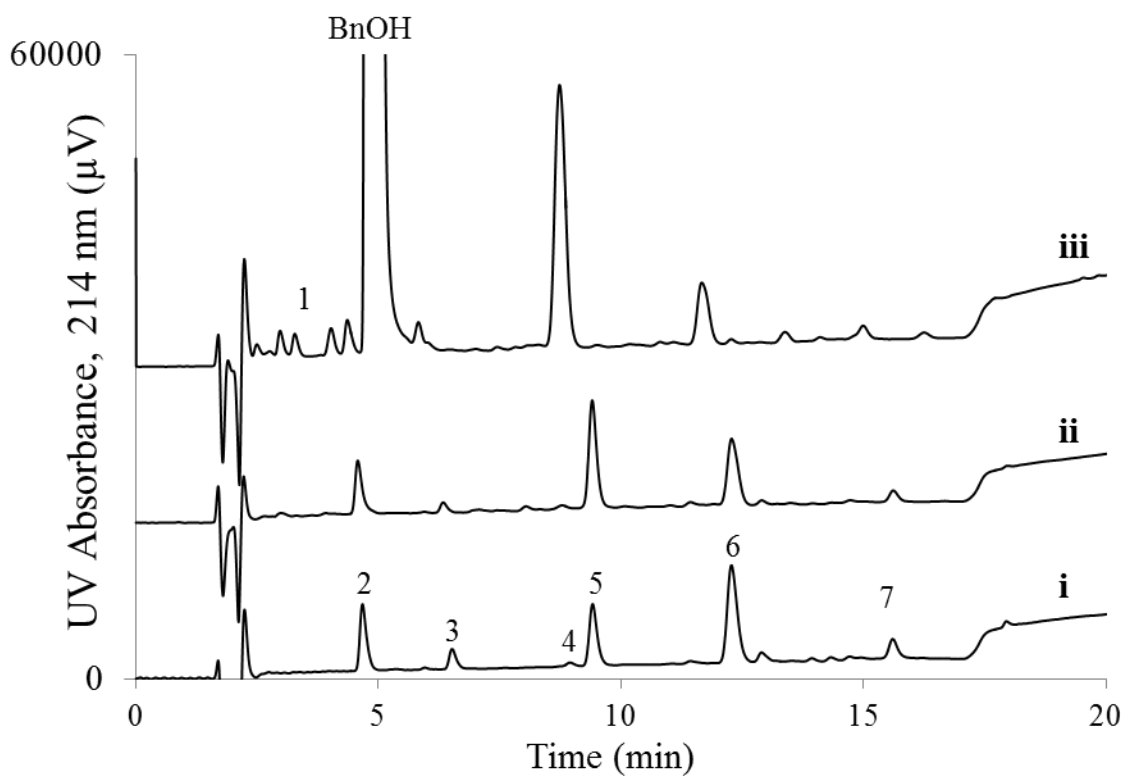


Figure 7: Comparison of the degradation products formed after 48 h at 70 °C oxytocin formulated in i) water pH 4, ii) water pH 4 with 0.5% w/v tert-butanol, and iii) water pH 4 with 0.5% w/v benzyl alcohol. Peak assignments: 1) monodesamino OT, 2) OT, 3) trisulfide OT, 4) tetrasulfide OT, 5) dimer, 6) dimer, 7) higher order aggregates.

#### 4.3.4.3. Trichloro group

To investigate the effect CB's trichloro group on the stability of the oxytocin, solutions containing either trichloroacetic acid (TCA, formulation H) or trichloroethanol (TCE, formulation I) were tested (Table 2). The presence of TCA showed a slight increase the % OT remaining after 48 h heat-stress, compared to the unbuffered formulation without additives (Figure 8ii). However, the plot of the degradation kinetics was linear with a calculated half-life of 1.2 days (Figure 8i), which is less than the buffered formulation with no additives (1.5 days). This added stability compared to the formulation in water could simply be due to the increased buffering capacity of the ammonium acetate that was necessary to increase the pH to 4 after the addition of the TCA. The LC-UV-MS data shows the formation of primarily cyclic polysulfides with dimers present at low concentration (Figure 9iii).

TCE on the other hand, elicits very similar behavior to CB in OT formulations. After 48 h at 70° C there is still 70% OT remaining in the formulation (Figure 8ii). Again, the data diverges from the expected pseudo first order kinetics, with the OT disappearance leveling off after 8 h (Figure 8i). Like CB, the LC-UV chromatogram shows that OT in the presence of TCE does not form dimers (Figure 9ii). Additionally, with TCE, an unidentified peak is produced. This peak has a different retention time to the unidentified peak seen in the CB formulation, indicating that it is a different product. If the CB and TCE are increasing the stability of OT through a new reaction mechanism, this peak could be a byproduct. Further studies are needed to identify this peak.

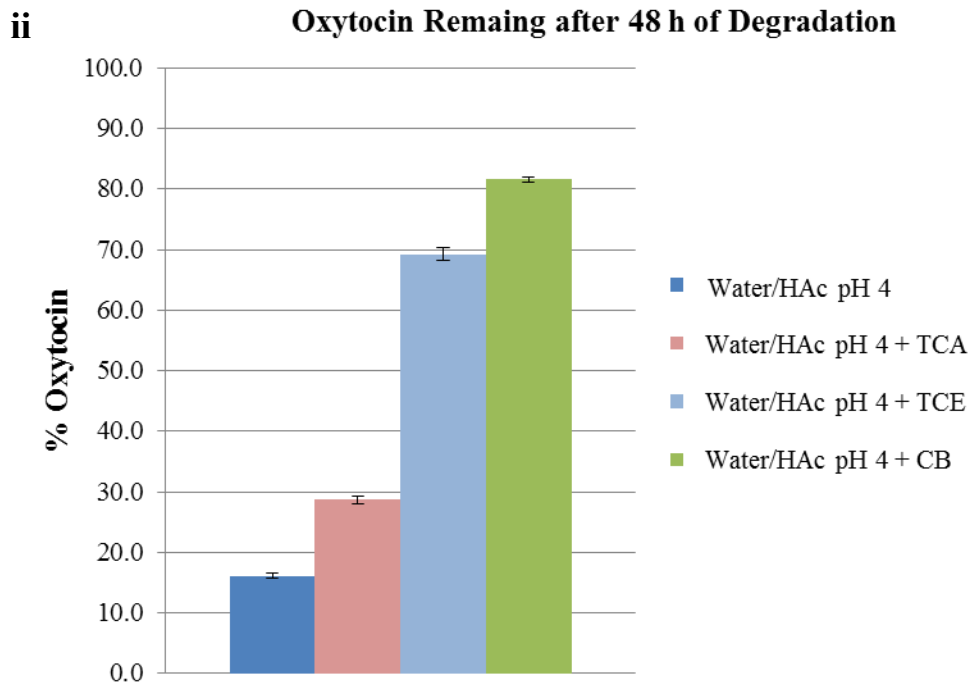
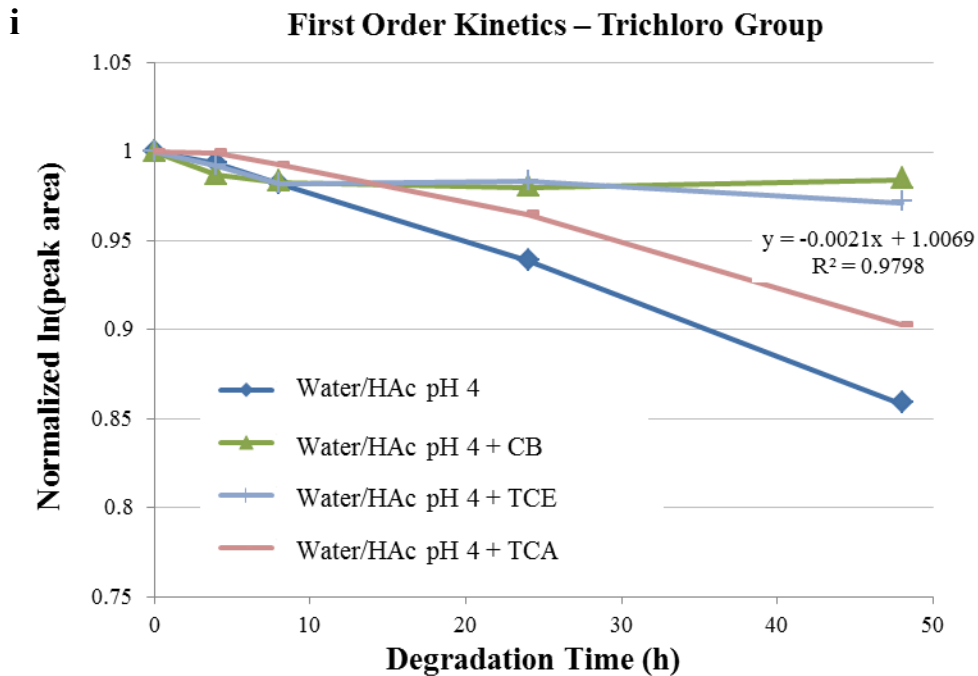


Figure 8: Comparison of the i) pseudo first order degradation kinetics and ii) amount of oxytocin remaining after 48 h 70 °C heat-stress in unbuffered formulations, with 0.5% w/v additives

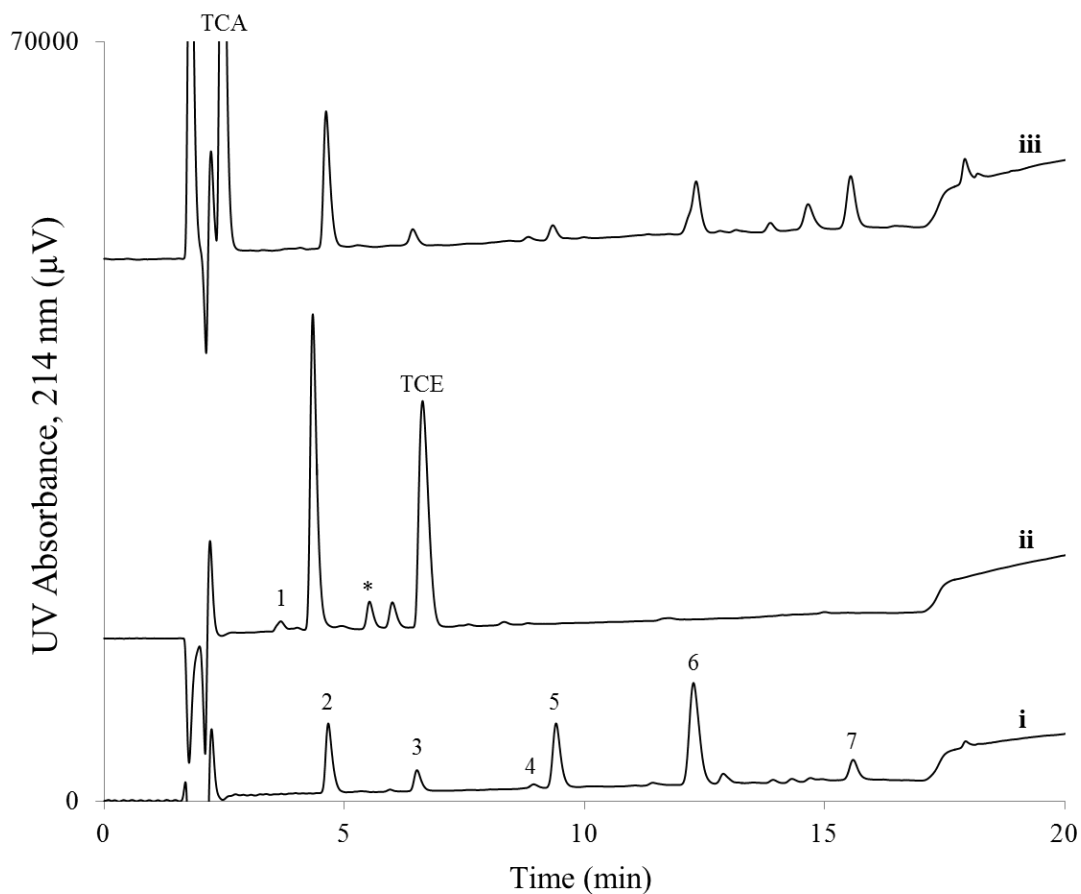


Figure 9: Comparison of the degradation products formed after 48 h at 70 °C oxytocin formulated in i) water pH 4, ii) water pH 4 with 0.5% w/v trichloroethanol, and iii) water pH 4 with 0.5% w/v trichloroacetic acid. Peak assignments: 1) monodesamino OT, 2) OT, 3) trisulfide OT, 4) tetrasulfide OT, 5) dimer, 6) dimer, 7) higher order aggregates, \*unidentified species.

#### 4.3.5 Potential rationale for increased OT stability in the presence of CB and TCE

OT in the presence of CB and TCE does not appear to form dimers. A few reports in the literature have suggested that the presence of CB reduces the likelihood of aggregation of proteins in blood samples; however, the mechanism for this stabilization was not provided [21, 22]. For OT specifically, the mechanism of degradation postulated by Wisniewski et al. indicates that the dimer products are formed from linear OT peptides after they undergo the loss of a sulfur following  $\beta$ -elimination of the disulfide bond (Figure 1) [12]. It is possible that both CB and TCE are associating with the peptide in a way that is preventing further reactions.

The conformation of OT in solution consists of two  $\beta$ -turns stabilized by the disulfide bond and considerable hydrogen bonding between multiple residues [23]. As heated cyclic OT denatures, or becomes linear following  $\beta$ -elimination of the disulfide bond, the secondary structure is removed, allowing the hydrophobic amino acid residues Tyr<sup>2</sup>, Leu<sup>8</sup>, and Ile<sup>3</sup> to interact with the solution. Tryptophan fluorescence quenching studies have shown that TCE (logP octanol-water, 1.42) associates with hydrophobic regions of proteins [24, 25], inducing stable alpha-helical secondary structure. This effect has also been seen with peptides using other halogenated alcohols, such as trifluoroethanol [26-29]. CB is even more hydrophobic, with a logP (octanol-water) value of 2.03. Therefore, it is possible that CB has an even stronger association with the hydrophobic regions of the peptide. With such a small peptide, any association of CB to the hydrophobic residues of OT could prevent nearby thiols and N-termini from interactions that lead to the formation of dimers. To investigate the effect of CB on the peptide structure, further studies by nuclear magnetic resonance and circular dichroism should be done on the peptide-preservative mixtures.

In addition to the mechanism for the degradation products previously discussed, it is possible for OT to undergo disulfide scrambling through radical-based reactions in the presence of light and heat. Mozziconacci has reported the formation several products [30] that had not been described in the previous published reports [11, 12, 17]. Through personal discussions with Mozziconacci, it was postulated that



under high temperature conditions, the generation of sulfur centered radicals could lead to the formation of both the cyclic polysulfides and dimers. In this case, it is possible that CB and TCE could be acting as electron scavengers and preventing degradation before it can occur.

Regardless of the mechanism, structural identification of the additional peak seen in the chromatograms for both the TCE and CB formulation is necessary to gain more information on how it could be formed. MRM analysis should be performed on the new peak before and after reduction and alkylation. These studies will provide further structural information and allow for product identification and direction of additional experiments.

#### **4.4 Concluding remarks**

Despite the widespread use of OT for clinical purposes in maternal health, not much is known regarding the mechanism of degradation of this peptide in its commercial pharmaceutical formulation. In this chapter, a preliminary look at the degradation products when OT is formulated in solution similar to its pharmaceutical preparation was accomplished. Oddly, in the presence of the antimicrobial preservative CB, the stability of oxytocin is increased. In an attempt to determine the reason for this increased stability, a variety of compounds of structural similarity to CB were tested in accelerated degradation studies. Of all of the compounds tested, only 0.5% w/v TCE was capable of inducing a similar stabilizing effect in the OT formulation. TCE also showed similarities to CB in the lack of dimer products formed during degradation. Additionally, in both the CB and TCE samples, an unidentified peak was seen in the LC-UV chromatogram. Further studies to determine identity of this peak are necessary.

In addition to investigating the mechanism by which CB improves OT stability, future directions of this project will be to further optimize the CE separation discussed in chapter 3 to include the dimer and cyclic polysulfide products. This will accomplish the goal of creating a low-cost assay to determine the stability of OT in the supply chains of developing countries.

## 4.5 References

- [1] Rohrbasser, C., Rheme, D., Decastel, S., Roth, S., Aja Montes, M. d. L., Veuthey, J.-L., Rudaz, S., *Chimia* 2009, 63, 890-891.
- [2] Marini, R. D., Rozet, E., Montes, M. L. A., Rohrbasser, C., Roht, S., Rheme, D., Bonnabry, P., Schappler, J., Veuthey, J. L., Hubert, P., Rudaz, S., *J. Pharm. Biomed. Anal.* 2010, 53, 1278-1287.
- [3] Creamer, J. S., Krauss, S. T., Lunte, S. M., *Electrophoresis* 2014, 35, 563-569.
- [4] Cornell Manning, M., Chou, D. K., Murphy, B. M., Payne, R. W., Katayama, D. S., *Pharm. Res.* 2010, 27, 544-575.
- [5] Hogerzeil, H. V., Walker, G. J. A., de Goeje, M. J., *Action Programme on Essential Drugs, World Health Organization.* 1993, 1-50.
- [6] Dudkiewicz-Wilczynska, J., Snyckerski, A., Tautt, J., *Acta Pol. Pharm.* 2000, 57, 403-406.
- [7] Krummen, K., Frei, R. W., *J. Chromatogr.* 1977, 132, 429-436.
- [8] Ohta, M., Fukuda, H., Kimura, T., Tanaka, A., *J Chromatogr* 1987, 402, 392-395.
- [9] Chaibva, F. A., Walker, R. B., *J. Pharm. Biomed. Anal.* 2007, 43, 179-185.
- [10] Wang, G., Miller, R. B., Melendez, L., Jacobus, R., *J. Liq. Chromatogr. Relat. Technol.* 1997, 20, 567-581.
- [11] Hawe, A., Poole, R., Romeijn, S., Kasper, P., van der Heijden, R., Jiskoot, W., *Pharm. Res.* 2009, 26, 1679-1688.
- [12] Wiśniewski, K., Finnman, J., Flipo, M., Galyean, R., Schteingart, C. D., *Peptide Science* 2013, 100, 408-421.
- [13] Meyer, B. K., Ni, A., Hu, B., Shi, L., *J. Pharm. Sci.* 2007, 96, 3155-3167.
- [14] Brange, J., Langkjaer, L., *Acta Pharm. Nord.* 1992, 4, 149-158.
- [15] Hutchings, R. L., M. Singh, S., Cabello-Villegas, J., Mallela, K. M. G., *J. Pharm. Sci.* 2013, 102, 365-376.
- [16] de Hoffmann, E., Stroobant, V., *Mass Spectrometry, Principles and Applications*, John Wiley and Sons LTD 2007.

- [17] Haselberg, R., Brinks, V., Hawe, A., de Jong, G. J., Somsen, G. W., *Anal. Bioanal. Chem.* 2011, *400*, 295-303.
- [18] Kuipers, B. J. H., Gruppen, H., *J. Agric. Food Chem.* 2007, *55*, 5445-5451.
- [19] Roy, S., Katayama, D., Dong, A., Kerwin, B. A., Randolph, T. W., Carpenter, J. F., *Biochemistry* 2006, *45*, 3898-3911.
- [20] Tobler, S. A., Holmes, B. W., Cromwell, M. E. M., Fernandez, E. J., *J. Pharm. Sci.* 2004, *93*, 1605-1617.
- [21] Chen, S. L., Yang, W. C., Huang, T. P., Wann, S., Teng, C. M., *Thromb. Haemostasis* 1990, *64*, 473-477.
- [22] Stewart, M. W., Gordon, P. A., *Thromb. Res.* 1991, *64*, 757-762.
- [23] Urry, D. W., Walter, R., *Proc. Nat. Acad. Sci. U. S.* 1971, *68*, 956-958.
- [24] Eftink, M. R., Zajicek, J. L., Ghiron, C. A., *Biochim. Biophys. Acta, Protein Struct.* 1977, *491*, 473-481.
- [25] Solt, K., Johansson, J. S., *Pharmacology* 2002, *64*, 152-159.
- [26] Jackson, M., Mantsch, H. H., *Biochim. Biophys. Acta, Protein Struct. Mol. Enzymol.* 1992, *1118*, 139-143.
- [27] Lee, C.-S., Lin, C.-H., Hsieh, W.-L., Chiao, S.-M., Tung, W.-C., *J. Nanosci. Nanotechnol.* 2014, *14*, 5568-5573.
- [28] Lee, C.-S., Tung, W.-C., Luo, W.-C., *Protein J.* 2012, *31*, 222-228.
- [29] Lehrman, S. R., Tuls, J. L., Lund, M., *Biochemistry* 1990, *29*, 5590-5596.
- [30] Mozziconacci, O., Schoeneich, C., *J. Pharm. Sci.* 2012, *101*, 3331-3346.

**Chapter Five:**

**Development of Methods for On-site Separation Based Analysis of Small Molecule**

**Pharmaceuticals for use in Developing Countries**

## 5.1 Introduction

Counterfeit drugs are reported to make up to 20% of the global market, and this number can be as high as 50-60% in developing countries [1, 2]. The term “counterfeit” covers a variety of products that are “deliberately and fraudulently mislabeled with respect to identify or source” [3]. In a survey published by the World Health Organization (WHO), all counterfeit drugs seized over a two-year period were classified into several categories. Of the 46 reports, only 17.8% of the products were the correct drug at the correct amount that was being distributed in falsified packaging. The remaining 82.2% were substandard medicines: 32.1% contained no active ingredient, 20.2% had an incorrect amount of active ingredient, 21.4% contained of the wrong active ingredient, and 8.5% had high levels of impurities and contaminants [4].

The presence of these substandard medicines in developing countries has a huge negative impact on public health. Medications that contain little-to-no active ingredient can prolong sickness and increase the likelihood of death, while taking a drug containing the wrong active ingredient can lead to serious side effects. Additionally, any inconsistency in the source of the drugs that leads to switching from authentic drug to counterfeit and back again, can lead to the emergence of drug-resistant bacteria, which pose a global health threat. Due to the increasing prevalence of counterfeit drugs in developing countries, quality control of pharmaceuticals must now be performed at multiple checkpoints throughout the distribution system, in addition to the screening that occurs when products enter the country. The ability of a government to maintain an effective regulatory authority directly impacts the likelihood of counterfeits getting to market. Of the 191 WHO member states, only 20% can maintain a functioning regulatory presence, while 30% have no regulation at all [4].

A major roadblock to a reliable regulatory effort in developing countries is the lack of appropriate instrumentation to screen the supply chain for counterfeit drugs. Quality control of pharmaceuticals is normally accomplished in a permanent laboratory that contains state of the art instrumentation (i.e. HPLC and MS), and most USP and EUP methods have been developed with this environment in mind.

Unfortunately, these types of laboratories do not exist in developing countries for many reasons, including the lack of funding, access to trained personnel, and improper infrastructure (electricity and running water) needed to support HPLC or MS. Therefore, portable, user-friendly, and inexpensive alternatives are needed to perform high-throughput screening of pharmaceuticals in the absence of a traditional laboratory setting.

Due to the large number of samples that need to be screened each day, non-destructive methods, that do not require extensive sample preparation, are popular. One strategy has been to develop innovative tracking codes and anti-counterfeit packaging to maintain a more secure distribution of pharmaceuticals across the world by providing a simple visual-based inspection to verify identity [5, 6]. Recently, the FDA developed a multiple wavelength emitter (CD-3) that can be used to visually screen tablet coatings and packaging in comparison to the authentic product [7-9]. The latest version of this device is handheld and battery operated, allowing it to be transported to wherever it is needed. While the CD-3 is a very useful and groundbreaking technique for first-pass screening of products, it gives no chemical information about the drug.

For products that fail the first-pass inspection, a secondary analysis is needed to get more information regarding chemical composition. Handheld devices for X-ray fluorescence [10], Raman [11, 12] or infrared [13, 14] spectroscopy are commercially available and well suited for this task. However, the cost of these devices is far beyond what is reasonable for developing countries. For example, a single handheld Raman spectrometer can cost anywhere from 20,000 to 50,000 USD. With this high start-up cost, it is unlikely enough devices could be purchased to cover the multiple distribution lines, store houses, and clinics located throughout a large country. Additionally, while these spectrometers are able to provide qualitative information regarding the chemical composition of the tablet based on spectra matching of the compounds to a library, they have limited quantitative ability [15, 16], making them unable to detect counterfeits containing the wrong amount of active ingredients.

Thin-layer chromatography (TLC) kits by Minilab™ that use colorimetric detection have been widely used as an inexpensive, portable method for monitoring pharmaceutical quality [17]. While TLC is capable of providing semi-quantitative results for a wide variety of drugs commonly used in developing countries [18, 19], the downside of this technique is that it is both time and resource intensive. Each test requires several sample preparation steps to get the tablet into solution, and then mL amounts of organic solvents are needed to perform the separation and detection. This whole process can take upwards of 30 min per plate to accomplish. Additionally, to obtain reproducible and accurate results, the test is best performed by trained personnel.

Paper-based lateral-flow assays, on the other hand, are more environmentally friendly and easy to use. These tests have been thoroughly investigated for low-cost diagnostics for developing countries [20-23]. More recently, this approach has also been explored for on-site pharmaceutical quality control. For example, Weaver et al. described simple, yet specific paper-based tests for beta-lactam antibiotics and anti-tuberculosis (TB) drugs [24]. In this assay, the tablet is scraped across a test card, eliminating the crushing and dissolving sample preparation steps. The test card contains several lanes of dried reagents that react with the formulation to produce colored products. Using water in the place of organic solvents, the small amount of powdered tablet, deposited on the paper, is dissolved and brought into the reagent zones via capillary action. These reagents are designed to react with specific functional groups known to be present in the active ingredient and excipients that make up the formulation. While these tests are only qualitative, they give much more information regarding the structure of the drug compared to TLC.

Microchip electrophoresis (ME) is a versatile separation technique that can be used to supplement the information gained from the qualitative analysis methods that are currently available in developing countries. A separation-based assay allows for simultaneous identification of degradation products and active ingredient that is not possible with the lateral-flow tests. Further coupling of ME to a universal detection system can also be used for quantitative analysis, giving a more accurate assessment of active ingredient concentration than is possible with the handheld spectrometers. Due to the small dimensions of

the separation channel, ME requires only a few microliters of sample and reagent, keeping the cost-per-test low and leading to a short total analysis time. Additionally, because fluid movement is accomplished through the application of voltage, there is no need for expensive small-volume pumps.

In the laboratory, ME can be coupled to a variety of detectors depending on the needs of the assay. However, the ability to incorporate electrodes directly into the design of the microchip and miniaturize the associated electronics, makes electrochemical detection a more attractive method for on-site analysis compared to spectroscopic methods such as UV or LIF [25, 26]. With the micrometer pathlengths and picoliter sample plugs characteristic of ME, the limits of detection (LOD) achievable with UV spectroscopic detection are extremely high. LIF detection exhibits lower the LODs; however, derivatization chemistry for molecules that do not contain a fluorophore is required, increasing the complexity of the assay. For a more useful and universal detection of charged species, capacitively coupled contactless conductivity detection ( $C^4D$ ) can be used. ME was first coupled with  $C^4D$  in 2001 [27] and it has since been used for the analysis of biological, environmental, and pharmaceutical samples as described in an several excellent reviews [28].

Conductivity detection works by placing two electrodes (working and detection) opposite each other within the separation channel. In direct conductivity detection the electrodes are placed inside the separation channel (Figure 1a). A low frequency alternating signal is applied to the working electrode to compensate for the formation of the electric double layer at the electrode surface. The signal received at the second electrode is inversely proportional to the resistance of the fluid in the channel between the two electrodes  $G = 1/R = 1/V$ , where  $G$  is conductance,  $R$  is resistance, and  $V$  is voltage. If the analyte zone is charged and therefore less resistive than the BGE, it will be more conductive and will yield a positive peak in the electropherogram. On the other hand, if the zone is more resistive than the background electrolyte, a negative peak will be observed.



In  $C^4D$ , the electrodes are isolated from the fluid in the separation channel by an insulating layer. In this system the electrode, insulating layer, and solution behave similarly to a parallel plate capacitor (conductor/dielectric/conductor) (Figure 1b). To overcome the high impedance of the signal transmission across the insulating layer, a high frequency signal must be used. The generation of a high frequency alternating current at the working electrode creates the polarization of the dielectric. As the signal travels through the solution to the second electrode, the resulting current that is measured depends on the capacitive reactance of the dielectric ( $C_w$ ), the resistance of the solution, and the reactance of the stray capacitance ( $C_0$ ) (the direct capacitive coupling between the electrodes) as shown in the simple circuit diagram in Figure 1c. By keeping  $C_w$  low and  $C_0$  high, the current varies linearly with the conductivity of the solution [28].  $C^4D$  has less background noise than contact conductivity due to the isolation of the electrodes, and it also prevents electrode fouling and bubble formation that can occur when the electrodes are placed in the solution.

For implementation in developing countries, single-use disposable components coupled with reusable instrumentation are an excellent way to achieve high-performance, low-cost analysis of samples [23]. Since the electrodes in  $C^4D$  are placed outside of the channel and isolated from the fluid, it is possible to build a device that reuses the electrode board. The electrodes are the most expensive part of the microchip, and reusing them will help keep the cost-per-test low. The part of the microfluidic that houses the channels for ME can be fabricated from a variety of low-cost materials. While glass has been traditionally employed for the fabrication of these devices due to its well characterized surface properties, glass microchips are expensive and time consuming to produce. More robust and inexpensive microchips can be manufactured from polymers and plastics [29-32] using large scale manufacturing processes. These plastic chips can be easily aligned within the electrode board, used once, and disposed of, allowing for a much cheaper portable test than the handheld spectrometer, with greater analytical capability than TLC or paper-based devices.

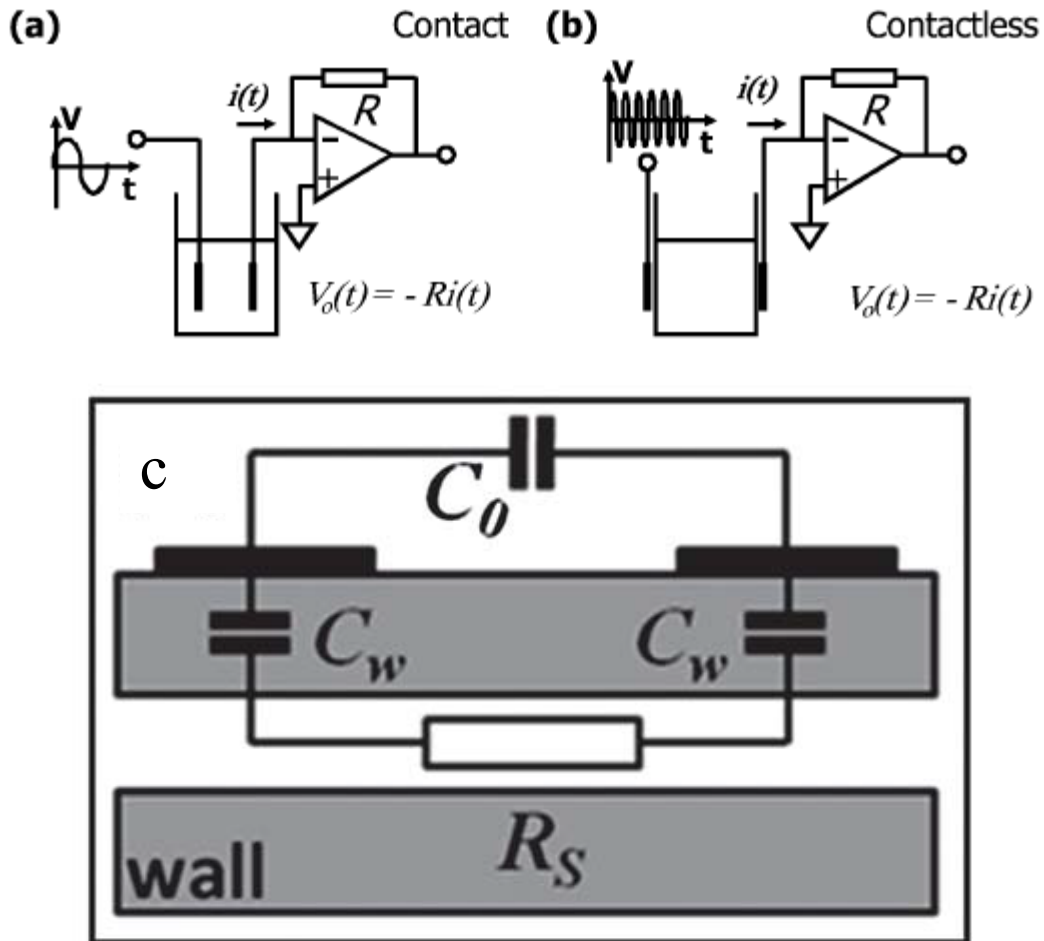


Figure 1: Comparison between the a) contact and b) contactless conductivity detection. C) A simplified electrical circuit diagram of the electrodes relationship to the solution. The grey blocks represent the top and bottom microchannel walls with the solution between them. The top wall has the capacitively coupled electrodes on it.  $C_w$ , wall capacitance;  $C_0$ , stray capacitance;  $R_s$ , solution resistance. Reprinted with permission from Coltro et al (ref 28).

In this chapter, a ME-C<sup>4</sup>D method is developed for the determination of two first-line anti-TB drugs, ethambutol (EMB) and isoniazid (INH) (Figure 2). Tuberculosis is a deadly communicable disease that, despite being treatable, is responsible for 1.5 million deaths per year worldwide. One of the major factors directly impacting access to life-saving medication is the distribution of counterfeit drugs within developing countries via unregulated supply chains. Both CE-UV and CE-C<sup>4</sup>D have been evaluated as fast and inexpensive methods for the analysis of first-line anti-TB drugs [33, 34]. To improve the portability and, therefore, feasibility of on-site analysis, ME-C<sup>4</sup>D was used to separate EMB and IHN, and partially separated EMB from its major degradation product 2-aminobutanol (2-AMB).

## 5.2 Materials and methods

### 5.2.1 Chemicals and reagents

HEPES, lactic acid, MES, histidine, diethylamine (DEA), ethylenediamine (EDA), EMB, INH, and 2-AMB were obtained as analytical grade reagents from Sigma Aldrich (St. Louis, MO). The acetone was received from Fisher Scientific (Fair Lawn, NJ). For the studies involving the commercial formulated drug, EMB hydrochloride (EMB HCl) produced by Teva pharmaceuticals (Petah Tikva, Israel) was used. All BGE and sample solutions were prepared with 18 M $\Omega$  ultrapure water (Millipore, Billerica, MA) and filtered through a 0.2  $\mu$ m pore nylon filters prior to use (GE Water and Process Technologies, Trevose, PA, USA).

The following supplies were used as received: 100 mm Si wafers (Silicon Inc, Boise, ID); AZ 1518 photoresist and AZ 300 MIF developer (Mays Chemical, Indianapolis, IN); SU-8 10 negative photoresist and SU-8 developer (MicroChem, Newton, MA); Slygard 184 Silicone Elastomer Kit: PDMS (Ellsworth Adhesives, Germantown, WI, USA); Borosilicate float glass, 4" x 1.1 mm (Precision Glass and Optics, Santa Ana, CA); Pt (99.99% purity) and Ti (99.97% purity) targets (2 in. diameter  $\times$  0.125 in. thick; Kurt J. Lesker Co., Clairton, PA); gloss laminating sheets – acid free (U.S. Stamp & Sign, Cookeville, TN); and Ag colloidal paste (Ted Pella, Redding, CA, USA).

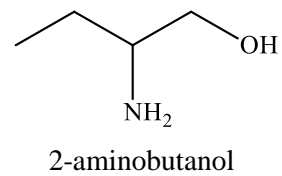
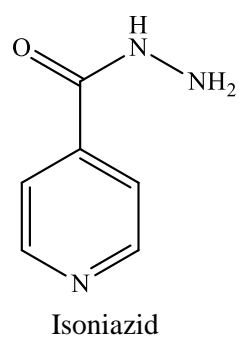
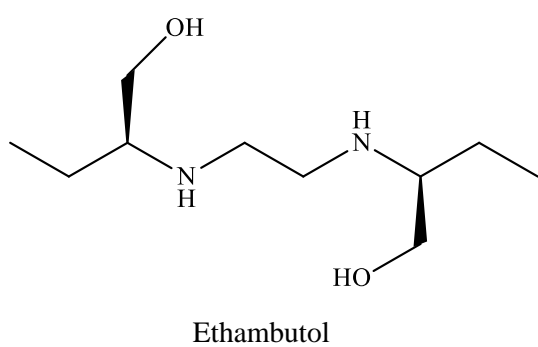


Figure 2: Structures of first line anti-TB drugs ethambutol and isoniazide. Structure for 2-aminobutanol, the major degradation product of ethambutol.

### 5.2.2 Background electrolyte preparation

For ME-C<sup>4</sup>D experiments, two BGEs were used. A BGE composed of 30 mM MES and 50 mM histidine was prepared by combining the correct amount of both components to nanopure water to achieve the desired concentration. At this ratio of MES to histidine the pH of the solution is  $6.0 \pm 0.1$  and no additional pH adjustment is needed. To prepare the 60 mM HEPES, pH 4.0 BGE, a stock solution of 200 mM HEPES was made weekly and diluted daily. A 5 M lactic acid solution was used to adjust the pH of the 60 mM HEPES BGE to pH 4.0 (final concentration of lactic acid was approximately 0.1 mM).

### 5.2.3 Sample preparation

Stock solutions of EMB, INH, EDA, and DEA were prepared at a concentration of 20 mM in ultrapure water. These solutions were stored at 4 °C and diluted to the desired concentration with BGE prior to use. The stock solution of 2-AMB was prepared day of the experiment at a concentration of 5 mM in BGE.

For the analysis of the pharmaceutical formulations, three EMB tablets were weighed and pulverized with a mortar and pestle. Based on the reported drug concentration of 400 mg per tablet, and the average weight of the three pills, the appropriate amount of powder was weighted out to produce a 5 mL solution of 5 mM EMB in BGE. This solution was sonicated for 30 min and filtered through a 0.2 µm pore nylon filters prior to use.

The lab-made counterfeits were created by mixing the correct amount of powered EMB tablet and sucrose to create formulations of 0, 25, 50, and 100% ETB. These formulations were dissolved in 10 mL (final concentration was 10 mM for the 100% solution), sonicated for 30 min, and filtered through a 0.2 µm pore nylon filters. Finally they were diluted by a factor of 10 in BGE (1 mM for the 100% solution) prior to use.

## 5.2.4 Microchip design

### 5.2.4.1 PDMS microchannel fabrication

The channels of the ME device were molded into PDMS using a previously described procedure [35, 36]. Briefly, a 100 mm silicon wafer was coated with SU-8 10 negative photoresist using a spin coater. The photoresist was cross-linked in the pattern of the channels by exposure to UV light for 16 s through a negative mask with the transparent microchip features on a black field (Infinite Graphics, Minneapolis, NM). After exposure, the unreacted photoresist was removed with SU-8 developer, leaving raised microchannel features on the wafer (40  $\mu\text{m}$  wide and 15  $\mu\text{m}$  tall). A 10:1 mixture of PDMS to curing agent was poured over the wafer and placed in an oven to cure at 70  $^{\circ}\text{C}$  for 2 h. The PDMS layer was then peeled off, leaving an imprint of the microchannels in the polymer. Access to these channels was provided through reservoirs made by a 4 mm biopsy punch at the end of each channel (Harris Uni-Core, Ted Pella, Redding, CA). All experiments were performed with a 5 cm separation channel and 0.75 cm side arms in the design of the simple-t microchip (Figure 3a).

### 5.2.4.2 Electrode fabrication

A lift-off process was used to fabricate the platinum electrodes that were used for conductivity detection. The process has been previously described by Vazquez et al [37]. Borosilicate float glass was coated with positive photoresist (AZ 1518) and exposed to a UV light through a negative mask (transparent electrode features on a black field) for 10 s. After exposure, the plate was placed in 300 MIF developer to remove unreacted photoresist, leaving exposed glass in the shape of the electrodes surrounded by photoresist. The plate was subjected to a plasma de-scum to etch the exposed glass, remove impurities, and prepare the surface for better metal adhesion. It was then immediately placed in the thin layer deposition chamber where a 200  $\text{\AA}$  Ti adhesion layer was deposited followed by a 4000  $\text{\AA}$  Pt layer. To complete the process, the photoresist (covered by excess Ti and Pt) was removed by placing the plate in an acetone bath for 5 min, leaving behind the Pt electrodes (Figure 4) of 650  $\mu\text{m}$  wide with a

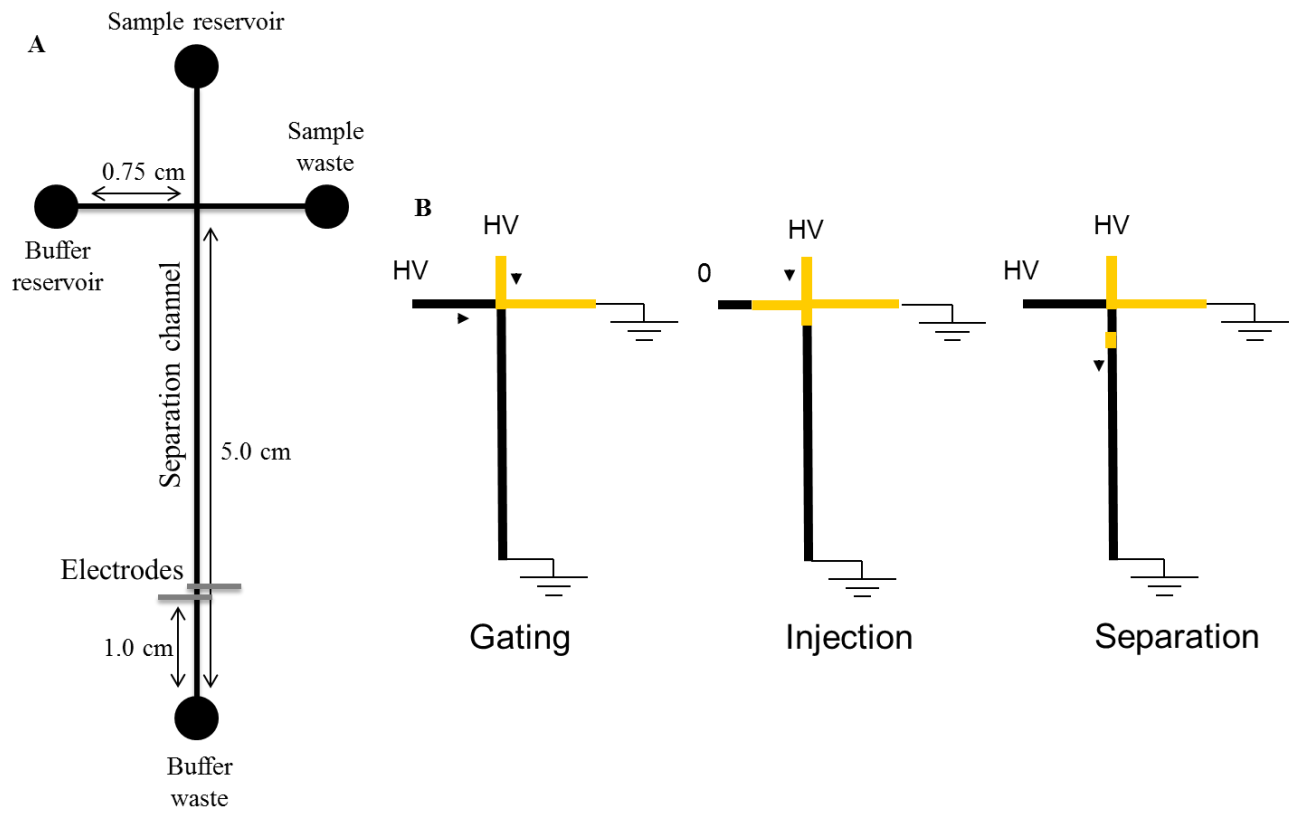


Figure 3: Cartoon schematic of the A) simple-t microchip dimensions and B) gated injection

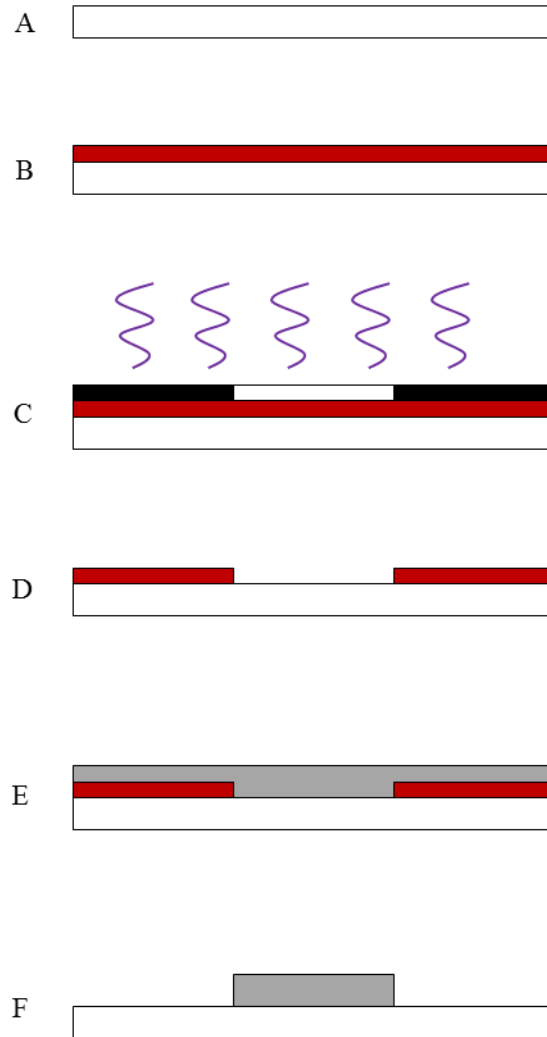


Figure 4: Step-by-step cartoon schematic of the lift-off electrode fabrication. A) borosilicate glass plate, B) spin-coated photoresist, C) UV exposure through negative mask, D) remove exposed photoresist, E) Ti and Pt sputtered over photoresist and glass, F) “lift off” remaining photoresist with acetone.



200  $\mu\text{m}$  gap between them. Pt wires were connected to the electrodes with colloidal silver paste and secured to the plate with quick-set epoxy.

#### 5.2.4.3 Microchip construction

The face of the glass plate containing the  $\text{C}^4\text{D}$  electrodes was covered by a thin layer of an adhesive polyester laminating sheet to isolate the metal electrode from the separation channel. The cured PDMS layer, containing the microchannels, was then aligned and reversibly sealed over the polyester layer (Figure 5). The electrodes were placed perpendicularly to the separation channel 1 cm from the buffer waste reservoir (Figure 3a).

#### 5.2.5 Microchip operation

A gated injection scheme was used to introduce sample into the separation channel of the simple-t microchip for analysis. The voltages were applied to the appropriate reservoirs using a programmable Jenway Microfluidic Power Supply (Dunlow, Essex, UK) controlled by an in-house Labview program (National Instruments, Austin, TX). To establish the gate, one high-voltage lead was placed in the sample reservoir and one in the buffer reservoir, with an earth ground in the sample waste and buffer waste reservoirs. To inject, the high-voltage at the buffer reservoir was floated, allowing the sample to fill the channel intersection. After a defined period of time, the voltage was reapplied and the gating was reestablished, leaving a discrete plug of sample in the separation channel to undergo electrophoresis (Figure 3b).

#### 5.2.6 Instrumentation for $\text{C}^4\text{D}$

A BK Precision function generator (Yorba Linda, CA) was used to apply a signal of 400-500 kHz (optimized daily) with an amplitude of 10  $V_{\text{pp}}$  at the working electrode. The detection circuitry was fabricated in-house by members of the Instituto de Química de São Carlos at the University of São Paulo, Brazil [38, 39]. The voltage output was collected and converted from analog to digital through an

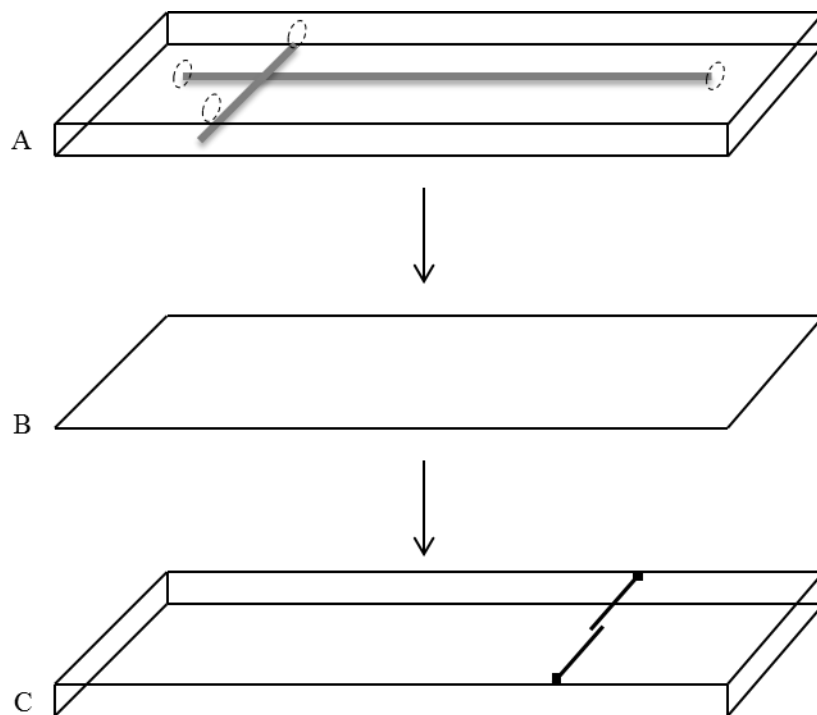


Figure 5: Construction of the ME with C4D chip. A) PDMS layer with embedded microchannels, B) polyester insulating layer, and C) glass plate with electrodes.

in-house Labview program. To reduce the background interference, the whole microchip was placed inside a Faraday cage (Figure 6).

### 5.3 Results and discussion

#### 5.3.1 Rational for BGE composition

To decrease the background current in  $C^4D$ , low-conductivity BGEs are typically used. The zwitterionic collection of Good's buffers and amino acids are particularly attractive for this purpose. A previous report for the CE- $C^4D$  separation and detection of EMB and 2-AMB used a BGE composed of 30 mM MES and 50 mM histidine at pH 6.0 [34].

The initial investigation of EMB on-chip was performed using the same MES/histidine BGE. A standard solution of 5 mM EMB was analyzed on the 5 cm simple-t microchip discussed in section 5.2.4.3 (Figure 7a). With this BGE it was possible to resolve EMB and 2-AMB (Figure 7b). However, detection of INH is not possible at this pH because it has no charge. Figure 8 shows a plot prepared by Faria et al that shows the effect of the BGE pH on the electrophoretic mobilities of EMB and INH [33]. At pH values above 5.5, INH is neutral and will give no response in  $C^4D$ . As can be seen from the graph, there is a small window between pH 3.5 and 4.5 where both EMB and INH are charged and can be separated based on difference in mobilities.

To achieve a BGE at pH 4.0, where both EMB and INH are positively charged, a BGE consisting of 60 mM HEPES, 0.1 mM lactic acid at pH 4.0 was chosen. In our studies, with the 5 cm long channel, EMB and INH were fully resolved (Figure 9c). Unfortunately, EMB and 2-AMB were only partially resolved using with this system (Figure 10b). It is possible that the resolution could be improved by using a chip with a longer separation channel, or by further optimization of the BGE; however, other chip designs and BGEs were not investigated at this time.

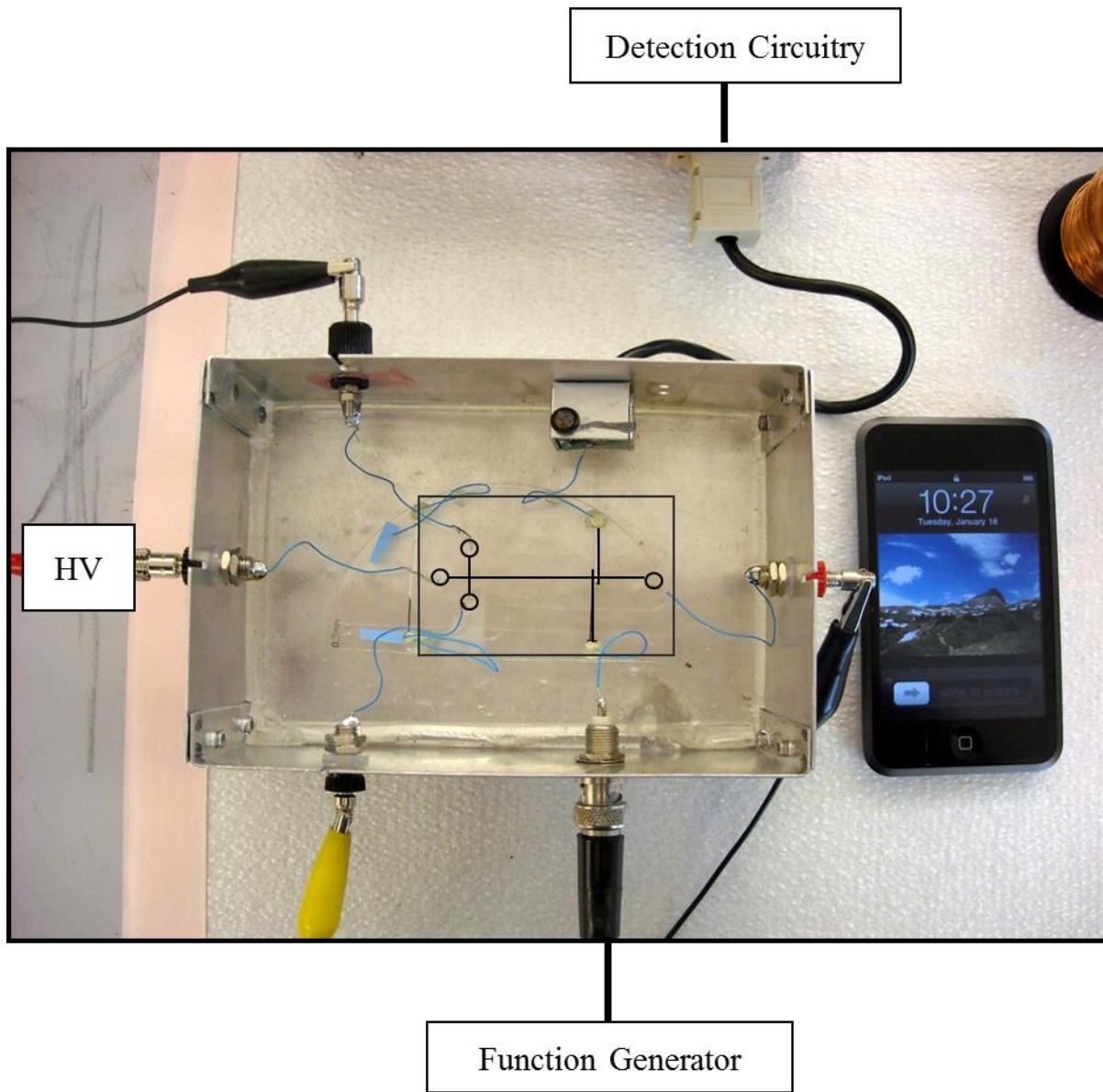


Figure 6: Photo of the microchip sitting inside the C<sup>4</sup>D box containing electrical leads for the high-voltage (HV) power supply, function generator, and detection circuitry. iPhone for scale.

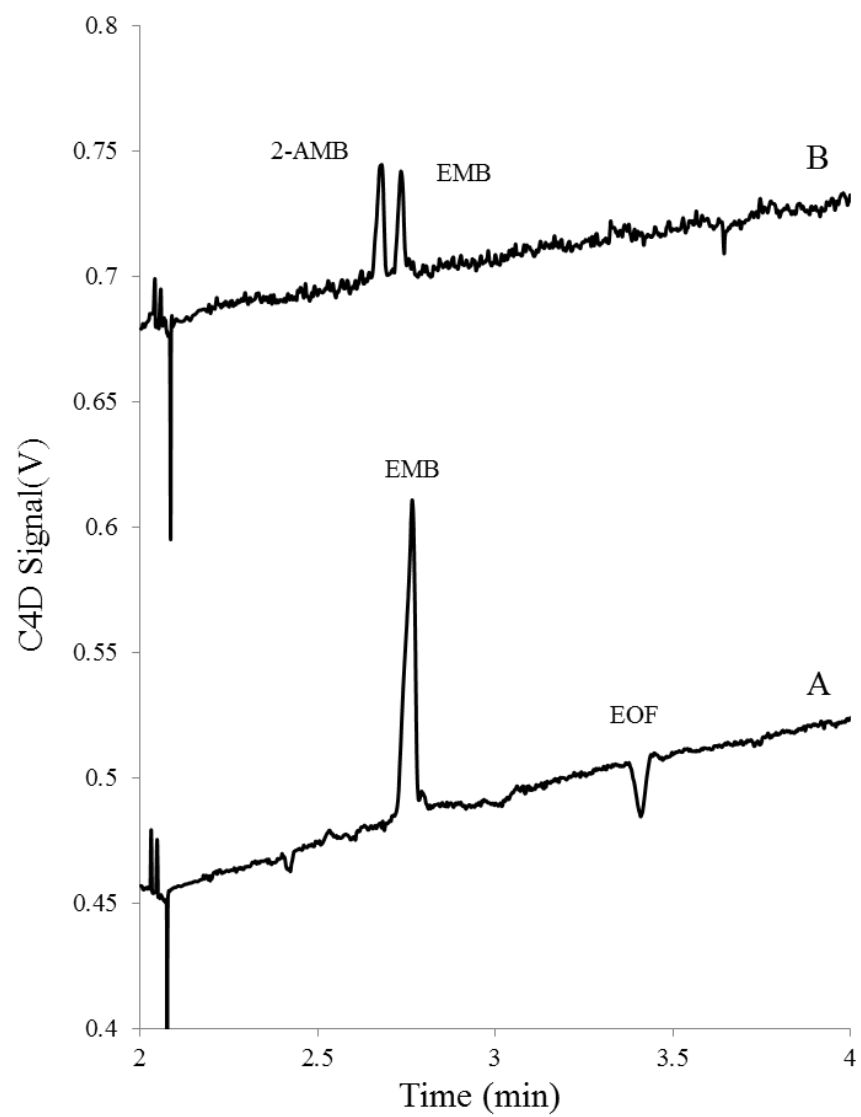


Figure 7: Electropherograms of A) 5 mM EMB, and B) separation of 1 mM 2-AMB and 1 mM EMB.

BGE: 30 mM MES, 50 mM His, pH 6.0.

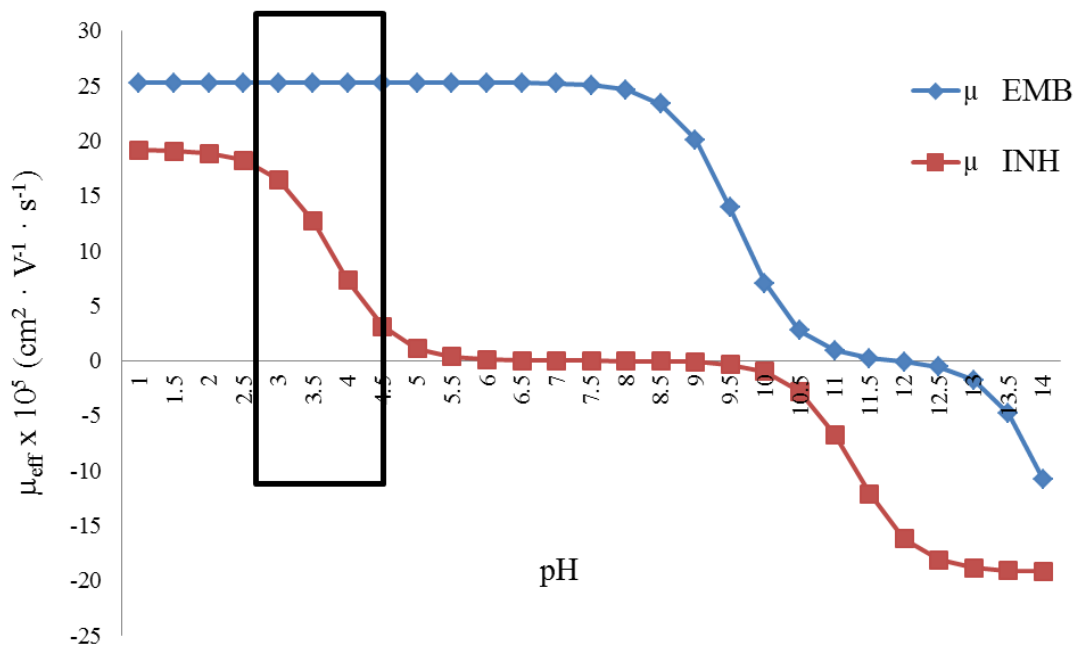


Figure 8: The effective mobility curve of EMB and INH. Data provided by Professor Marcone de Oliveira from the Departamento de Química, Instituto de Ciências Exatas, Universidade Federal de Juiz de Foravia via personal communication.

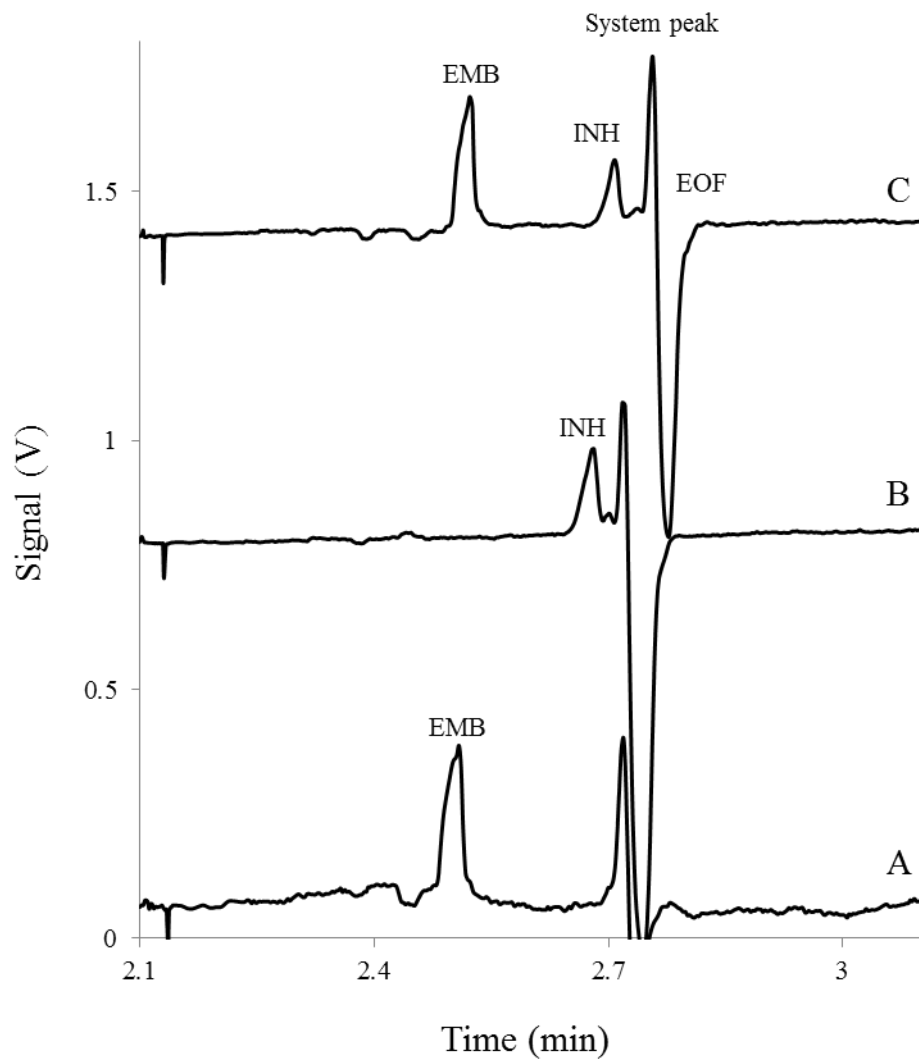


Figure 9: Electropherograms of A) 1 mM EMB, B) 5 mM INH, and C) separation of 1 mM EMB and 5 mM INH. BGE: 60 mM HEPES, 0.1 mM lactic acid, pH 4.0

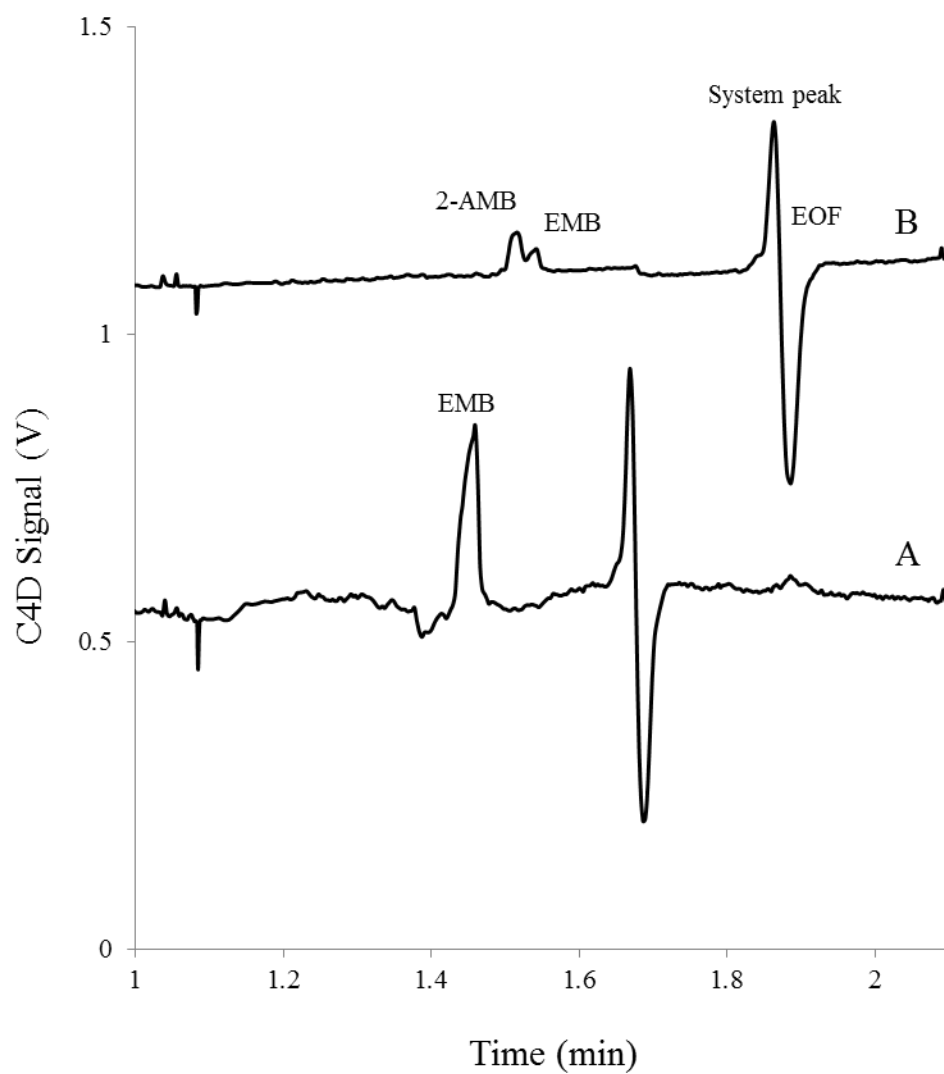


Figure 10: Electropherograms of A) 1 mM EMB and B) separation of 1 mM 2-AMB and 0.25 mM EMB.  
BGE: 60 mM HEPES, 0.1 mM lactic acid, pH 4.0



To determine the utility of ME-C<sup>4</sup>D for quantitation of both drugs, calibration curves were prepared for EMB and INH. Since the concentration of the sample is determined during sample preparation when a specified amount of the crushed tablet is dissolved into the BGE, the test can easily be run at a concentration that falls within the linearity of the method. Calibration curves for EMB and INH were linear over a range of 0.25-5.0 mM with R<sup>2</sup> values of 0.9973 and 0.9991, respectively. The LODs, estimated at a S/N =3, were 18 μM for EMB and 180 μM for INH. Luckily, sensitivity is not a main concern for the analysis of these compounds since the solid dose formulations contain a large amount of active ingredient, 400 mg per EMB HCl tablet and 300 mg per INH tablet.

### 5.3.2 ME separation performance for EMB standards vs pharmaceutical formulation

To assess the analytical performance of the separation, the % RSD for migration time, peak height, and peak area, along with theoretical plates/meter were calculated for the EMB standard dissolved in BGE and are shown in Table 1. The commercial EMB HCl tablet is formulated with several excipients including gelatin, hydroxypropyl methylcellulose, sodium lauryl sulfate, sorbitol, steric acid, sucrose, and titanium dioxide. To insure that the presence of excipients did not affect the separation, or the ability to quantitate the drug, a crushed tablet was dissolved into BGE and analyzed. Surprisingly, the migration time reproducibility improved significantly with the addition of the excipients, as did the calculated number of theoretical plates (Table 1). This could possibly be explained by the presence of the lauryl sulfate surfactant in the formulation. With the initially high concentrations of the drug and surfactant found in the injection plug, it is possible that the negatively charged surfactants present in the formulation associate with EMB, through a combination of hydrophobic or electrostatic interactions. This association would decrease the electrophoretic mobility of the EMB, and induce a stacking effect. Then, as the sample plug diffuses, becoming diluted by BGE in the separation channel, these interactions would diminish, causing the free drug to separate based on its own electrophoretic mobility. A similar phenomena of sample pre-concentration by surfactant micelle collapse has been described by Quirino et al [40].

Table 1 – Separation Performance for ETB in a Standard vs Tablet Formulation

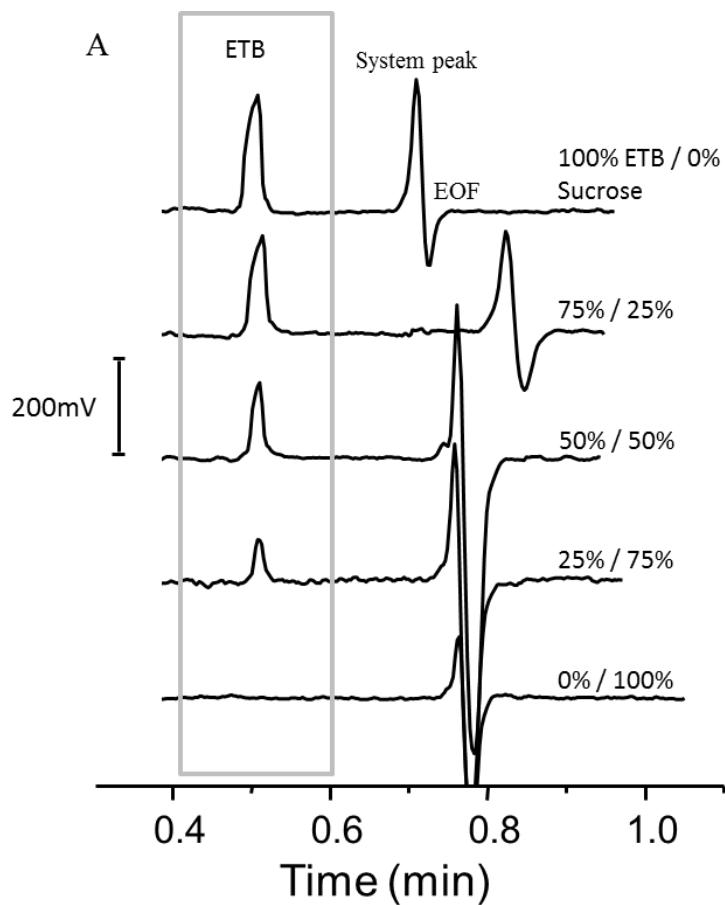
Drug (n=9)	Migration Time %RSD	Peak Height %RSD	Peak Area %RSD	Theoretical Plates Plates/meter
Standard	3.5	1.6	2.8	290,000
Tablet	0.38	1.8	3.4	410,000

### 5.3.3 Analysis of a lab-made counterfeit

As previously stated, approximately one fifth of counterfeit drugs contain the wrong amount of active ingredient [4]. The available paper-based devices and handheld spectrometers are currently unable to perform quantitative analysis. According to the European Pharmacopoeia monograph for EMB HCl, the tablet must contain between 90-110% of the amount listed on the label [41]. To assess the capability of the ME-C<sup>4</sup>D system to measure the amount of active ingredient in adulterated products, lab-made counterfeits were formulated by cutting EMB tablets with sucrose. Then, using the peak area of the counterfeit formulations divided by the peak area of a 100% EMB standard, the percentage of EMB in the counterfeit was determined. The actual percentage fell within a 95% confidence interval for all counterfeit formulations except for the 25% ETB counterfeit, where the ME-C<sup>4</sup>D results gave a confidence interval of 25.9-28.1 for an n=9 injections (Figure 11). However, 25% is far outside of the acceptable concentration range for EBT HCl and even with a confidence of 90% this product would be rejected. While further studies will need to investigate counterfeits covering a %EMB closer to the acceptable range of 90-110%, this study suggests that a peak area comparison of the sample to a standardized solution of EMB could be used accurately assess the amount of active ingredient in the product.

### 5.3.4 Identification of an internal standard

For the application of in-field analysis in developing countries, the assay will need to be robust and reproducible under a wide range of external conditions. Temperature, in particular, can greatly affect the migration time of analytes due to the change in BGE viscosity. To help account for environmental error, as well as any chip-to-chip variation, an internal standard should be used. Additionally, having the internal standard will provide a more accurate way to identify drugs based on their relative migration time.



Actual	Ave Calculated (95% MOE)
25%	27% ( $\pm 1.1$ )
50%	49% ( $\pm 2.0$ )
75%	80% ( $\pm 5.3$ )
100%	100% ( $\pm 2.2$ )

Figure 11: A) Electropherograms of various concentrations of EMB cut with sucrose to simulate a counterfeit formulation. BGE: 60 mM HEPES, 0.1 mM lactic acid, pH 4.0. B) back calculation of the concentration in the formulation as compared to the actual value (n=9).

Several amine-containing compounds were assessed as internal standards using the simulation software Peakmaster. Peakmaster is a program developed by Jaroš et al in 2001 that uses equations derived from electrophoresis theory to predict analyte migration times. Based on user imputed BGE, sample, and instrumentation conditions a theoretical electropherogram is generated. The 60 mM HEPES, 0.1 mM lactic acid BGE conditions were entered into the program from a predetermined database of possible constituents. Mobilities of EMB and INH were used as calculated by Faria et al., while the mobilities of the potential internal standards (ethylenediamine (EDA), diethylamine (DEA), and benzyl amine (BA)) were taken from the Peakmaster database of potential analytes. Using the specified parameters of all components in a 10 cm fused silica capillary was accomplished (Figure 12).

In Figure 13 it is possible to see that INH is fully resolved from all species, however, EMB completely co-migrated with BA but was separated from EDA and DEA. Based on this information, both EDA and DEA were tested on-chip. Using the ME-C<sup>4</sup>D, it was found that EMB and DEA co-migrated under the separation conditions (Figure 13a), while EDA was fully resolved from both IHN and EMB and will be used in the future as an internal standard (Figure 13b).

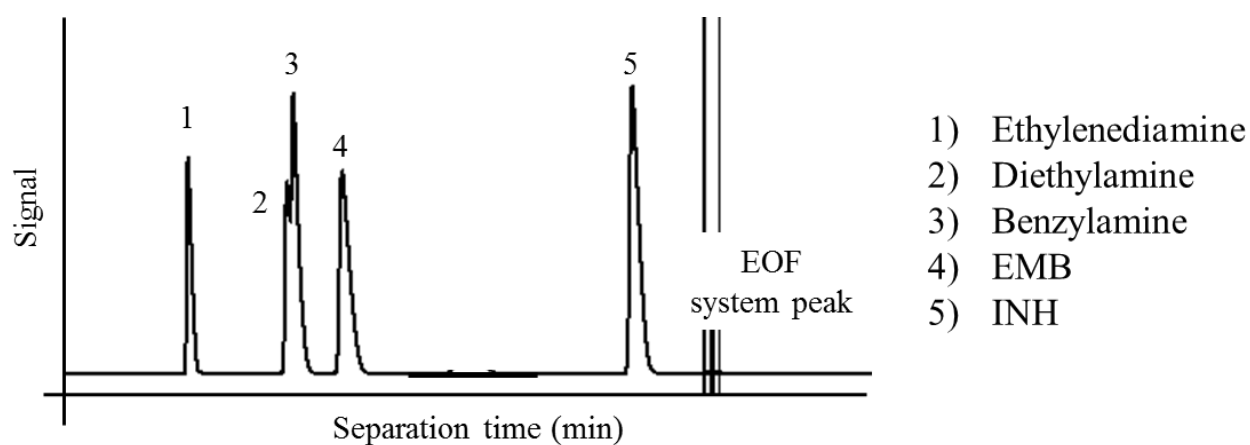


Figure 12: Peakmaster perdition of migration times of three potential internal standards based on the mobility from the database of compounds. Mobilities of EMB and INH were given to us by Marcone de Oliverira. Peakmaster run parameters: 40 cm capillary/10 cm to window, positive polarity, 10.8 kV driving voltage, EOF at 3 min. BGE constituents: 60 mM HEPES, 0.1 mM lactic acid. Signal: conductivity.

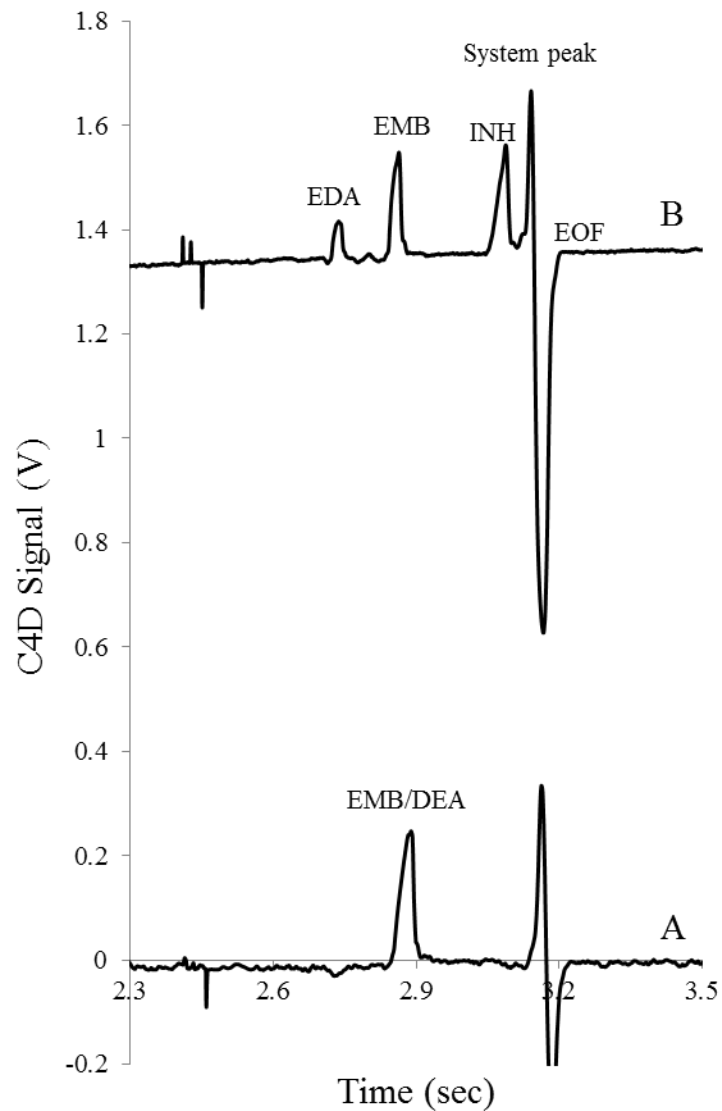


Figure 13: Electropherograms of A) 1.25 mM DEA and 0.5 mM EMB, B) 0.083 mM EDA and 0.67 mM EMB, and C) separation of 0.08 mM EDA, 1 mM EMB and 5 mM INH. BGE: 60 mM HEPES, 0.1 mM lactic acid, pH 4.0

## 5.4 Conclusions

This chapter describes the first steps towards the development of a portable ME-C<sup>4</sup>D assay for on-site pharmaceuticals testing. ME-C<sup>4</sup>D can provide separation-based analysis and necessary quantitative information for counterfeit drug screening in developing countries. Using a PDMS microchannel substrate with a 5 cm separation channel, a separation of two first-line anti-TB drugs (EMB and INH) was accomplished. TB medications are often prescribed in fixed dose combination formulations; making the simultaneous analysis of multiple active ingredients extremely useful. Using ME-C<sup>4</sup>D it is also possible to partially resolve EMB and its major degradation product, 2-AMB. The resolution of the separation could be improved through further optimization of the BGE or separation channel length.

To demonstrate the ability of this assay to provide quantitative results, a lab-made counterfeit of EMB was analyzed. The concentration of EMB in the adulterated product, EMB HCl tablet cut with sucrose, was determined by comparison of the peak area to a standard solution of EMB. Additionally, an internal standard was identified to help reduce chip-to-chip variability and assay error for future studies. While much work is needed before this device can be subjected to testing in the field, there is obvious potential in the utility of ME-C<sup>4</sup>D to provide low-cost portable and quantitative analysis of pharmaceuticals.



## 5.5 References

- [1] Storme-Paris, I., Rebiere, H., Matoga, M., Civade, C., Bonnet, P. A., Tissier, M. H., Chaminade, P., *Anal. Chim. Acta* 2010, 658, 163-174.
- [2] Zucker, H., Akunyili, D. N., Lee, R., in: IMPACT (Ed.), World Health Organization.
- [3] Kimura, K., Nishizawa, M., Sdogandji, T., ten Ham, M., Wondemangegehu, E., Department of Essential Drugs and Other Medicines, World Health Organization, Geneva, Switzerland 1999.
- [4] <http://www.who.int/medicines/services/counterfeit/overview/en/>, *World Health Organization; Medicines* 2014.
- [5] Power, G., in: IMPACT (Ed.), <http://www.who.int/impact/events/IMPACT-ACTechnologiesv3LIS.pdf>, World Health Organization.
- [6] Shah, R. Y., Prajapati, P. N., Agrawal, Y. K., *J Adv Pharm Technol Res* 2010, 1, 368-373.
- [7] Fischer, A., U.S. Food and Drug Administration 2013.
- [8] <http://www.fda.gov/downloads/ForConsumers/ConsumerUpdates/UCM349206.pdf>, Food and Drug Administration, Consumer Health Information.
- [9] <http://www.fda.gov/downloads/NewsEvents/Newsroom/FactSheets/UCM349286.pdf>, in: Services, D. o. H. a. H. (Ed.), U.S. Food and Drug Administration 2013.
- [10] Ida, H., Kawai, J., *Forensic Sci. Int.* 2005, 151, 267-272.
- [11] Ricci, C., Nyadong, L., Yang, F., Fernandez, F. M., Brown, C. D., Newton, P. N., Kazarian, S. G., *Anal. Chim. Acta* 2008, 623, 178-186.
- [12] Yang, D., Thomas, R., *Am. Pharm. Rev.* 2012, 15, 1-10.
- [13] Hargreaves, M. D., Green, R. L., Jalenak, W., Brown, C. D., Gardner, C., John Wiley & Sons Ltd. 2012, pp. 275-287.
- [14] Moffat, A. C., Assi, S., Watt, R. A., *J. Near Infrared Spectrosc.* 2010, 18, 1-15.
- [15] Assi, S., Watt, R., Moffat, T., *Spectroscopy* 2011, 36, 38-44, 46-47.
- [16] Hajjou, M., Qin, Y., Bradby, S., Bempong, D., Lukulay, P., *J. Pharm. Biomed. Anal.* 2013, 74, 47-55.

- [17] Sherma, J., *Acta Chromatogr.* 2007, 19, 5-20.
- [18] Flinn, P. E., Kenyon, A. S., Layloff, T. P., *J. Liq. Chromatogr.* 1992, 15, 1639-1653.
- [19] Kaale, E., Risha, P., Layloff, T., Sherma, J., *Chromatogr. Sci. Ser.* 2014, 106, 247-263.
- [20] Martinez, A. W., Phillips, S. T., Whitesides, G. M., Carrilho, E., *Anal. Chem. (Washington, DC, U. S.)* 2010, 82, 3-10.
- [21] Fu, E., Liang, T., Spicar-Mihalic, P., Houghtaling, J., Ramachandran, S., Yager, P., *Anal. Chem.* 2012, 84, 4574-4579.
- [22] Lutz, B., Liang, T., Fu, E., Ramachandran, S., Kauffman, P., Yager, P., *Lab Chip* 2013, 13, 2840-2847.
- [23] Yager, P., Edwards, T., Fu, E., Helton, K., Nelson, K., Tam, M. R., Weigl, B. H., *Nature (London, U. K.)* 2006, 442, 412-418.
- [24] Weaver, A. A., Reiser, H., Barstis, T., Benvenuti, M., Ghosh, D., Hunckler, M., Joy, B., Koenig, L., Raddell, K., Lieberman, M., *Anal. Chem.* 2013, 85, 6453-6460.
- [25] Lacher, N. A., Garrison, K. E., Martin, R. S., Lunte, S. M., *Electrophoresis* 2001, 22, 2526-2536.
- [26] Wang, J., *Talanta* 2002, 56, 223-231.
- [27] Guijt, R. M., Baltussen, E., Van der Steen, G., Frank, H., Billiet, H., Schalkhammer, T., Laugere, F., Vellekoop, M., Berthold, A., Sarro, L., Van Dedem, G. W. K., *Electrophoresis* 2001, 22, 2537-2541.
- [28] Coltro, W. K. T., Lima, R. S., Segato, T. P., Carrilho, E., Pereira de Jesus, D., Lucio do Lago, C., Fracassi da Silva, J. A., *Anal. Methods* 2012, 4, 25-33.
- [29] Becker, H., Gaertner, C., *Anal. Bioanal. Chem.* 2008, 390, 89-111.
- [30] Becker, H., Locascio, L. E., *Talanta* 2002, 56, 267-287.
- [31] Fiorini, G. S., Chiu, D. T., *BioTechniques* 2005, 38, 429-446.
- [32] Tsao, C.-W., DeVoe, D. L., *Microfluid. Nanofluid.* 2009, 6, 1-16.
- [33] Faria, A. F., de Souza, M. V. N., Bruns, R. E., de Oliveira, M. A. L., *Talanta* 2010, 82, 333-339.
- [34] Fracassi da Silva, J. A., Vitorazzi de Castro, N., Pereira de Jesus, D., Faria, A. F., De Souza, M. V. N., Leal de Oliveira, M. A., *Electrophoresis* 2010, 31, 570-574.

- [35] Duffy, D. C., McDonald, J. C., Schueller, O. J. A., Whitesides, G. M., *Anal. Chem.* 1998, 70, 4974-4984.
- [36] McDonald, J. C., Duffy, D. C., Anderson, J. R., Chiu, D. T., Wu, H., Schueller, O. J. A., Whitesides, G. M., *Electrophoresis* 2000, 21, 27-40.
- [37] Vazquez, M., Frankenfeld, C., Coltro, W. K. T., Carrilho, E., Diamond, D., Lunte, S. M., *Analyst* 2010, 135, 96-103.
- [38] Fracassi da Silva, J. A., do Lago, C. L., *Analytical Chemistry* 1998, 70, 4339-4343.
- [39] Fracassi da Silva, J. A., Guzman, N., do Lago, C. L., *Journal of Chromatography A* 2002, 942, 249-258.
- [40] Quirino, J. P., Haddad, P. R., *Anal. Chem.* 2008, 80, 6824-6829.
- [41] Pharmacopia, *Ethambutol Hydrochloride*, Council of Europe, Strasbourg 2005.

## **Chapter Six**

### **Conclusions and Future Directions**

## 6.1 Conclusions

### 6.1.1 Oxytocin project

The ultimate goal of the project described in the first half of this thesis was to develop a capillary electrophoresis (CE) method for the separation and detection of the degradation products formed by oxytocin (OT) under thermal stress. Having a reliable, low-cost assay for OT integrity could help maintain a more secure supply chain in developing countries. Currently the biggest threat to the supply of OT is the absence of proper shipping and storage of these heat-sensitive products [1] as OT is known to generate several degradation products under heat-stress conditions [2].

Initially, studies were focused on the CE-based separation of the desamino degradation products of OT, as discussed in chapter 3 [3]. OT has three possible sites where deamidation can occur, leading to seven different desamino degradation products. Chapter 3 described the systematic optimization of the background electrolyte (BGE) for the CE separation to provide greater selectivity between species with similar electrophoretic mobilities. The final BGE composition included sulfobutyl ether  $\beta$ -cyclodextrin as a pseudo stationary phase and MeOH as an organic modifier. Under these conditions it was possible to achieve baseline resolution of all seven desamino species from OT. Using this method, the heat-stress degradation of OT at pH 2.0 was monitored over a period of 96 h at 70 °C. This CE method offers faster analysis times and lower costs-per-test than the current HPLC method.

However, deamidation is not the only degradation pathway for heat-stressed OT samples. Previous studies have shown that the major products formed at pH > 3 are dimers and cyclic polysulfides. The cyclic polysulfides are formed by the addition of one to two sulfurs to the disulfide bridge of OT between Cys<sup>1</sup> and Cys<sup>6</sup>. The mechanism by which both the dimers and the cyclic polysulfides are formed was postulated by Wisniewski et al [4]. These previous studies to determine the degradation products of OT were performed in phosphate buffered solutions to control pH. While this was necessary for controlled OT degradation, it does not account for the fact that injectable OT is formulated in unbuffered

water, adjusted between pH 3-5 with the addition of acetic acid, and 0.5% w/v chlorobutanol (CB) as a preservative. Before continuing the optimization of our CE method to include the dimer and cyclic polysulfide compounds, confirmation that the degradation products formed in the pharmaceutical preparation are identical to those reported in the buffered formulation was needed.

Chapter 4 presents a preliminary study of the OT degradation products formed under heat-stress conditions in a variety of liquid formulations, including an unbuffered water solution with CB that is similar to the pharmaceutical preparation. Over the course of two days, multiple samples were analyzed at regular time intervals while the samples were heated at 70° C. The analysis of the samples was accomplished with LC-UV-MS. MS was used for mass identification of the peaks present in the LC-UV chromatogram, while the LC-UV data at 214 nm was used for quantitative analysis to determine degradation kinetics.

In these studies, it was determined that the presence of CB in the unbuffered and buffered formulations increased the thermal stability of OT. This effect was much more pronounced in the unbuffered formulations where the percentage of OT remaining after 48 h at 70 °C was improved by a factor of five. In the formulations that did not contain CB, all of the expected degradation products of OT (dimers and cyclic polysulfides) were observed. However, with the addition of CB, the dimer products were no longer formed, indicating a change in the degradation mechanism of OT. Additionally, a new peak was observed in the LC-UV chromatogram that eluted after the trisulfide product (4.9% of t=0 oxytocin peak area).

Several compounds of structural similarity to CB were tested in the unbuffered OT formulation in an attempt to determine mechanism by which CB decreases the degradation rate. Of all of the compounds tested, only 0.5% w/v 2,2,2-trichloroethanol (TCE) produced a similar stabilizing effect in the OT formulation, as well as preventing the formation of dimer products. Additionally, an unidentified peak was seen in the LC-UV chromatogram of the TCE sample (5.8% of t=0 oxytocin peak area). If CB and

TCE are reacting with the OT in a way that prevents the formation of dimers, this new peak could be a useful tool in determining the mechanism. Future studies will focus on confirming its identity.

#### 6.1.2 ME-C<sup>4</sup>D portable analysis project

The overall goal of this project was to take the initial steps towards developing a portable analysis system for on-site drug quality control screening. Resource-low countries are plagued by the counterfeit drug products that make up to 50% of the market in some areas. Without proper regulatory control by governmental agencies, these substandard products can pass unchecked into the country and be distributed causing prolonged sickness, potential side effects, and death. Currently, the analytical methods available for screening pharmaceutical supply chains range from high-tech handheld spectrometers, to low-tech TLC and lateral-flow assays. These methods cover a variety of innovative ways to qualitatively assess drug quality; however, their quantitative abilities are limited. This prevents the identification of the subset of counterfeits that contains the wrong amount of active ingredient.

To supplement the qualitative methods mentioned above, while keeping the cost-per-test low, microchip electrophoresis (ME) is an attractive separations-based analysis method. ME can be coupled with a universal detector, such as C<sup>4</sup>D, that allows for quantitative analysis of multiple products simultaneously. The work in chapter 5 discusses the uses of ME coupled with capacitively coupled contactless conductivity detection (C<sup>4</sup>D) for the analysis of anti-tuberculosis (TB) drugs. Using this methods, two first-line anti-TB drugs, ethambutol (EMB) and isoniazid (INH), separated and detected using a BGE consisting of 60 mM HEPES with 0.1 mM lactic acid at pH 4.0. Additionally, this system was used to analyze lab-made counterfeits of various concentrations of EMB. The assay was useful for determining the concentration of formulations containing 50, 75, and 100% drug within a 95% confidence interval.

## 6.2 Future Directions

### 6.2.1 CE separation of all oxytocin degradation products

In addition to further investigations into the mechanism of the stability enhancement of oxytocin in the presence of CB as discussed at the end of chapter 4, we would like to continue working towards a CE-based separation for OT integrity screening. As mentioned previously, OT and the cyclic polysulfides have roughly the same size-to-charge ratio at all pH values, making them impossible to separate by CZE. Additionally, the cyclodextrin used in chapter 3 does not provide any selectivity between these three peptides. However, metals such as copper (II) have been used previously to form complexes with peptides, imparting an additional negative charge and thereby changing their mobility [5].

We have hypothesized that the addition of copper (II) or another divalent metal ion to the BGE could lead to varying degrees of complexation for the three cyclic peptides based on the length of the disulfide bridge. Due to the presence of the disulfide bond, OT does have some inherent secondary structure. Structural studies have shown that hydrogen bonding occurs between the hydroxyl group of the Tyr2 and the carboxamide of Asn5 due to their proximity in the cyclic form of the peptide. With the addition of each new sulfur molecule to the disulfide bridge, this structure could change, possibly allowing access to more of the peptide backbone for metal complexation, introducing selectivity between the di-, tri-, and tetrasulfide OTs. The trouble with testing this hypothesis has been the lack of commercially available standards for the cyclic polysulfides that could be used to optimize the separation. However, both Ferring Pharmaceuticals and the Schoenich lab at KU have offered their support in the donation or preparation of said species.

### 6.2.2 Continuing development for on-site ME analysis

#### 6.2.2.1. ME-C<sup>4</sup>D for small molecule analysis

It going forward, the next goal of this project is to further develop the ME-C<sup>4</sup>D system so it can be used for the analysis of counterfeit drugs in developing countries. This includes further miniaturization of



the associated electronics needed to run the device. Through work in our laboratory by Ryan Grigsby, and through collaboration with Pinnacle Technologies, development of a miniaturized high voltage power supply (HVPS) and associated software needed to operate the voltage for fluid flow on-chip has been accomplished. This instrumentation was developed as part of our “lab-on-a-sheep” project; however, the technology is transferable to on-site microchip based analytical systems. The C<sup>4</sup>D circuitry is already quite small and can be housed in a 2”x4” box. To be fully autonomous, all the components including HVPS and C<sup>4</sup>D, must run on a laptop battery. Again, this has been demonstrated with the “lab-on-a-sheep” project and just needs to be modified for the ME-C<sup>4</sup>D system.

To further improve this assay for use in developing countries, another area of future research that needs to be addressed is investigating alternative microchip substrates to PDMS that are still inexpensive and easy to fabricate. While PDMS is an excellent choice for prototyping, it will not be useful for the final product because PDMS loses its elasticity overtime, making long-term storage impractical. Many plastic options exist [9-11] for just this application and further work will be done to test the separation performance in a few of these materials.

In addition, before ME-C<sup>4</sup>D can be implemented in developing countries in areas that do not have functioning laboratories, sample preparation methods that can be performed on-site without the need of a mortar and pestle and sonicator to grind the tablet need to be developed. The sample preparation protocols used in conjunction with the Minilab™ TLC tests have been very successful in this regard [12, 13]. In this method, the tablet in a small bag and dissolved in a predetermined volume of solvent to achieve the correct concentration. We will adapt their methods to develop a working protocol. Additionally, the effect of ambient temperature variability on the ME separation must also be investigated since in elevated temperatures can lead to changes in the migration time of the analytes. More work, using the internal standard discussed in chapter 5, is needed to show that separation performance is acceptable under various external temperatures.

And then finally, once the generic ME-C<sup>4</sup>D system has been fully developed, assays for other drugs used frequently in developing countries should be developed using the same basic platform. Once these goals have been realized, it will be possible to portable field ready analysis system that could provide much needed quantitative analysis of pharmaceuticals on-site and at a low-cost.

#### 6.2.2.2. ME-LIF for protein and peptide drug analysis

The downside of the ME-C<sup>4</sup>D system for protein and peptide drug analysis is the poor limits of detection. Peptide and protein drugs are generally formulated at low concentrations; oxytocin for example is prepared as 10 IU/mL or roughly 20  $\mu$ M. In CE, the small pathlength leads to poor limits of detection (LOD) with UV-Vis spectroscopic detection. While the UV is useful for conventional CE for universal detection of biologics, it does not make an attractive option for microchip. As an alternative to UV, LIF provides very specific and sensitive detection. Work towards a fully portable LIF detection system has been underway in our laboratory for the past two years. The current system has a total cost of less than \$500 and can easily fit in an 8x8 inch box (Figure 2). Preliminary separations of fluorescently derivatized amino acids have been achieved and LODs in the low  $\mu$ M are possible. While these initial studies show significant promise, much work is needed to get this system to a place where it can be implemented in the field.

Additionally, microchip electrochromatography (MEC) is being investigated as a separation mechanism for the peptide products. MEC combines chromatographic retention and electrophoretic migration, with bulk fluid flow created by the EOF. This combination enhances the selectivity and efficiency of the separation and enables the separation of neutral species not possible with CZE. Gold nanoparticles affixed to the surface of the capillary as an open tubular column (OTCEC) have been used for the separation of peptides [6]. As compared to packed-bed columns, OTCECs have the benefit of easy and reproducible preparation, while maintain the high peak efficiency of CE [7]. This approach could allow for a portable and inexpensive peptide assay without the use of BGE additive to achieve a

separation of the degraded products. Optimization of peptide separations on both conventional CE and a microchip design from the Garcia lab [8] is being currently under way.

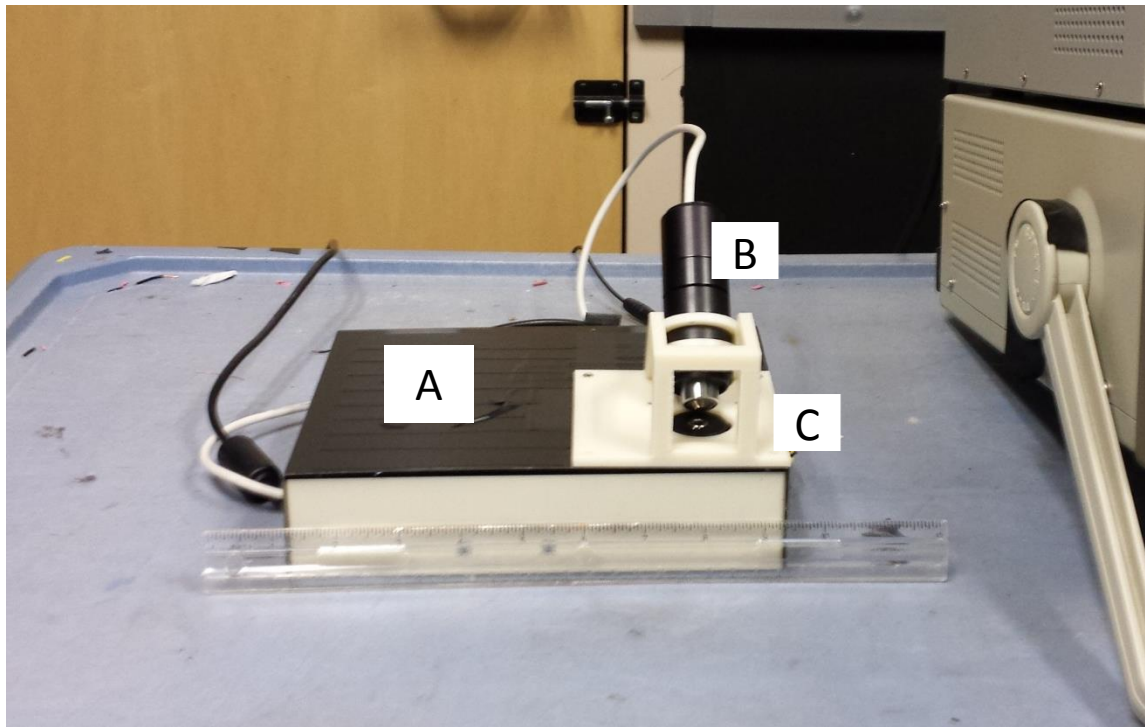


Figure 1: Current image of the portable LIF detector as developed by Nathan J. Oborny in the Susan Lunte Lab. A) Box housing the electronics, battery to power the system, and 420nm LED with focusing lenses. B) Objective, filter, and custom photodiode amplifier for detection. C) 3D printed prototype optics mount to hold objective 45 degrees to LED source.

### 6.3 References

- [1] Hogerzeil, H. V., Walker, G. J. A., de Goeje, M. J., *Action Programme on Essential Drugs, World Health Organization*. 1993, 1-50.
- [2] Hawe, A., Poole, R., Romeijn, S., Kasper, P., van der Heijden, R., Jiskoot, W., *Pharm. Res.* 2009, 26, 1679-1688.
- [3] Creamer, J. S., Krauss, S. T., Lunte, S. M., *Electrophoresis* 2014, 35, 563-569.
- [4] Wiśniewski, K., Finnman, J., Flipo, M., Galyean, R., Schteingart, C. D., *Peptide Science* 2013, 100, 408-421.
- [5] Kuhnline, C. D., Lunte, S. M., *J. Sep. Sci.* 2010, 33, 2506-2514.
- [6] Hamer, M., Yone, A., Rezzano, I., *Electrophoresis* 2012, 33, 334-339.
- [7] Cheong, W. J., Ali, F., Kim, Y. S., Lee, J. W., *J. Chromatogr. A* 2013, 1308, 1-24.
- [8] Segato, T. P., Bhakta, S. A., Gordon, M. T., Carrilho, E., Willis, P. A., Jiao, H., Garcia, C. D., *Anal. Methods* 2013, 5, 1652-1657.
- [9] Becker, H., Locascio, L. E., *Talanta* 2002, 56, 267-287.
- [10] Fiorini, G. S., Chiu, D. T., *BioTechniques* 2005, 38, 429-446.
- [11] Tsao, C.-W., DeVoe, D. L., *Microfluid. Nanofluid.* 2009, 6, 1-16.
- [12] Kaale, E., Risha, P., Layloff, T., Sherma, J., *Chromatogr. Sci. Ser.* 2014, 106, 247-263.
- [13] Flinn, P. E., Kenyon, A. S., Layloff, T. P., *J. Liq. Chromatogr.* 1992, 15, 1639-1653.